THE UNIVERSITY OF ALBERTA

ANALYSIS OF STRENGTH AND DEFORMATION FOR BONDED PRESTRESSED CONCRETE BEAMS

by

LESLIE BAKAR

A THESIS

SUBMITTED TO THE FACULTY OF GRADUATE STUDIES

IN PARTIAL FULFILMENT OF THE REQUIREMENTS FOR THE DEGREE OF

MASTER OF SCIENCE

DEPARTMENT OF CIVIL ENGINEERING

EDMONTON, ALBERTA

MAY 1966

UNIVERSITY OF ALBERTA

FACULTY OF GRADUATE STUDIES

The undersigned certify that they have read, and recommend to the Faculty of Graduate Studies for acceptance, a thesis entitled ANALYSIS OF STRENGTH AND DEFORMATION FOR BONDED PRESTRESSED CONCRETE BEAMS submitted by LESLIE BAKAR in partial fulfilment of the requirements for the degree of MASTER OF SCIENCE.

ABSTRACT

This thesis presents an analytical study of the strength and deformation of bonded prestressed beams with rectangular cross-sections. The beams were analyzed for strength and deformation using each of six stress blocks. The results obtained using each stress block were compared with those obtained from tests and also those derived using the other stress blocks.

For the two-point loaded beams, the correlation between the theoretical moment-curvature relationship and that derived from strain measurements in the tests was good, except at the stage of loading just beyond cracking. The moment-curvature relationship for the one-point loaded beams could not be predicted accurately. The ultimate moment could be predicted but there were large discrepancies between the predicted and measured ultimate curvatures mainly because of unbonding of the reinforcement. These discrepancies were even more pronounced on the shorter one-point loaded beams. In general, for the two-point loaded beams, there was better agreement between the theoretical and measured load-deflection curve because the beams had a substantial portion of their length subjected to a constant moment as compared to that for the one-point loaded beams.

The closest approximations to the test curves were obtained using a Jensen type stress block. Using Hognestad's stress block, the derived curves were also close to the test curves but were slightly more conservative than those obtained using Jensen's stress block.

ACKNOWLEDGEMENTS

This investigation was conducted under the supervision of Dr. J. Warwaruk, Associate Professor in the Department of Civil Engineering. His assistance, guidance and checking of the manuscript are sincerely appreciated.

The author also wishes to thank the staff of the Computing Science Department for their assistance with the computer program.

TABLE OF CONTENTS

TABLE OF CONTENTS (Continued)

LIST OF TABLES

LIST OF FIGURES

LIST OF FIGURES (Continued)

LIST OF FIGURES (Continued)

CHAPTER I

INTRODUCTION

1.1 Introductory Remarks

This thesis deals with the analysis of the deformation characteristics of pretensioned prestressed concrete beams. The method of analysis used was the same as that described in Reference (12)* and the results of the analysis were compared with the results of beams tested at the University of Alberta (Edmonton) reported in References (1) and (9).

1.2 Object

The object of this investigation is to analyze prestressed concrete beams for strength and deformations, using all available stress blocks. The method of analysis (12) originally used only a simplified stress block consisting of two straight lines. With this analysis, the effects of different stress blocks were studied in this thesis and compared with test results. Thus, a stress block could be chosen which would predict accurately the moment-curvature relationship at all stages of loading.

The analysis is directly applicable to short-time loading since tension in the concrete was neglected and creep effects due to sustained loads were not considered. The method of analysis requires that the ultimate and cracking moments for the beams are known. The ultimate moment

---

*The numbers in parenthesis refer to the entries in the list of references.

determination was straight-forward; however, difficulties were encountered in predicting the cracking moment. The cracking moments obtained exhibited considerable scatter. In this investigation, a consistent substitute for the usual cracking moment was assumed as that point where a crack had progressed up to a position such that the neutral axis of the beam was at the level of the reinforcement. In this connection, a part of this thesis deals with a comparison of the modulus of rupture predicted by two empirical equations given in Appendix A.1 and that calculated from beam tests.

CHAPTER II

LITERATURE REVIEW

2.1 Introduction

Many investigators, in the early 1900's recognized the non-linear behavior of the stress-strain relationship for concrete. A number of investigators have tried to approximate the stress-strain curve of concrete by mathematical curves. Some have tried to approximate the actual compressive stress block by using equivalent rectangular or trapezoidal stress blocks. A complete study of all the available stress blocks up to the year 1950 was made by Hognestad and summarised (3). The most significant of these are Stussi's, Jensen's and that proposed by Hognestad. The stress-blocks which were published after 1951 will be discussed in the following sections of this chapter.

All stress blocks can be broken down into three distinct groups. The first group consists of those stress blocks which can be derived on the basis of the concrete strength, f'_c , only; the second depends on f'_c and the corresponding strain, ϵ_o , at which f'_c occurs; and finally those stress blocks which are derived experimentally from measurements of strains, moments and axial loads applied directly to a member.

2.2 Stress Blocks Depending on f'_c only

2.2.1 Introductory Remarks

The first group of stress blocks deals with those stress blocks

whose entire shape can be determined if f'_c is known. Properties such as the modulus of elasticity E , the strain, ϵ_o , corresponding to maximum stress and the ultimate strain, ϵ_u , can be determined. The stress blocks that fall into this group are Stussi's (3), Jensen's (5), Hognestad's (3) and Kriz and Lee's (6).

2.2.2 Stussi 1932

Stussi (3) in his analysis of rectangular concrete beams reinforced in tension only, assumed a very general type of stress block as shown in Figure 2.1(a). An arbitrary form of the concrete stress block was assumed which was more or less the same shape of the stress-strain curve of a standard concrete cylinder or prism. This stress block was then completely defined by the parameters k_1, k_2, f'_c and ϵ_u as shown in Figure 2.1(a). Stussi, however, was concerned only with the ultimate moment M_u , of the concrete beams. Using the stress-strain curve derived from a standard prism test, he found that k_1 ranged from 0.70 to 0.77, k_2 ranged from 0.39 to 0.41 and ϵ_u was taken to be between 0.002 and 0.0025. He did not realize that the standard prism could be strained beyond the point at which the ultimate prism load was reached. Thus his values of k_1 , k_2 and ϵ_u were smaller than those used in current practice. Hognestad (3) has pointed out that Stussi's approach was of such a general nature that many later ultimate strength theories could be considered as refinements and improvements of Stussi's work.

2.2.3 Jensen 1943

A complete study of rectangular concrete beams reinforced in tension only was made by Jensen in 1943 (5). His proposed stress block

was based on the concept that concrete stress-strain properties could be defined by two parameters, namely, the initial modulus of elasticity E , and the plasticity ratio β . The plasticity ratio was defined as the ratio of the plastic strain to the total strain of the concrete at rupture. Jensen noted that concrete of high strength exhibited almost a straight line on the stress-strain curve and final rupture occurred at a strain just beyond ϵ_o . On the other hand, concrete of low strength exhibited a stress-strain curve which could be closely approximated by a second degree parabola, with the final strain at rupture much greater than that of higher strength concrete. As a result, the modulus of elasticity was given in terms of the compressive strength of the concrete:

$$E = \frac{30,000,000}{5 + 10,000/f'_c} \text{ psi} \qquad (2.1)$$

the plasticity ratio was given by

$$\beta = \frac{1}{1 + (\frac{f'_c}{4000})^2} \qquad (2.2)$$

the strain corresponding to maximum stress was given by

$$\epsilon_o = \frac{f'_c}{E} \qquad (2.3)$$

From the above three relationships the ultimate strain was derived and expressed as

$$\epsilon_u = \frac{f'_c}{(1 - \beta)E} \qquad (2.4)$$

FIGURE 2.1 STRESS BLOCKS

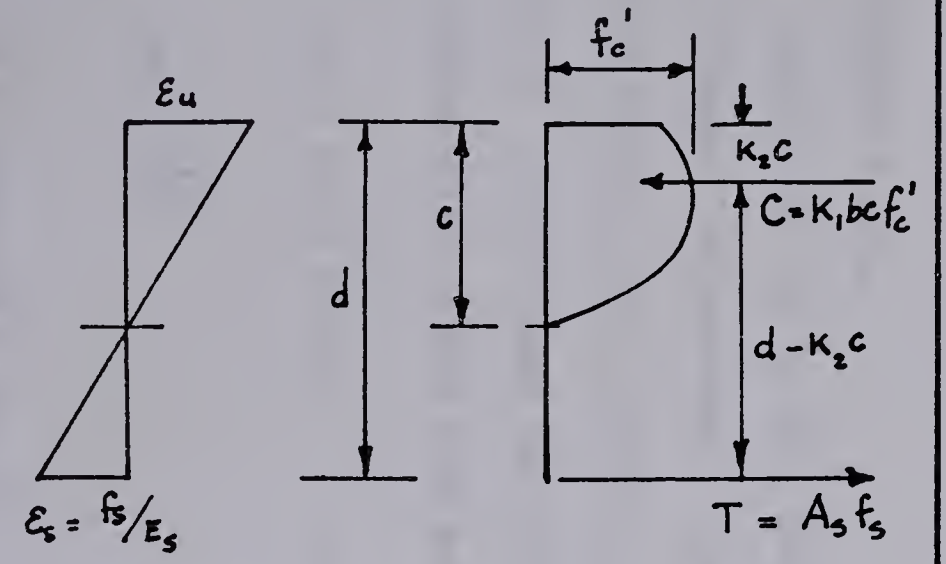

a. STUSSI'S STRESS BLOCK

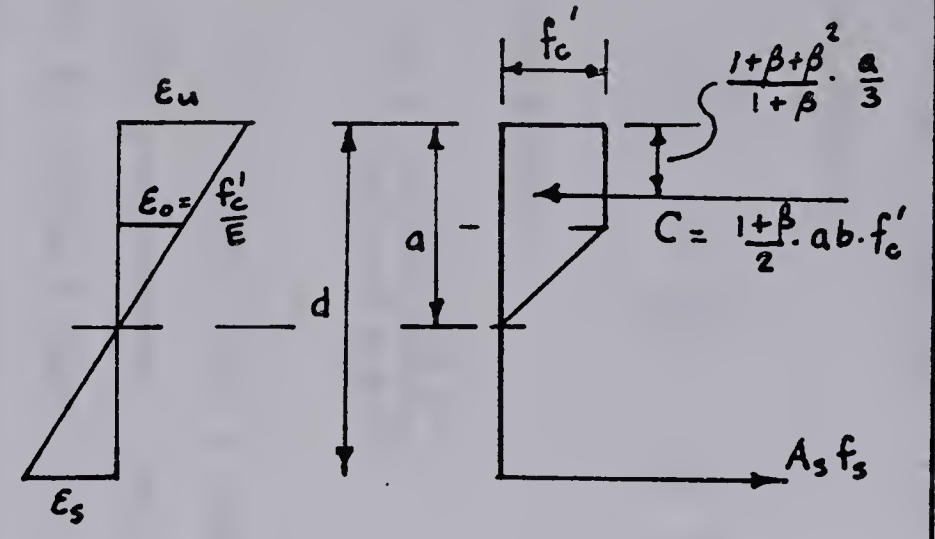

b. JENSEN'S ORIGINAL STRESS BLOCK

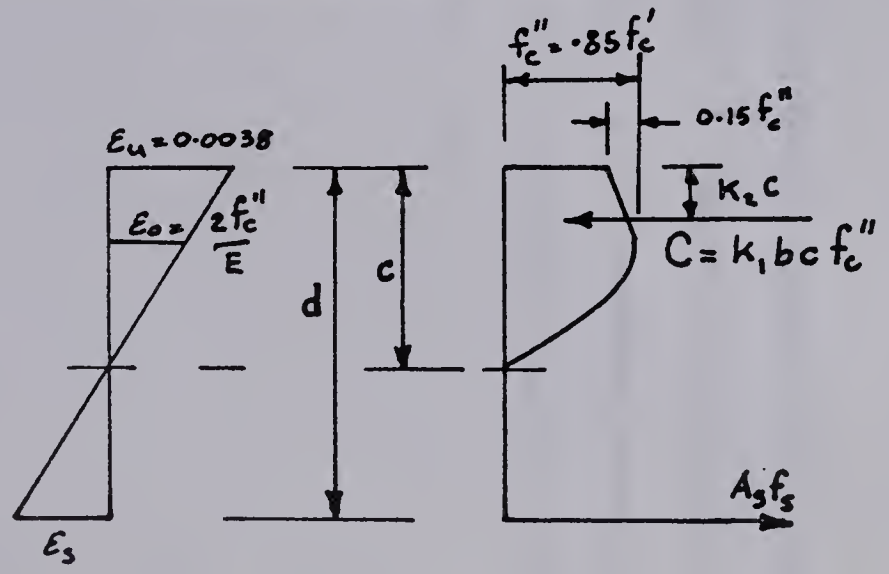

C. HOGNESTAD'S STRESS BLOCK

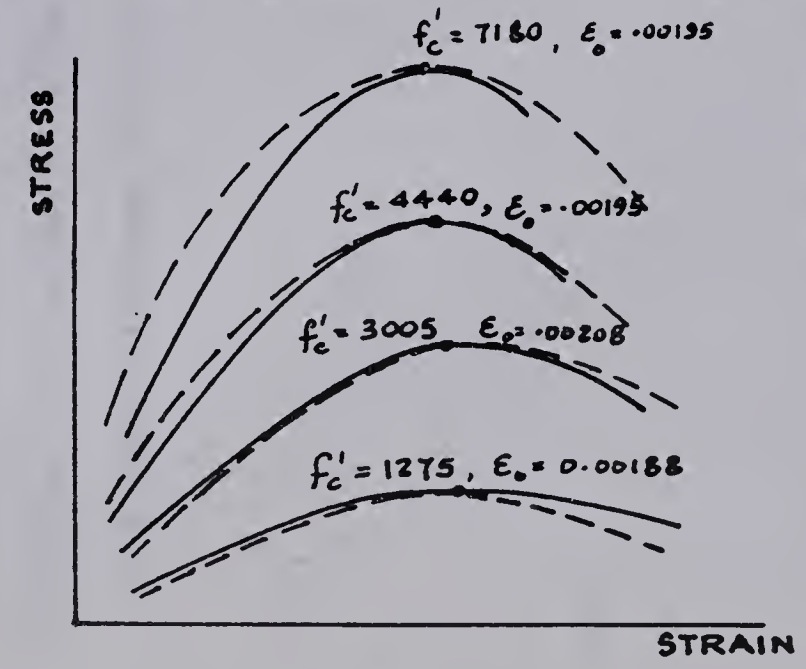

d. SMITH AND YOUNG'S STRESS BLOCK

Jensen's stress block is shown in Figure 2.1(b). Using the assumptions and expressions given above, an expression for the ultimate moment was derived,

$$\frac{M_u}{bd^2 f'_c} = p \frac{f_s}{f'_c} \left(1 - \frac{1}{N} \frac{pfs}{f'_c}\right) \tag{2.5}$$

N was derived from

$$N = \frac{3\,(1+\beta)^2}{2(1+\beta+\beta^2)} \tag{2.6}$$

It was found that N ranged from 2.0 for 1000 psi concrete to 1.83 for 6000 psi concrete. The ultimate moment equation (2.5) was then simplified by taking N equal to 2.0 in all cases. By doing so, Jensen justified using f'_c instead of $0.85\, f'_c$.

2.2.4 Hognestad 1951

Hognestad (3) in 1951 conducted a study of eccentrically loaded concrete columns. He assumed a stress block for compressed concrete such as shown in Figure 2.1(c). Choosing the value of the maximum stress f''_c to be $0.85\, f'_c$, he obtained the expression for a parabolic relationship for the stress-strain curve from zero strain to ϵ_o ,

$$f_c = f''_c \left[2\,\epsilon/\epsilon_o - (\epsilon/\epsilon_o)^2\right] \tag{2.7}$$

where $$\epsilon_o = \frac{2f''_c}{E} \tag{2.8}$$

and $$E = 1{,}800{,}000 + 460\, f''_c \tag{2.9}$$

After ϵ_o was reached, the stress-strain relationship was linear from ϵ_o to ϵ_u . The limiting strain was taken as 0.0038 inch per inch, regardless of concrete strength.

2.2.5 Kriz and Lee 1960

In a study of over-reinforced rectangular concrete beams, Kriz and Lee (6) used a generalised second-degree equation to approximate the relationship between stress and strain in the compressed concrete in a beam. The generalised equation was

$$f^2 + A\epsilon^2 + Bf\epsilon + Cf + D\epsilon = 0 \qquad (2.10)$$

where the strain, ϵ , was given in 10^{-3} inch per inch and the corresponding stress f , in kips per square inch.

The coefficients A, B, C and D were functions of f'_c and could be obtained by substituting four known values of f and the corresponding values of ϵ into equation (2.10) and solving simultaneously.

The four known values of f could be obtained from the equation

$$f = F + Gf'_c + H\,(f'_c)^2 \qquad (2.11)$$

where coefficients F, G and H were functions of ϵ and were previously determined for four known strains of 0.006, 0.0012, 0.0018, and 0.0024 inch per inch.

Using equation 2.10, curves were plotted for f'_c ranging from 1000 psi to 6000 psi. It was noted that for f'_c of 3000 psi and lower, the maximum stress on the stress-strain curve was equal to f'_c. In the case of f'_c equal to 4000 psi or greater, the maximum stress on the

stress-strain curve was always less than the value of f'_c . For example, the maximum stress for 6000 psi concrete was found to be about 5600 psi.

In the following chapters of this thesis, the stress block proposed by Kriz and Lee is referred to as the PCA stress block, for convenience.

2.3 Stress Blocks Depending on f'_c and ϵ_o

2.3.1 Introductory Remarks

Some stress blocks can be expressed by means of mathematical curves. To define the curve completely two parameters are required, namely, the concrete strength f'_c and the corresponding strain ϵ_o which is obtained from the standard cylinder test. Two stress blocks fall into this group, Smith and Young's (10) and Desayi and Krishnan (2) stress blocks.

2.3.2 Smith and Young 1956

A single continuous function was derived by Smith and Young for the stress-strain relationship of concrete in compression. The function was an exponential type given by the equation

$$f = \epsilon \, Me^{-N\epsilon} \tag{2.12}$$

This function gave a decrease in the stress-strain curve after the maximum stress f'_c was reached. The constants M and N were evaluated from the actual properties of a 6 x 12-in. cylinder and the boundary conditions

$$f = f'_c \text{ when } \epsilon = \epsilon_o \tag{2.13}$$

and

$$\frac{df}{d\epsilon} = 0 \quad \text{when } \epsilon = \epsilon_o \tag{2.14}$$

where $\frac{df}{d\epsilon}$ is the slope of the stress-strain curve. From these boundary conditions the following equation was obtained,

$$f = f'_c \cdot \frac{\epsilon}{\epsilon_o} \cdot e^{\left(1 - \frac{\epsilon}{\epsilon_o}\right)} \qquad (2.15)$$

Equation 2.15 depends not only on a knowledge of f'_c but also on the strain ϵ_o , which is obtained from a standard cylinder test. The advantage of using such a curve is that the compressive force and its location can be determined mathematically for any value of strain in the extreme concrete fibre. No limiting strain was proposed. The authors suggested that reliable tests be conducted to determine ϵ_u , for different strength and curing conditions of concrete.

Figure 2.1(d) shows a comparison of the actual test curves (solid lines) for a standard test cylinder and the curves predicted by Smith and Young (broken lines). It can be seen that the continuous function approximates very closely the test curves for concrete strength of 4000 psi and lower. For very high concrete strength of the order of 7000 psi, the compressive force predicted by the continuous function was about 10 per cent greater than the actual force.

2.3.3 Desayi and Krishnan 1964

Desayi and Krishnan (2) proposed the following equation for the stress-strain curve for concrete in compression

$$f = \frac{E\epsilon}{1 + (\epsilon/\epsilon_o)^2} \qquad (2.16)$$

which could be extrapolated beyond the maximum stress in order to compute

the ultimate moment in concrete beams. The initial tangent modulus E is obtained from a computation similar to Hognestad's

$$E = \frac{2f'_c}{\epsilon_o} \tag{2.17}$$

The strain ϵ_o at which the maximum stress f'_c occurred was obtained from the stress-strain curve of a standard cylinder test. Thus equation 2.16 depended on a knowledge of the parameters f'_c and ϵ_o . An ultimate strain was not specified. The plots of the stress-strain curves predicted by Desayi and Krishnan were very similar to those of Smith and Young (10). The proposed curves plotted slightly lower than Smith and Young's curves for all values of strain less than ϵ_o and slightly higher for strains greater than ϵ_o . The predicted curves approximated very closely the test curves for concrete strengths of 4000 psi and less. The compressive force predicted for high concrete strength was approximately 10 per cent greater than that of the actual compressive force.

2.4 Experimentally Derived Stress Blocks

2.4.1 Introductory Remarks

Some investigators have derived stress-strain relationships for concrete from actual measurements of strains, moments and axial loads applied directly to a concrete beam. Stress blocks which fall into this group are Lee's (7), Hognestad, Hanson and McHenry's (4) and Smith's (11).

2.4.2 Lee 1953

L.H.N. Lee (7) derived a method of obtaining the stress-strain curve for concrete from beam test data by numerical differentiation. He

expressed the stress-strain relationship in the following form

$$f = A\epsilon - B\epsilon^2 \qquad (2.18)$$

$$\text{for } 2\epsilon_o > \epsilon > o$$

The coefficients A and B were functions of f'_c and ϵ_o, and were expressed by the relationships,

$$A = \frac{2f'_c}{\epsilon_o} \qquad (2.19)$$

and

$$B = \frac{f'_c}{\epsilon_o^2} \qquad (2.20)$$

A plot of this curve is shown in Figure 2.2. With the aid of compatibility and equilibrium equations, the neutral axis was given by

$$\frac{c}{d} = \frac{\epsilon}{\epsilon + \epsilon_s} \qquad (2.21)$$

(see Figure 2.2)

Considering the equilibrium of internal forces,

$$C = T = \frac{bc}{\epsilon} \int_o^c F(\epsilon_x)\, d(\epsilon_x) \qquad (2.22)$$

$$= A_s E_s \epsilon_s \quad \text{for } \epsilon_y > \epsilon_s > o$$

$$= A_s f_y \text{ for } \epsilon_s > \epsilon_y$$

substituting equation 2.21 into equation 2.22 and differentiating with respect to ϵ , he obtained the equations

$$f = \frac{A_s}{bd} E_s \left(\epsilon \frac{d\epsilon_s}{d\epsilon} + 2\epsilon_s \frac{d\epsilon_s}{d\epsilon} + \epsilon_s\right) \qquad (2.23)$$

for $\epsilon_y > \epsilon_s > o$

and

$$f = \frac{A_s}{bd} f_y \left(1 + \frac{d\epsilon_s}{d\epsilon}\right) \qquad (2.24)$$

for $\epsilon_s > \epsilon_y$

The strains ϵ_s and ϵ were measured in tests on beams which were loaded in increments and a curve of f against ϵ was plotted using equation 2.23 and 2.24, replacing the differential $\frac{d\epsilon_s}{d\epsilon}$ by the finite difference $\Delta\epsilon_s/\Delta\epsilon$.

Hognestad in Reference (4), pointed out that certain experimental errors tended to amplify the numerical differentiation. For example, at low loads some tensile stress is carried by the concrete. Also, the measured value of ϵ_s is influenced by the position of the strain gauges in relation to the cracks in the tension zone.

2.4.3 Hognestad, Hanson and McHenry, 1955

The complete stress-strain curve for concrete in compression was determined by Hognestad, Hanson and McHenry (4) by testing the specimen shown in Figure 2.3. The specimen had a rectangular cross section 5 x 8-in. in the middle portion. A major thrust P_1 was applied to the specimen and the strain at the lower surface was adjusted to zero by varying a minor thrust P_2 . Thus the lower surface simulated the neutral axis of an actual beam.

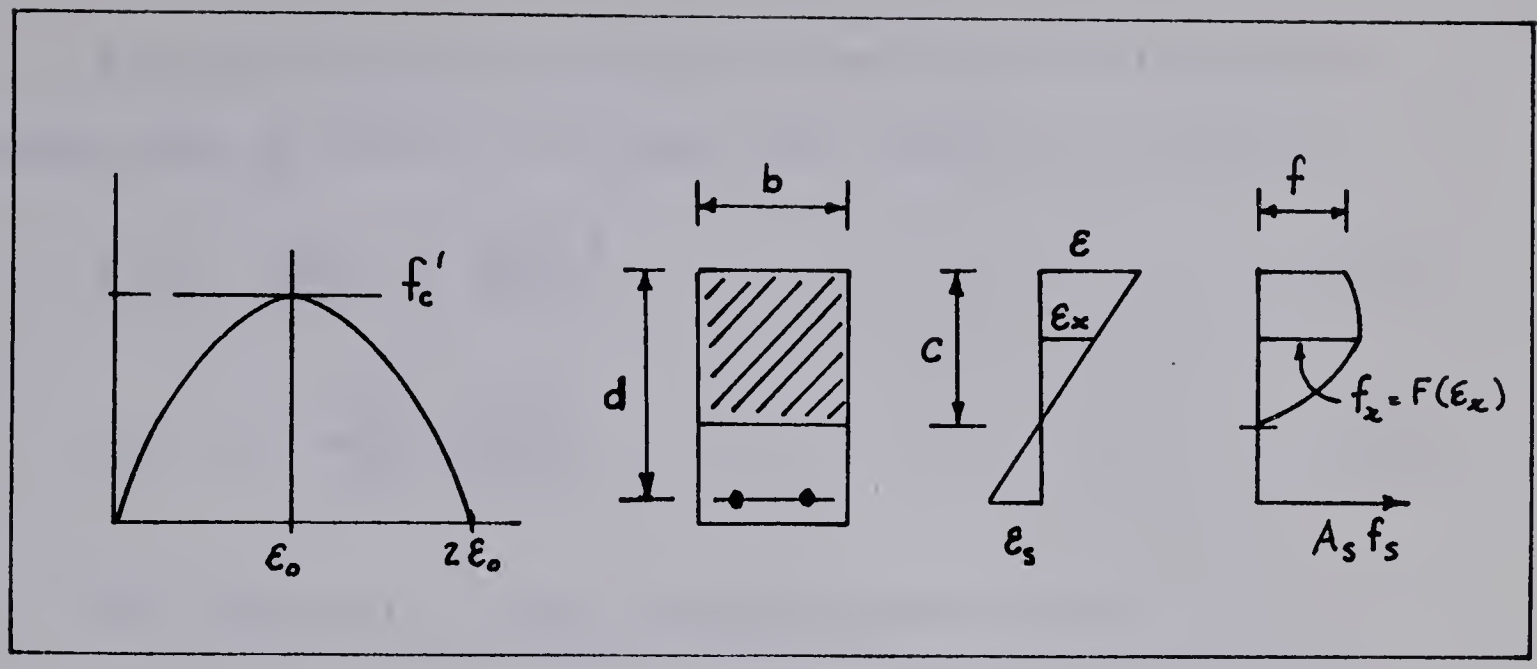

FIGURE 2.2 LEE'S STRESS BLOCK

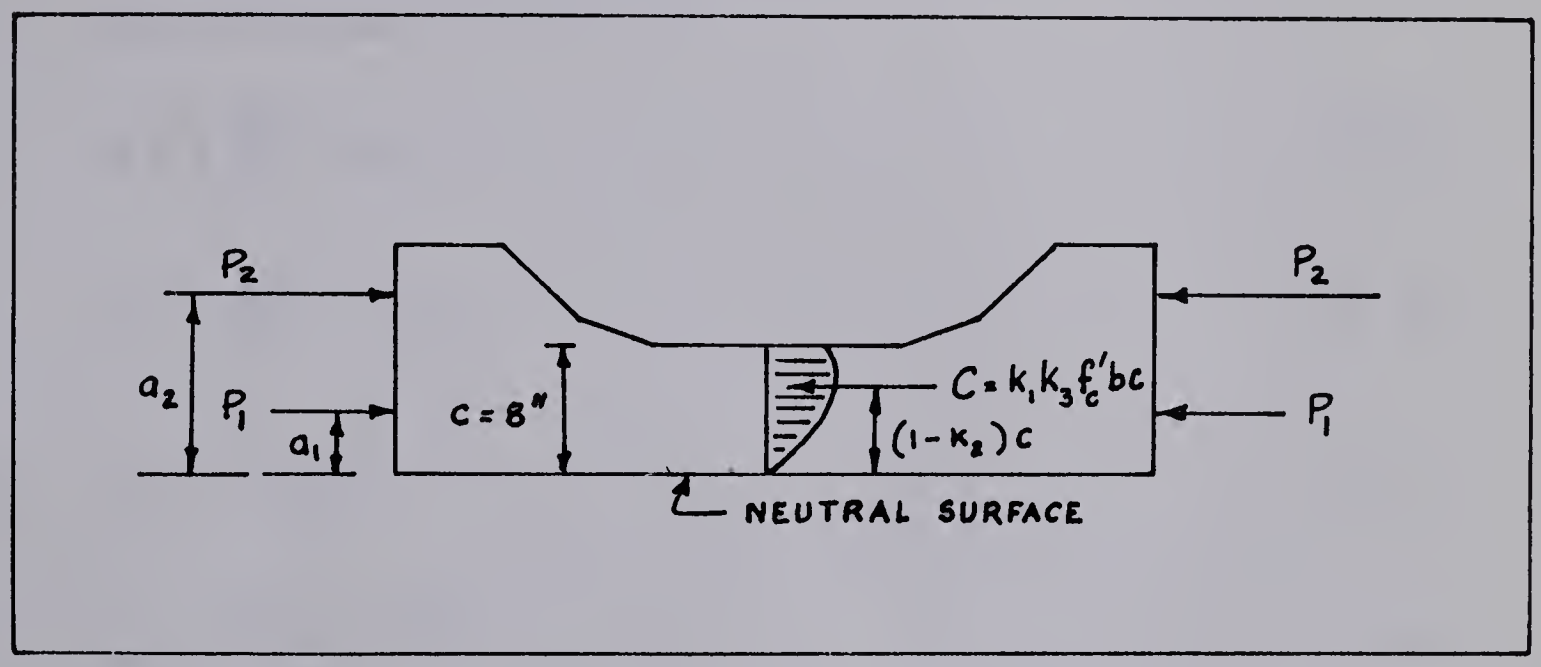

FIGURE 2.3 TEST SPECIMEN [HOGNESTAD, HANSON AND McHENRY]

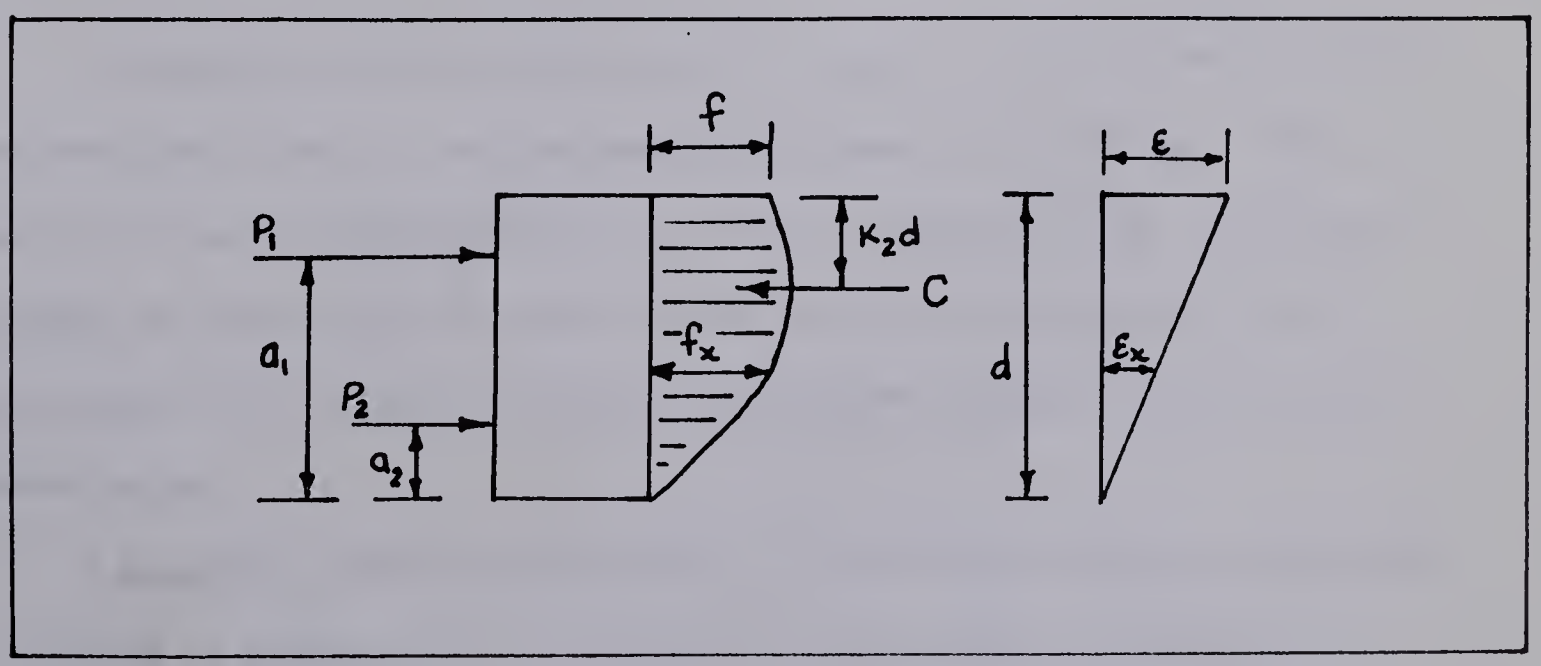

FIGURE 2.4 SMITH'S TEST PRISM

From the equilibrium of forces and moments the following relationships were derived for all values of P_1 from zero to ultimate.

$$k_1 k_3 = \frac{C}{b_c f'_c} = \frac{P_1 + P_2}{b_c f'_c} \tag{2.25}$$

and

$$k_2 = 1 - \frac{P_1 a_1 + P_2 a_2}{(P_1 + P_2)c} \tag{2.26}$$

By assuming (1) A linear strain distribution and

(2) Stress is a function of strain only

they obtained the expressions,

$$f = \epsilon \frac{df_o}{d\epsilon} + f_o \tag{2.27}$$

and

$$f = \epsilon \frac{dm_o}{d\epsilon} + 2m_o \tag{2.28}$$

where

$$f_o = \frac{P_1 + P_2}{bc} \tag{2.29}$$

and

$$m_o = \frac{P_1 a_1 + P_2 a_2}{bc^2} \tag{2.30}$$

Equations 2.27 and 2.28 gave the concrete stress f as a function of the measured strain ϵ and the measured values of f_o and m_o . The differentials were approximated by finite differences $\Delta f_o/\Delta\epsilon$ and $\Delta m_o/\Delta\epsilon$. An average of equations 2.27 and 2.28 was used in deriving the stress-strain curves. The results obtained showed good agreement with standard cylinder tests.

Empirical relationships for k_1, k_2 and k_3 at ultimate condition were derived in terms of f'_c . It was also found that ϵ_u varied with

concrete strengths and was expressed by

$$\epsilon_u = 0.004 - f'_c/6.5 \times 10^6 \qquad (2.31)$$

For practical purposes the authors suggested that a constant value of 0.003 inch per inch was sufficiently conservative for ϵ_u .

2.4.4 Smith 1960

In determining the flexural compressive stress-strain curve for concrete, Smith (11) applied the same principle that was employed in (4).

In Figure 2.4 is shown a prism 6 x 4 x 12-in., which was subjected to forces P_1 and P_2. These forces were adjusted to obtain zero strain on the lower face. Smith showed that the compressive stress f , was independent of the strain ϵ and could be calculated at each stage of loading in terms of P_1 and P_2. The maximum strain ϵ , $k_2 d$ (see Figure 2.4) and the average stress could be obtained by direct measurement. The average stress was expressed as,

$$\text{average stress} = \frac{P_1 + P_2}{bd} \qquad (2.32)$$

$$= 1 - \frac{P_1 a_1 + P_2 a_2}{(P_1 + P_2)\, d} \qquad (2.33)$$

By considering the equilibrium of horizontal forces and differentiating with respect to ϵ , he then derived the expression,

$$f = \frac{1}{bd} \left[\frac{(P_1 + P_2)(\theta) - 2(P_1 a_1 + P_2 a_2)}{\theta - d} \right] \qquad (2.34)$$

where $$\theta = a_1 - \frac{(a_1 - a_2)}{1 + dP_1/dP_2} \qquad (2.35)$$

The value of dP_1/dP_2 was obtained from a plot of P_1 against P_2.

It was also shown that by considering increments of maximum strains, increments of P_1 and P_2 and increments of f , a relationship could be obtained for the ratio of strains between any two stages of loading in terms of P_1 and P_2 only. This relationship was

$$\frac{\epsilon'}{\epsilon} = \frac{bdf_a - (P_1 + P_2)}{bdf_a - (P_1' + P_2')} \qquad (2.36)$$

where f_a is the average stress between the increment of loading from P_1 and P_2 to P_1' and P_2' . Thus, if a value of ϵ were assumed for a given stage of loading, the value of ϵ for all other stages could be obtained using equation 2.36.

In the actual tests performed, the experimentally measured strains were 11 per cent greater than those predicted by equation 2.36. Smith assumed that this discrepancy was due to creep occurring during the tests.

2.4.5 Other Attempts

Numerous attempts to measure concrete stress directly have been made (4). Some of the methods used included photoelastic observations, stress meters and embedding small pressure cells in concrete beams. Experimental difficulties were encountered in these methods and the results obtained were not representative of the actual conditions of stress in the compression zone of the concrete beams. Because of these difficulties, a stress block suitable for analysis could not be obtained.

CHAPTER III

ANALYSIS

3.1 Introduction

3.1.1 Introductory Remarks

Most investigators have been concerned only with the ultimate strength of concrete beams. However, from the point of view of limit design, not only is the ultimate moment, M_u , a significant factor, but also the corresponding rotation, $\emptyset_u$.

Because of the inelastic behavior of concrete, its modulus of elasticity, E , is not constant but changes at each stage of loading. At the onset of cracking, the moment of inertia, I , of the beam section is reduced together with the modulus of elasticity of the concrete. This causes a reduction in EI which in turn reduces the stiffness of the particular beam. Thus, the usual moment-curvature relationship $M = EI\emptyset$, cannot strictly be applied to concrete beams except at the early stages of loading, before cracking occurs.

An extensive study of the strength and behavior of prestressed concrete beams was completed at the University of Illinois (12). In Reference (12), a method of determining the moment-curvature relationship at all stages of loading up to the ultimate condition is presented.

In this thesis, the method of analysis given in (12) was used except that a modification was introduced regarding the cracking stage of behavior. The method of analysis and modification are discussed in

detail in Appendix A. The actual computations were done with the aid of a computer.

3.1.2 Variables

The variables studied were the effect of different stress blocks and also the effect of varying the limiting strain on the moment-curvature relationship. On the load-deflection curves, only the effects of stress blocks were studied. The results of the analysis are shown in the form of plots. The results obtained from tests performed on prestressed beams at the University of Alberta, Edmonton, (1) (9) are shown on the same plot for the purpose of comparison. For convenience, the details of these beams are shown in Table 3.1. In Table 3.1(a) are presented the two-point loaded beams. Table 3.1(b) gives the long one-point loaded beams. Table 3.1(c) shows the short one-point loaded beams.

3.1.3 Concrete Stress Blocks

The stress blocks used in the analysis were those given by:

1. Hognestad
2. Smith and Young
3. Desayi and Krishnan
4. PCA
5. Jensen
6. Jensen modified by Hognestad

Stress blocks 1 to 5 have been described in Chapter II. Stress block 6 was used by Hognestad in Reference (3). It was essentially Jensen's stress block with the maximum stress f'_c changed to 0.85 f'_c. Thus, stress

TABLE 3.1 DETAILS OF BEAMS

(a) Two-Point Loaded Beams

Beam No.	f'_c psi	A_s in.^{2}	p/f'_c in^2/lb	P_{eff} ksi
1	6600	0.1156	2.94×10^{-7}	142
2	6400	0.2312	5.98×10^{-7}	133
3	7800	0.3468	7.36×10^{-7}	120
4	4800	0.1156	4.07×10^{-7}	139
5	5200	0.2312	7.37×10^{-7}	129
6	5400	0.3468	10.70×10^{-7}	123
11	4000	0.1156	4.78×10^{-7}	139
12	3600	0.2312	11.06×10^{-7}	139
13	3400	0.3468	17.10×10^{-7}	137

(b) One-Point Loaded 11-ft. Beams

Beam No.	f'_c psi	A_s in.^{2}	p/f'_c in^2/lb	P_{eff} ksi
7	7500	0.2312	5.09×10^{-7}	133
8	5400	0.3468	7.14×10^{-7}	133
1A	4300	0.2312	8.90×10^{-7}	138
2A	3400	0.3468	16.78×10^{-7}	137
3A	3500	0.4624	21.70×10^{-7}	130
4A	6000	0.2312	6.44×10^{-7}	146
5A	6800	0.3468	8.47×10^{-7}	142
6A	6900	0.4624	11.20×10^{-7}	144

(c) One-Point Loaded 5 ft. 6 in. Beams

Beam No.	f'_c psi	A_s in.^{2}	p/f'_c in^2/lb	P_{eff} ksi
9	6200	0.2312	6.20×10^{-7}	134
10	4300	0.2312	8.98×10^{-7}	133
1B	3500	0.2312	10.85×10^{-7}	141
2B	4200	0.3468	13.62×10^{-7}	136
3B	3500	0.4624	21.70×10^{-7}	137
4B	6300	0.2312	6.10×10^{-7}	143
5B	6500	0.3468	8.95×10^{-7}	143
6B	5900	0.4624	12.95×10^{-7}	144

block 6 was completely described by the parameters,

$$f''_c = 0.85\ f'_c \tag{3.1}$$

the plasticity ratio, $\beta = \dfrac{1}{1 + \left(\dfrac{0.85f'_c}{4000}\right)^2}$ (3.2)

and the modulus of elasticity, $E = \dfrac{30{,}000{,}000}{5 + \dfrac{10{,}000}{0.85f'_c}}$ psi (3.3)

This stress block was not described in Chapter II because nothing new was being presented.

One modification was made in all stress blocks. The ultimate strain ϵ_u , was assumed as 0.004 inch per inch except for high strength concrete which failed at an ultimate strain less than 0.004 inch per inch. For high strength concrete, using the stress blocks of Smith and Young, Desayi and Krishnan and PCA, the ultimate concrete strain was taken as that strain at which the stress dropped to zero.

For Smith and Young's stress block as well as Desayi and Krishnan's, ϵ_o was assumed as 0.002 inch per inch since no strain readings were taken in the tests of standard cylinders. For analytical purposes, an ϵ_o of 0.002 inch per inch was sufficiently accurate.

3.2 Moment-Curvature Relationship

3.2.1 Introductory Remarks

The results of the moment-curvature (M-Ø) analysis are shown in Figures 3.1 to 3.31 inclusive. Figures 3.1 to 3.9 show the M-Ø relationship for the two-point loaded beams. Figures 3.10 to 3.17 show the same relationship for the one-point loaded beams with eleven foot span

lengths. The M-Ø relationship for the five and one-half foot, one-point loaded beams are shown in Figures 3.18 to 3.25. The effect of varying ϵ_u on the M-Ø curves using Jensen's stress block is illustrated in Figures 3.26 to 3.31.

The values of the ratio of the predicted ultimate moments ($M_u$calc) to the ultimate moments ($M_u$test) of the test beams are given in Tables 3.2(a) (b) and (c). The ratios of the predicted ultimate curvatures ($\emptyset_u$calc) to the ultimate curvatures ($\emptyset_u$test) of the test beams are presented in Tables 3.3(a) (b) and (c).

The stress block proposed by Desayi and Krishnan gave results which were very close to those obtained using Smith and Young's stress block. Thus on all the M-Ø diagrams, the curves obtained using the Desayi and Krishnan stress block have been omitted for the sake of clarity.

3.2.2 Effect of Stress Blocks

The effect of varying the stress blocks in this analysis was not too significant. An examination of Figures 3.1 to 3.25 shows that the M-Ø curves predicted by the five different stress blocks fell within a narrow band at all stages of loading. This phenomenon was more pronounced for beams with low p/f_c' ratios such as beams 1, 4 and 11 shown in Figures 3.1, 3.4 and 3.7.

The use of Jensen's stress block in the analysis yielded M-Ø curves which best approximated the curves obtained from results of tests on beams. The ultimate moments and corresponding $\emptyset_u$ predicted by Jensen's stress block were, in the majority of cases, higher than those

TABLE 3.2 RATIO OF M_u PREDICTED TO M_u FROM BEAM TEST

(a) Two-Point Loaded Beams

Beam No.	Hognestad	Jensen	Jensen Modified	Smith and Young	PCA
1	0.90	0.91	0.91	0.91	0.90
2	0.95	0.98	0.96	0.97	0.95
3	0.92	0.96	0.93	0.95	0.90
4	0.92	0.94	0.93	0.93	0.92
5	0.93	0.97	0.95	0.96	0.91
6	0.88	0.95	0.91	0.93	0.84
11	1.03	1.05	1.07	1.04	1.03
12	0.97	1.05	1.00	1.02	0.98
13	0.89	1.00	0.93	0.95	0.92

(b) One-Point Loaded Long Beams

Beam No.	Hognestad	Jensen	Jensen Modified	Smith and Young	PCA
7	0.93	0.95	0.94	0.95	0.93
8	0.91	0.95	0.93	0.94	0.88
1A	0.86	0.91	0.89	0.89	0.85
2A	0.82	0.92	0.86	0.88	0.84
3A	0.87	0.99	0.92	0.94	0.91
4A	0.88	0.91	0.89	0.90	0.88
5A	0.85	0.89	0.86	0.88	0.84
6A	0.81	0.87	0.84	0.86	0.80

(c) One-Point Loaded Short Beams

Beam No.	Hognestad	Jensen	Jensen Modified	Smith and Young	PCA
9	0.89	0.92	0.90	0.91	0.89
10	0.91	0.96	0.95	0.95	0.90
1B	0.88	0.94	0.91	0.92	0.89
2B	0.84	0.92	0.91	0.89	0.84
3B	0.77	0.88	0.82	0.84	0.81
4B	0.89	0.92	0.90	0.91	0.89
5B	0.88	0.93	0.90	0.91	0.87
6B	0.89	0.97	0.92	0.94	0.88

TABLE 3.3 RATIO OF $\emptyset_u$ CALCULATED TO $\emptyset_u$ FROM TEST

(a) Two-Point Loaded Beams

Beam No.	Hognestad	Jensen	Jensen Modified	Smith and Young	PCA
1	1.25	1.52	1.36	1.50	1.21
2	0.74	0.88	0.80	0.87	0.73
3	0.68	0.78	0.72	0.79	0.65
4	1.25	1.53	1.37	1.46	1.21
5	0.73	0.86	0.78	0.83	0.70
6	0.81	0.91	0.85	0.89	0.77
11	0.75	0.91	1.06	0.85	0.77
12	0.91	1.04	0.96	0.99	0.93
13	0.77	0.86	0.81	0.82	0.80

(b) One-Point Loaded Long Beams

Beam No.	Hognestad	Jensen	Jensen Modified	Smith and Young	PCA
7	0.40	0.47	0.43	0.47	0.37
8	0.27	0.31	0.28	0.30	0.25
1A	0.44	0.52	0.49	0.49	0.45
2A	0.60	0.67	0.63	0.64	0.48
3A	0.87	0.95	0.90	0.92	0.89
4A	1.08	1.29	1.17	1.26	0.91
5A	0.74	0.85	0.79	0.85	0.73
6A	0.57	0.64	0.78	0.64	0.56

(c) One-Point Loaded Short Beams

Beam No.	Hognestad	Jensen	Jensen Modified	Smith and Young	PCA
9	0.48	0.57	0.52	0.56	0.48
10	0.56	0.64	0.62	0.62	0.57
1B	0.75	0.86	0.79	0.81	0.77
2B	0.52	0.58	0.56	0.56	0.52
3B	0.62	0.68	0.64	0.65	0.37
4B	0.58	0.69	0.62	0.67	0.57
5B	0.64	0.73	0.67	0.72	0.62
6B	1.29	1.45	1.35	1.46	1.28

predicted by the other stress blocks and slightly lower than those of the actual tests.

For most cases, the predicted M-Ø curve using Hognestad's stress block was always positioned slightly below the curves predicted by Jensen's stress block.

Using the Jensen's modified stress block, the series of M-Ø curves obtained plotted in an intermediate position between the Hognestad's curves and the Jensen's curves.

The predicted M-Ø curves using Smith and Young's stress block showed good correlation, at all stages of loading, with those of the other stress blocks, for concrete strengths of 4000 psi and lower. This effect can be seen in Figures 3.7 to 3.9, 3.13, 3.14, 3.20 and 3.22. For concrete strengths between 4000 psi and 5500 psi, the predicted curves using Smith and Young's stress block exhibited higher moments than those predicted by other stress blocks at the stage just beyond cracking, then dropped just below the Jensen's curves as the ultimate condition approached. This is illustrated in Figures 3.4 to 3.6, 3.12 and 3.21. For concrete strengths greater than 6000 psi, the predicted curves were well above the others at all stages of loading from the cracking load to some load just before the ultimate condition,when the predicted curves dropped slightly below the Jensen's curves. This condition is illustrated in Figures 3.1 to 3.3, 3.10, 3.15 to 3.17 and 3.22 to 3.25.

The PC A curves exhibited a maximum moment at some strain value less than 0.004 inch per inch and almost always had a downward slope at the limiting strain. For high concrete strengths, the PCA curves plotted well within the range of the Hognestad's and Jensen's curves at the inter-

mediate stages, then dropped off below the other curves at the ultimate condition. For low concrete strengths, the predicted M-Ø curves followed those of Smith and Young in the intermediate stages and again dropped off below the other curves as the ultimate condition approached. This phenomenon can be seen in Figures 3.7, 3.13 and 3.20.

It was noted on all analytical curves that there was a smooth transition from the point of cracking to the ultimate condition, on the M-Ø diagrams. On the other hand, the M-Ø curves obtained from tests showed a flattened region just beyond cracking, then almost coincided with the predicted curves as the ultimate condition approached. This characteristic was especially noticeable on the beams with low p/f_c' values, loaded at two points (See Figures 3.2, 3.7 and 3.8).

3.2.3 Effects of Type of Loading

The ratios of $M_u$calc/$M_u$test for all beams are shown in Table 3.2(a), (b) and (c). In all cases, the ultimate moment could be predicted within reasonable limits using any one of the five stress-blocks shown. The curvature ϕ_u , at ultimate condition could be predicted accurately in the case of the two-point loaded beams. The ratios $\phi_u$calc/$\phi_u$test, in Table 3.3(a) ranged from 0.78 to 1.53 using Jensen's stress block and 0.68 to 1.25 using Hognestad's stress block. In the case of the one-point loaded beams, using Jensen's stress block $\phi_u$calc/$\phi_u$test ranged from 0.31 to 1.29 for the eleven foot beams and 0.57 to 1.45 for the five and one-half foot beams. Using Hognestad's stress block the ratios $\phi_u$calc/$\phi_u$test ranged from 0.27 to 1.08 for the long beams and 0.48 to 1.29 for the short beams. All other stress blocks gave results which fell in some

intermediate position between those of Jensen's and Hognestad's stress blocks.

3.2.4 Effects of Varying the Limiting Strain

Using Jensen's stress block, limiting strains of 0.003, 0.004 and 0.006 inch per inch were used in the analysis of six representative beams. The M-Ø curves obtained are shown in Figures 3.26 to 3.31.

There was little difference in the predicted M_u and $Ø_u$ using an ϵ_u of either 0.003 or 0.006 inch per inch in the analysis. For beams with high p/f'_c values, the most significant effect was the slope of the initial part of the M-Ø diagram. This effect is shown in Figures 3.27, 3.28 and 3.31. The curves obtained using a limiting strain of 0.006 inch per inch were initially steeper than the curves obtained using limiting strains of 0.004 and 0.003 inch per inch. As the ultimate moment was approached, the difference between the three curves decreased and they merged almost into one curve. In the case of beams with low p/f'_c values, the effect of varying the limiting strain was essentially the same as for beams with high p/f'_c values. In the initial stages, however, the effect of a limiting strain of 0.006 inch per inch on the M-Ø curve was not as pronounced as was the case for beams with high p/f'_c values.

3.3 Load Deflection Relationship

3.3.1 Introductory Remarks

A knowledge of the moment and corresponding curvature for all points on the beam and at all stages of loading was required before the load-midspan deflection relationship (P-△) could be obtained. Since the moments and corresponding curvatures were already computed for all values

of strains up to 0.004 inch per inch in increments of 0.0002 inch per inch, the load corresponding to each moment increment was obtained from statics. The deflection of all stages was obtained by superimposing on the conjugate beam, the curvatures corresponding to the moments along the beam and taking moments of the area under the curvature diagram about midspan of the beam. This procedure was repeated for each increment of loading up to the ultimate load P_u . The computed values of load and corresponding midspan deflection together with those obtained from tests are shown in Figures 3.32 to 3.42 inclusive. In order to keep the P-Δ diagrams clear and legible, the only curves shown are those obtained using Hognestad's, Jensen's and Smith and Young's stress blocks. The other curves using PCA and Jensen's modified stress blocks plotted in the same relative positions as they did on the M-ϕ diagrams. Table 3.4 shows the ratios of the calculated midspan deflection (Δ_{calc}) to the actual midspan deflection (Δ_{test}) at ultimate condition, for all beams using Hognestad's, Jensen's and Smith and Young's stress blocks.

3.3.2 Two-Point Loaded Beams

The P-Δ curves for the two-point loaded beams are a direct reflection of the M-ϕ curves. The ratios $\Delta_{calc}/\Delta_{test}$ shown in Table 3.4(a) are slightly smaller than the ratios $\phi_u calc/\phi_u test$ shown in Table 3.3(a). The only exception was beam 11 which had a value of $\Delta_{calc}/\Delta_{test}$ almost twice the value of $\phi_u calc/\phi_u test$.

3.3.3 One-Point Loaded Beams

For the long beams, loaded at the centre, the ratios of $\Delta_{calc}/\Delta_{test}$ varied from a value of 0.23 to 0.62 using the Jensen's stress block and

TABLE 3.4

RATIO OF CALCULATED MAXIMUM MIDSPAN DEFLECTION TO MAXIMUM MIDSPAN DEFLECTION FROM TEST

(a) Two-Point Loaded Beams

Beam No.	Jensen	Hognestad	Smith and Young
1	1.26	1.05	1.24
2	0.79	0.67	0.76
3	0.74	0.64	0.73
4	1.10	0.91	1.04
5	0.73	0.63	0.70
6	0.76	0.67	0.73
11	1.69	1.41	1.59
12	1.29	1.13	1.22
13	0.82	0.74	0.78

(b) One-Point Loaded Long Beams

Beam No.	Jensen	Hognestad	Smith and Young
7	0.30	0.28	0.24
8	0.23	0.22	0.20
1A	0.59	0.55	0.52
2A	0.27	0.25	0.25
3A	0.32	0.29	0.28
4A	0.62	0.61	0.53
5A	0.29	0.27	0.24
6A	0.42	0.38	0.32

(c) One-Point Loaded Short Beams

Beam No.	Jensen	Hognestad	Smith and Young
9	0.06	0.06	0.05
10	0.06	0.06	0.06
1B	0.19	0.18	0.18
2B	0.19	0.17	0.16
3B	0.11	0.10	0.09
4B	0.22	0.21	0.18
5B	0.16	0.15	0.13
6B	0.26	0.24	0.20

0.20 to 0.53 using Smith and Young's stress block. The values obtained using Hognestad's stress block were intermediate between those obtained using Jensen's and Smith and Young's stress blocks. These ratios ranged from 0.22 to 0.61. On the short beams, the ratios of $\Delta_{calc}/\Delta_{test}$ varied from 0.06 to 0.26 using Jensen's stress block and 0.05 to 0.20 using Smith and Young's stress block. The values obtained using Hognestad's stress block were again intermediate between the other two sets and ranged from 0.06 to 0.24.

The ratio of $\Delta_{calc}/\Delta_{test}$ did not show any definite relationship to the ratio of $\phi_u calc/\phi_u test$ on the one-point loaded beams, except a general tendency to be smaller than the corresponding $\phi_u calc/\phi_u test$.

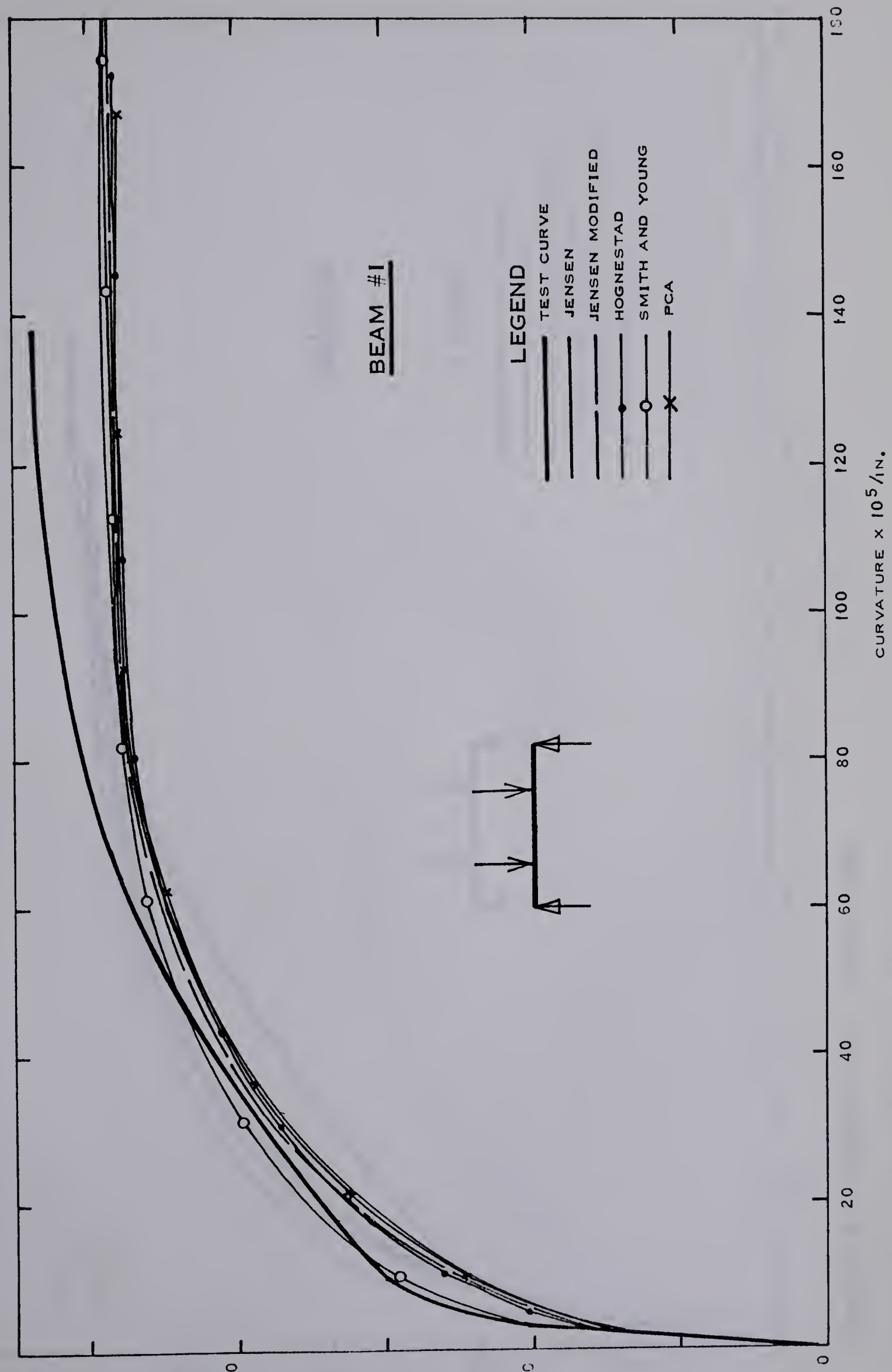

FIGURE 3.1 MOMENT VS. CURVATURE

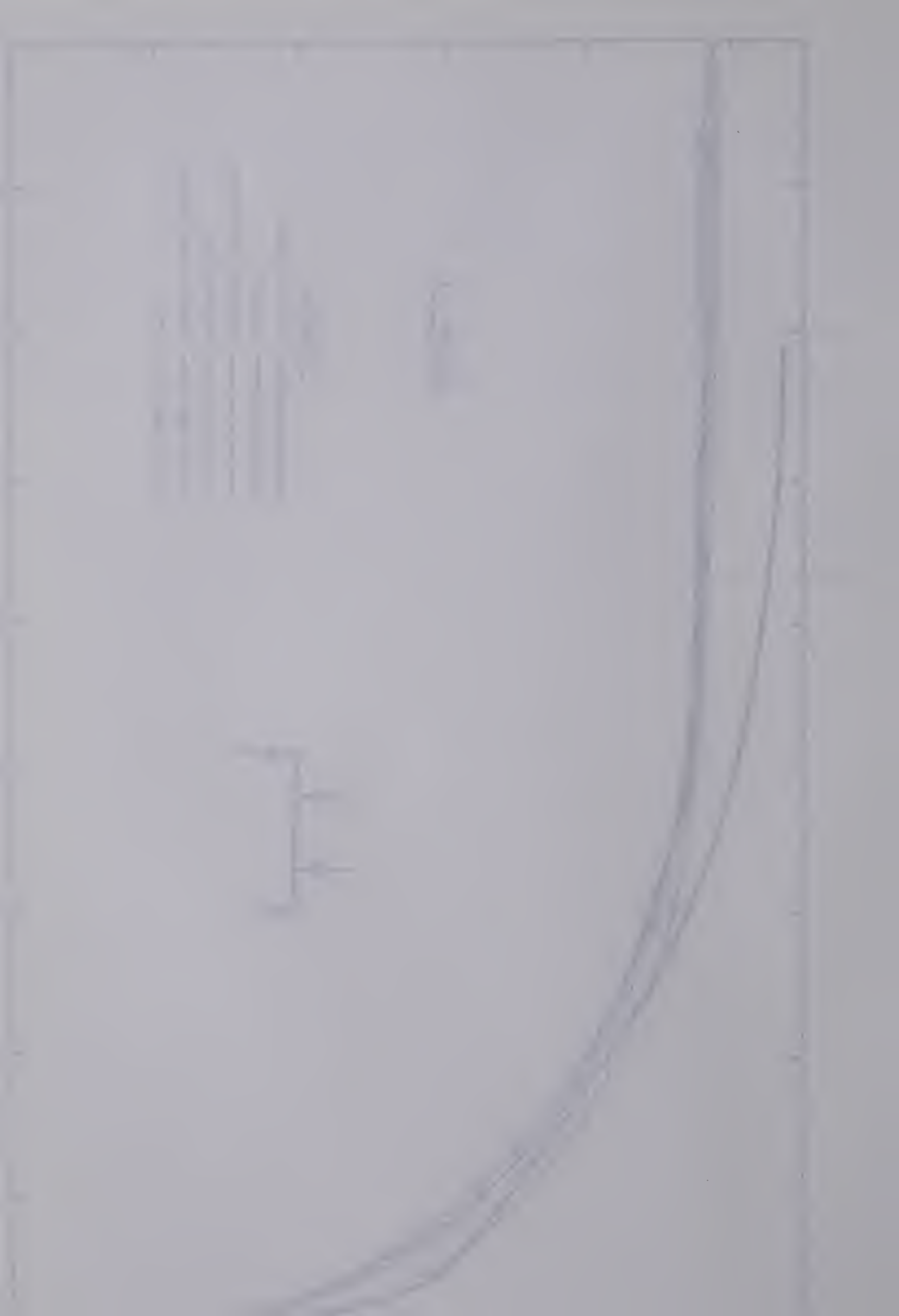

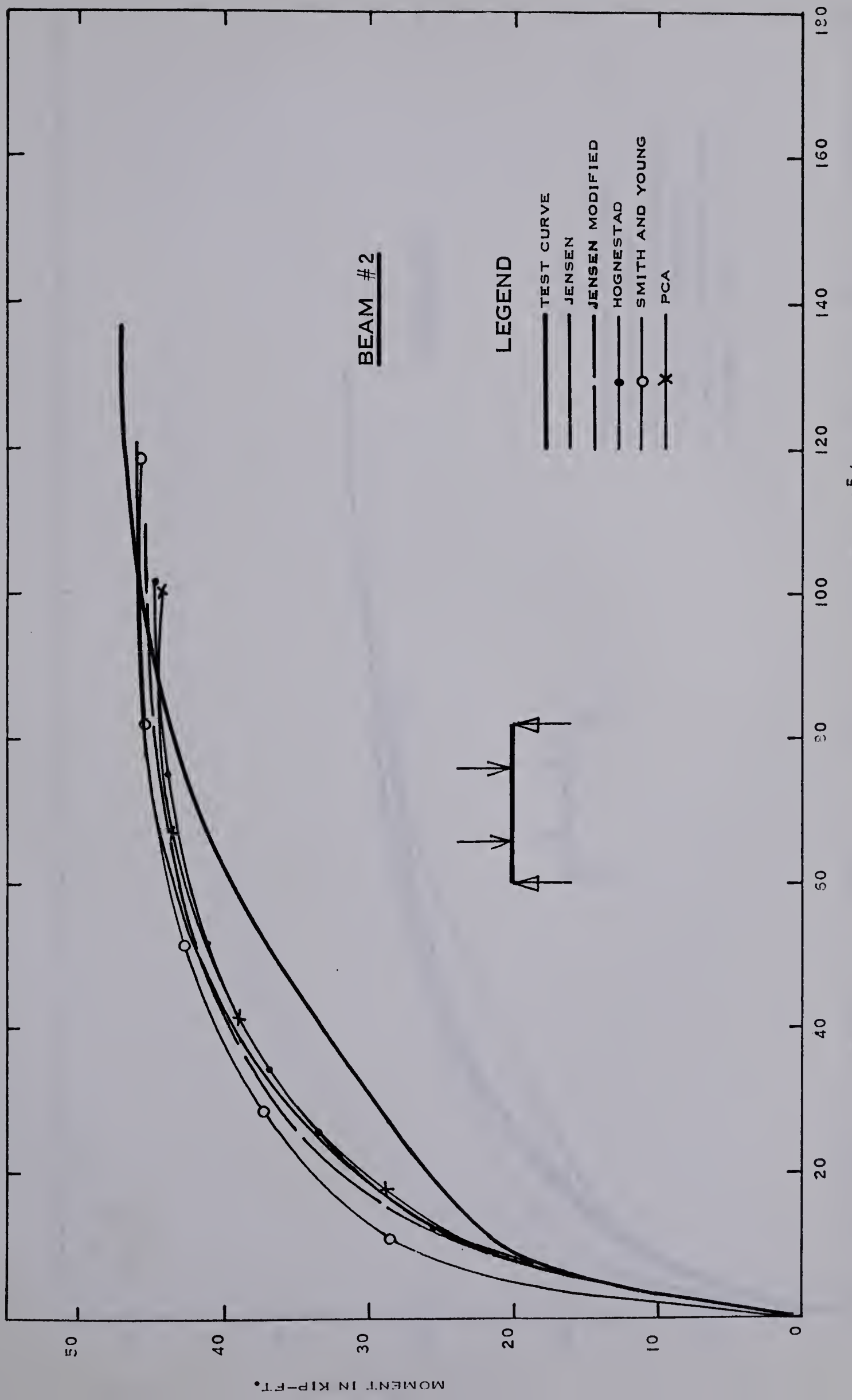

FIGURE 3.2 MOMENT VS. CURVATURE

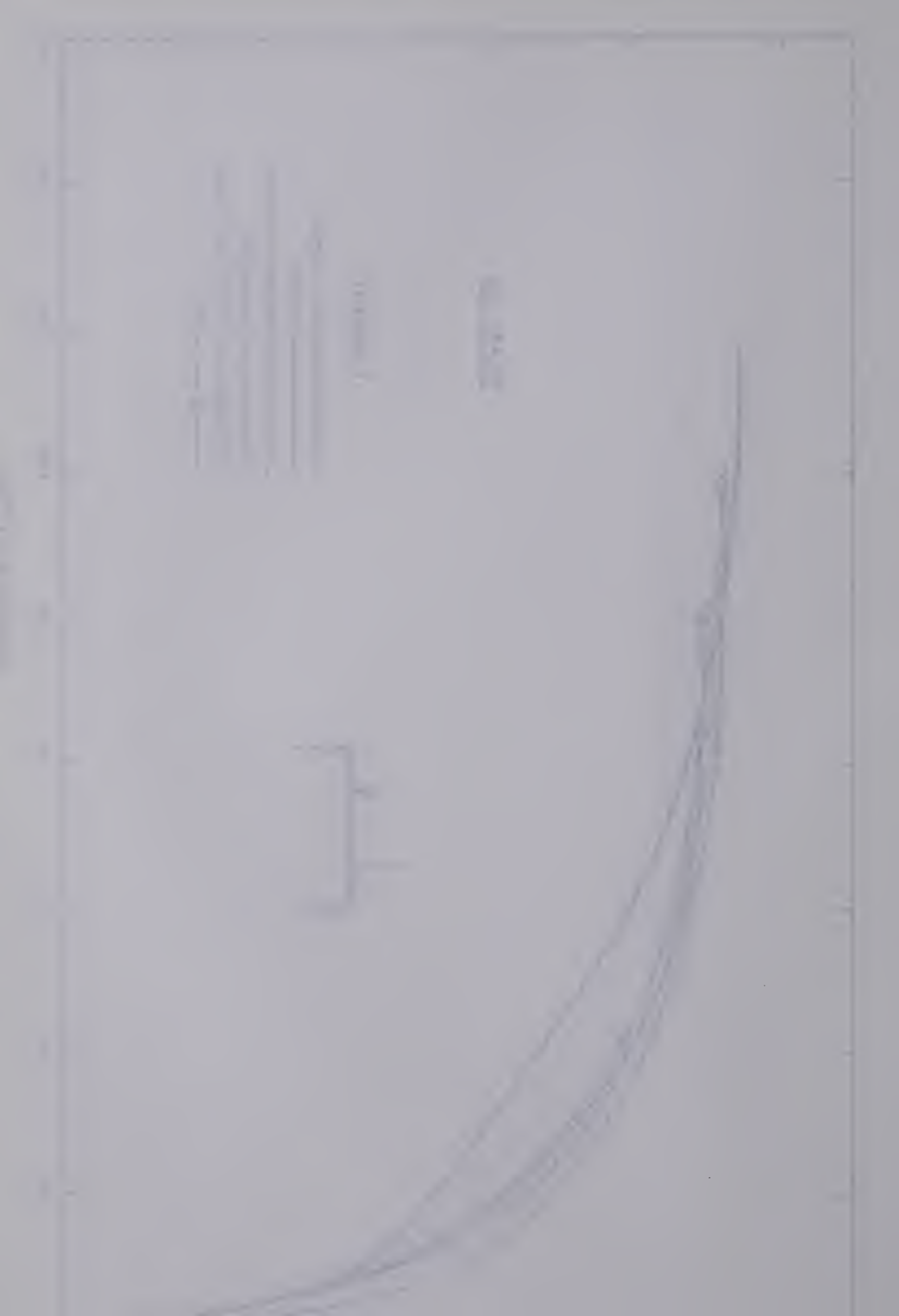

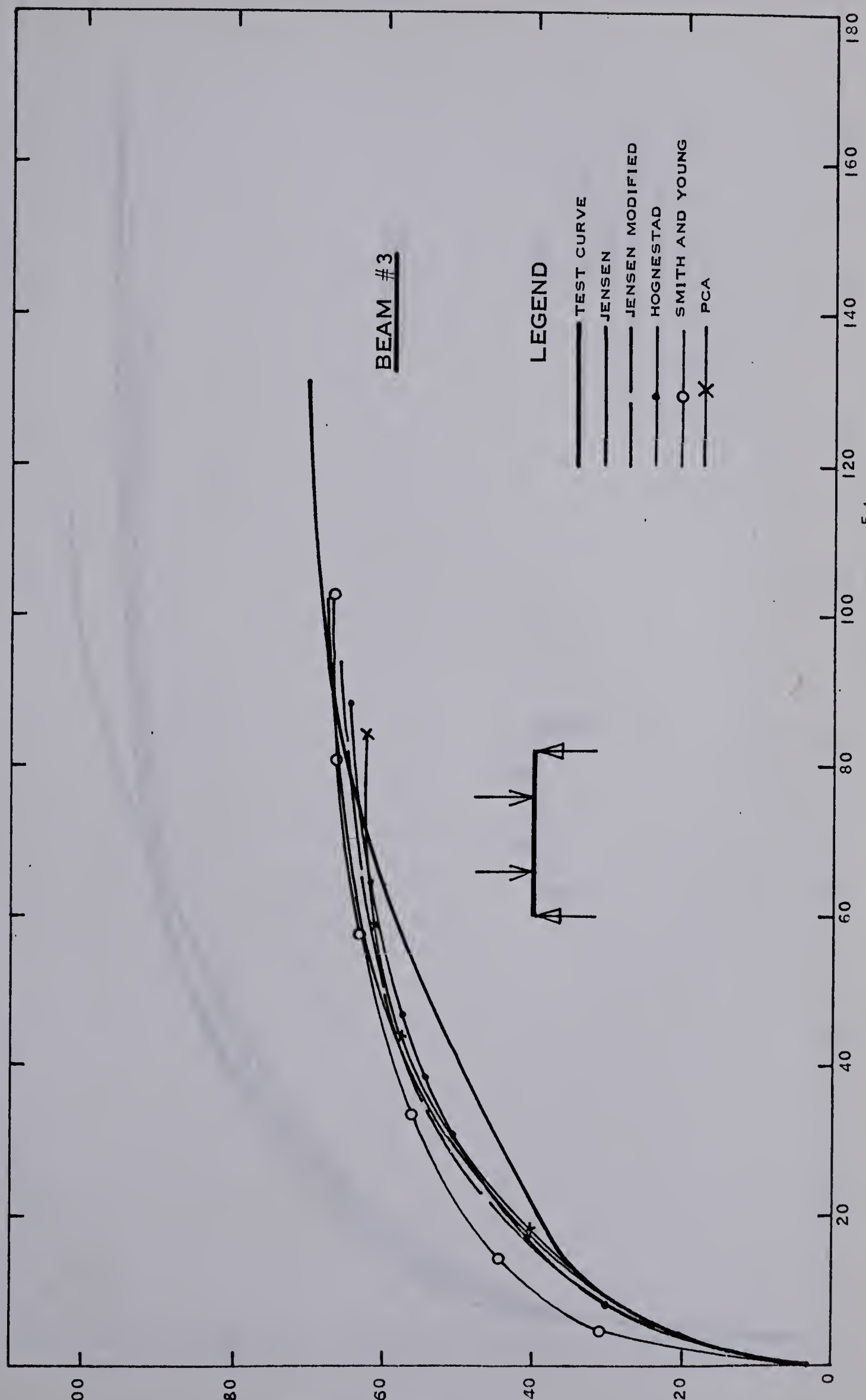

FIGURE 3.3 MOMENT VS. CURVATURE

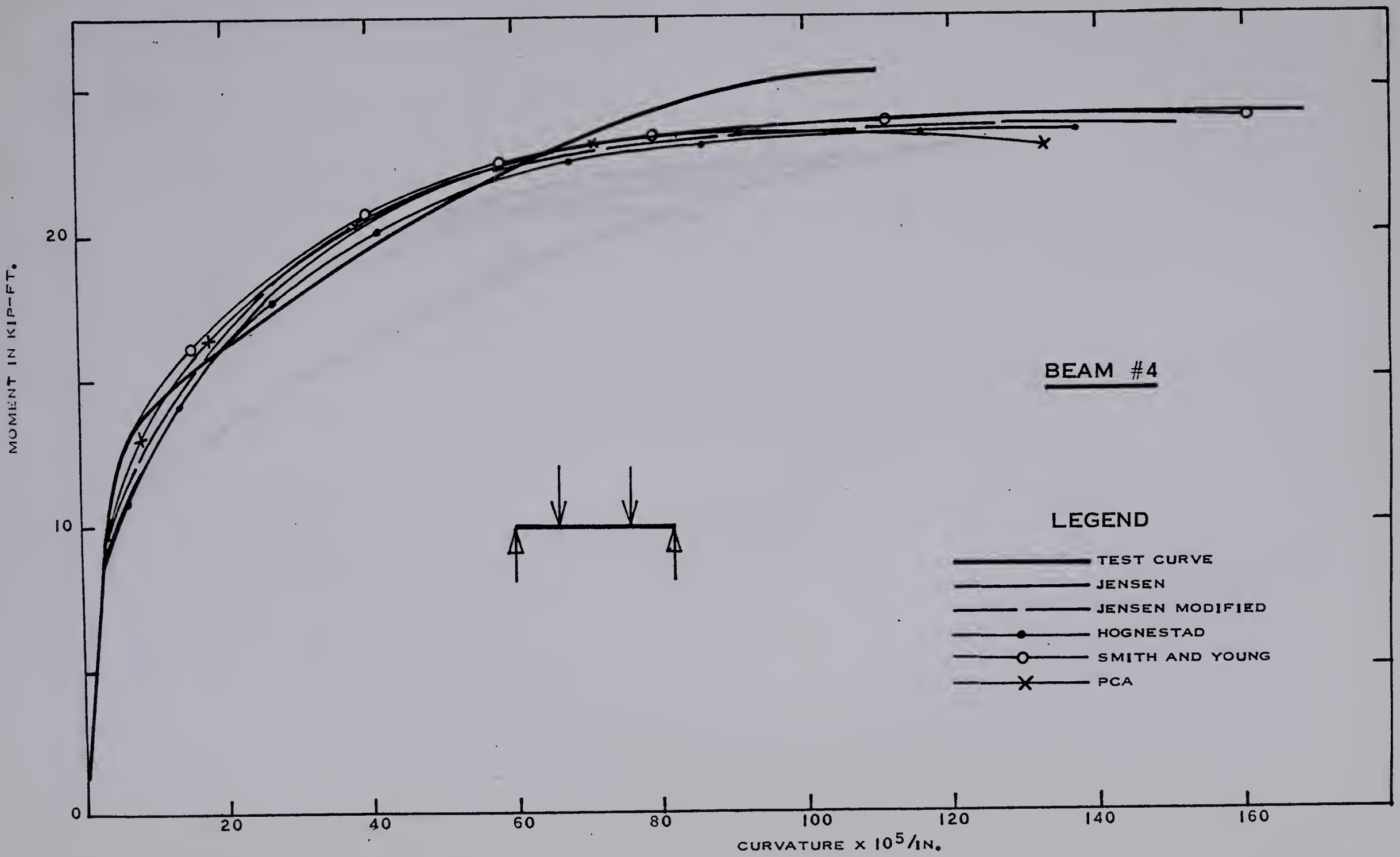

FIGURE 3.4 MOMENT VS. CURVATURE

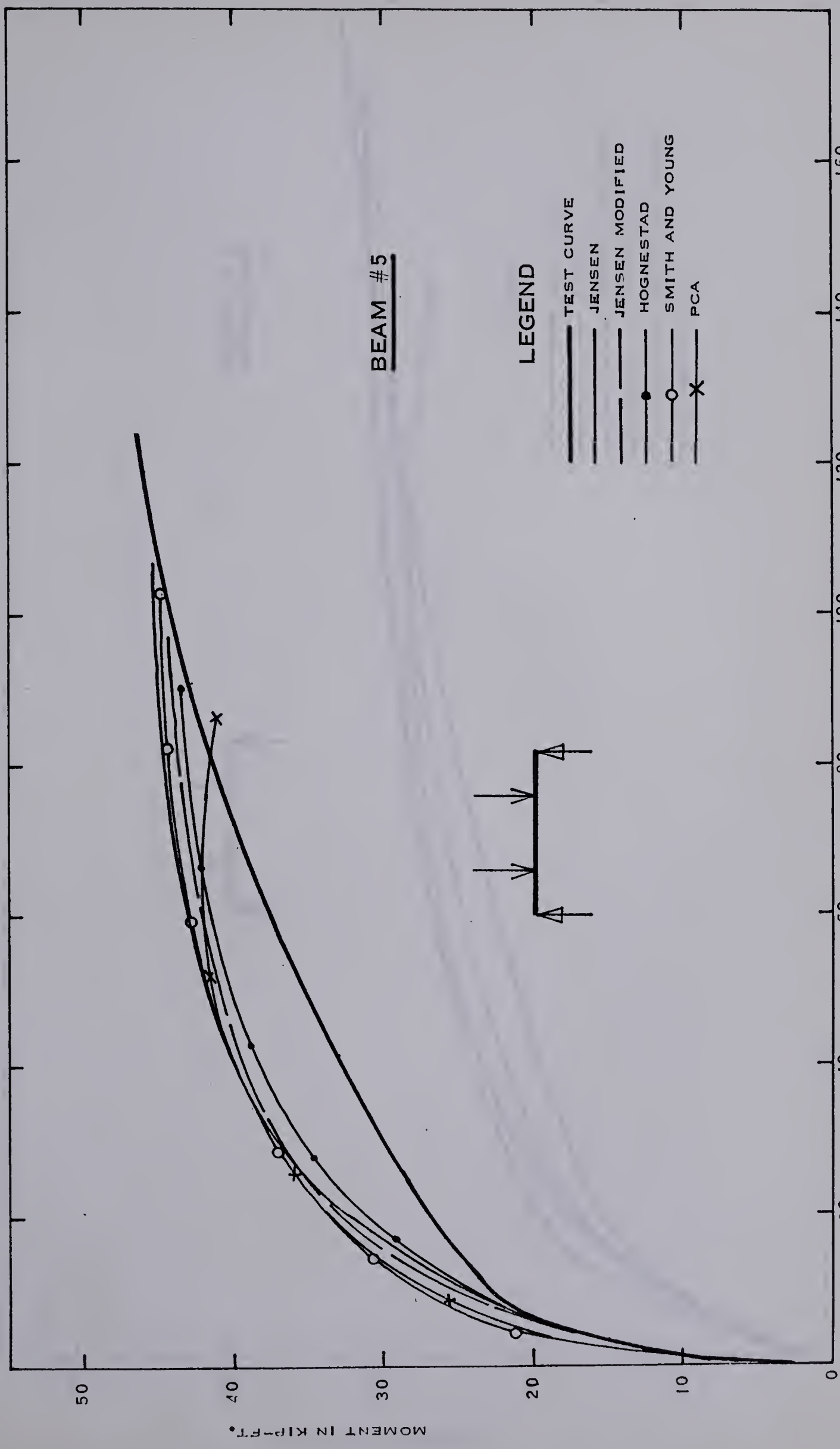

FIGURE 3.5 MOMENT VS. CURVATURE

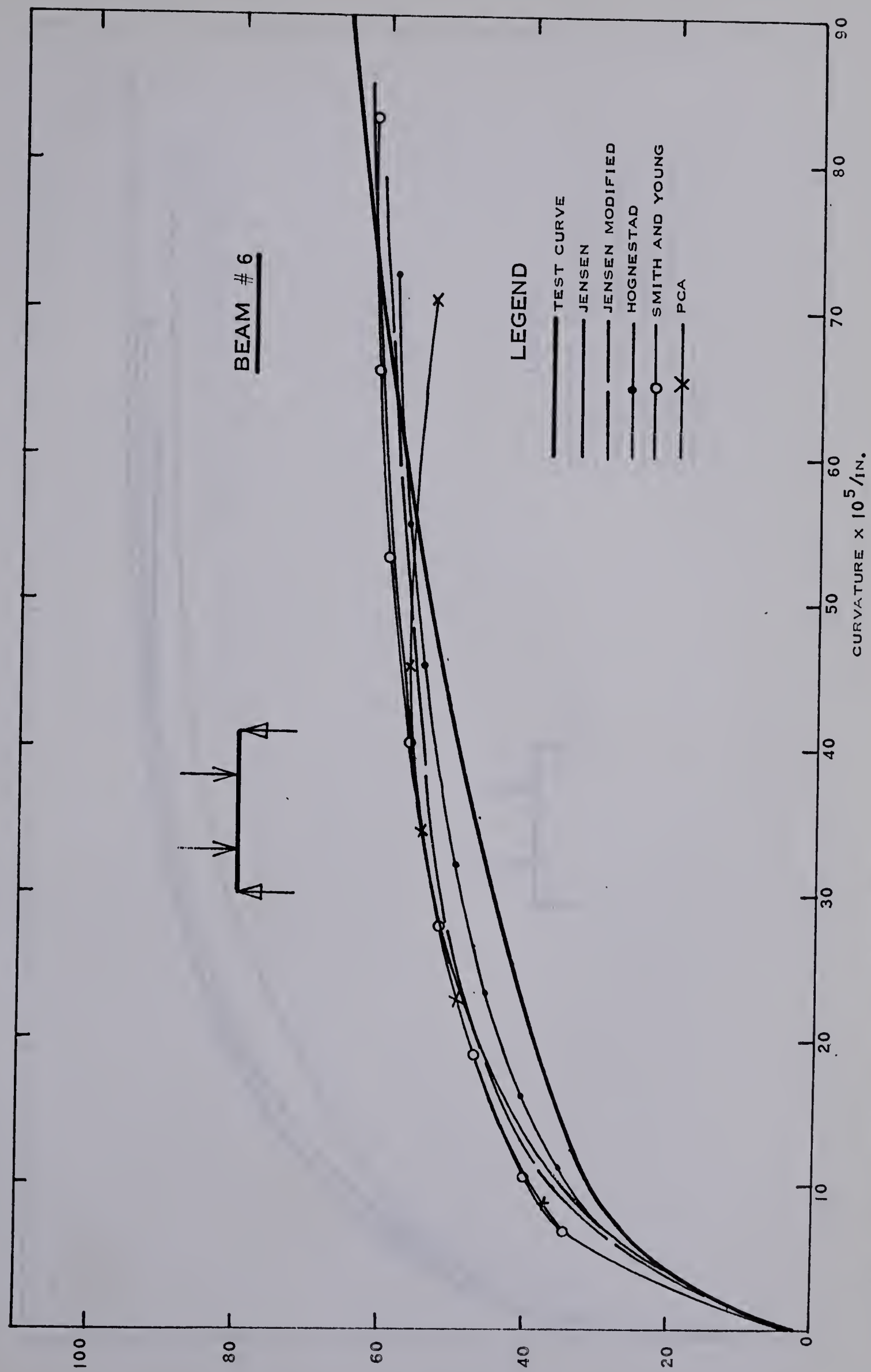

FIGURE 3.6 MOMENT VS. CURVATURE

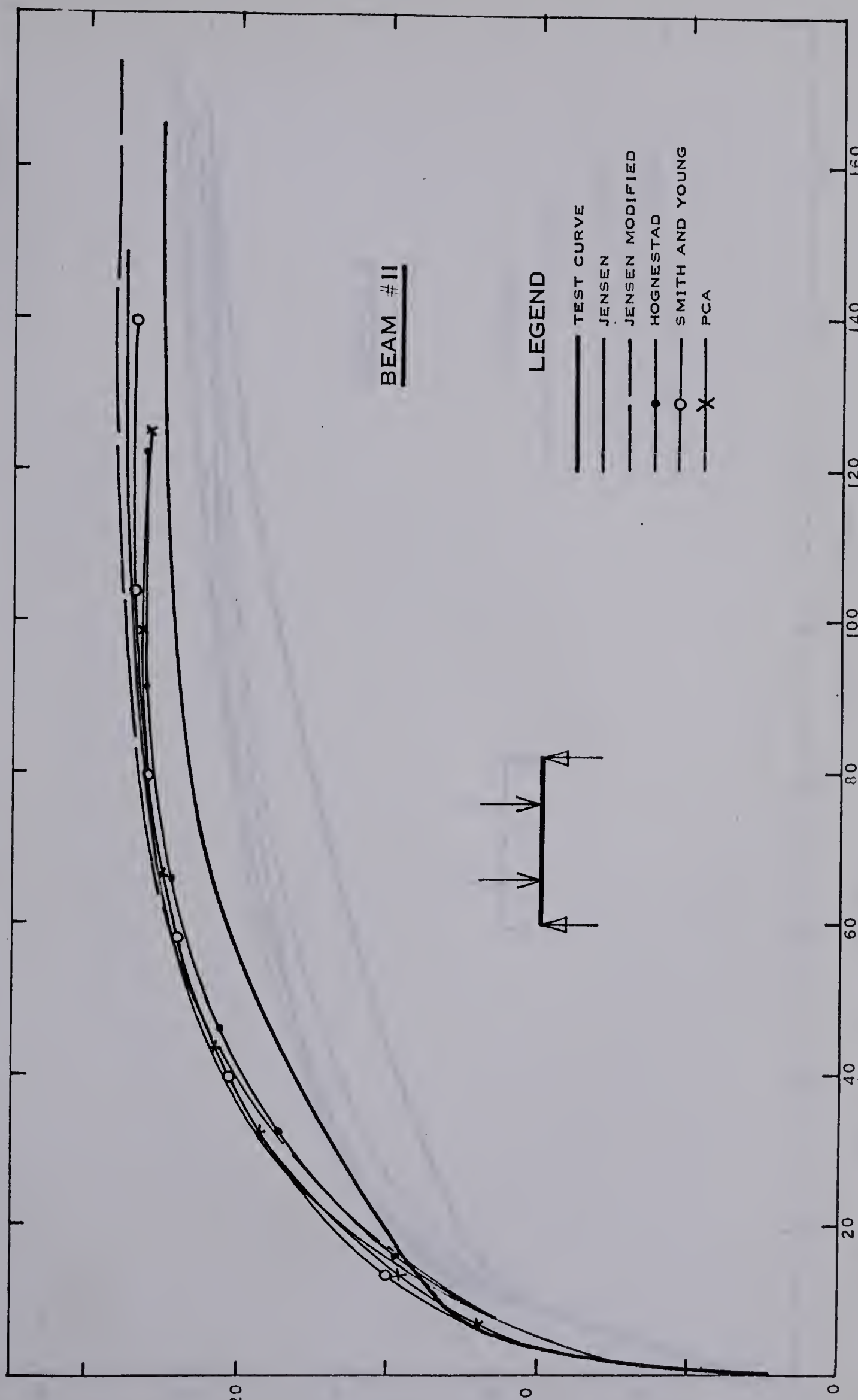

FIGURE 3.7 MOMENT VS. CURVATURE

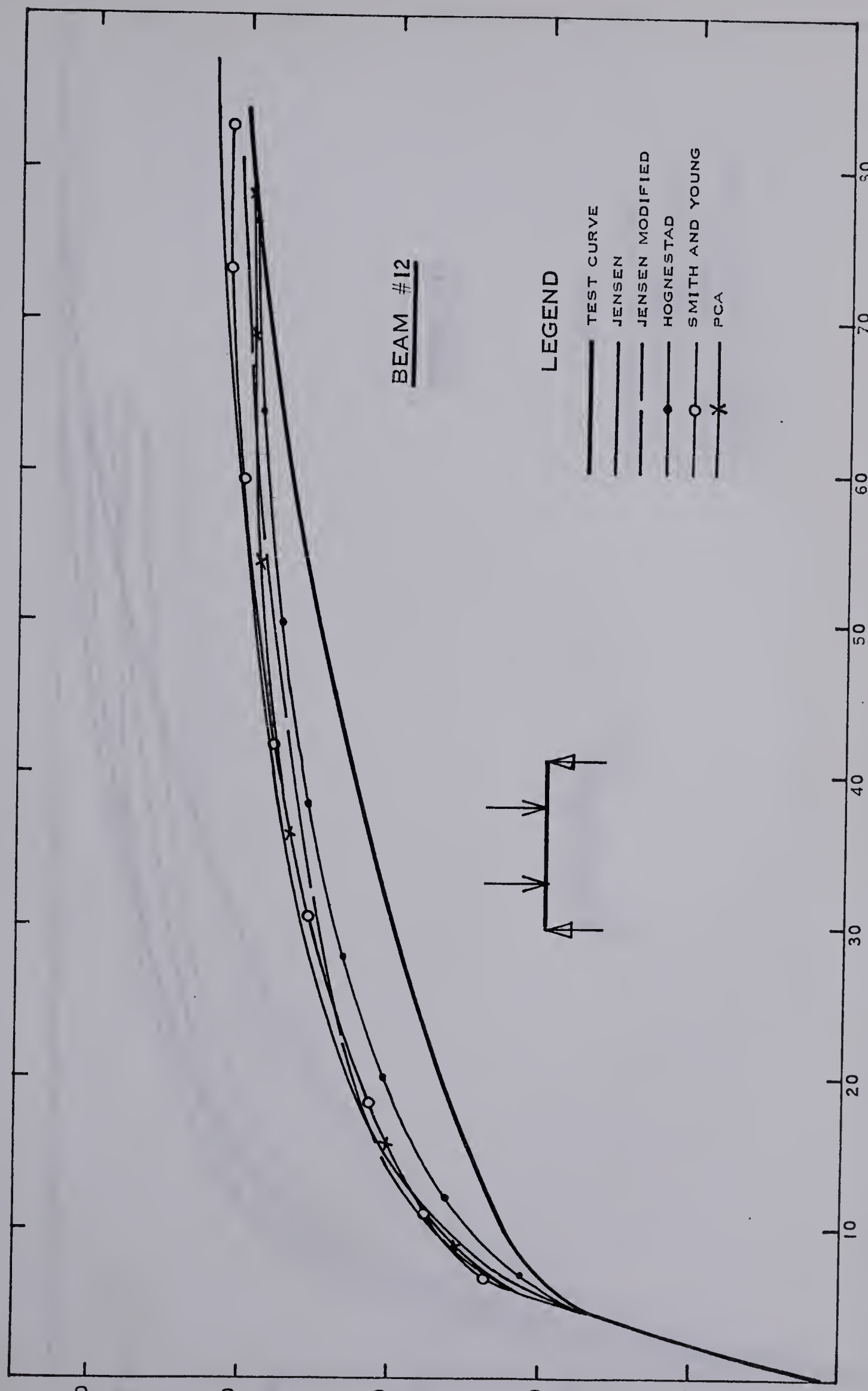

FIGURE 3.8 MOMENT VS. CURVATURE

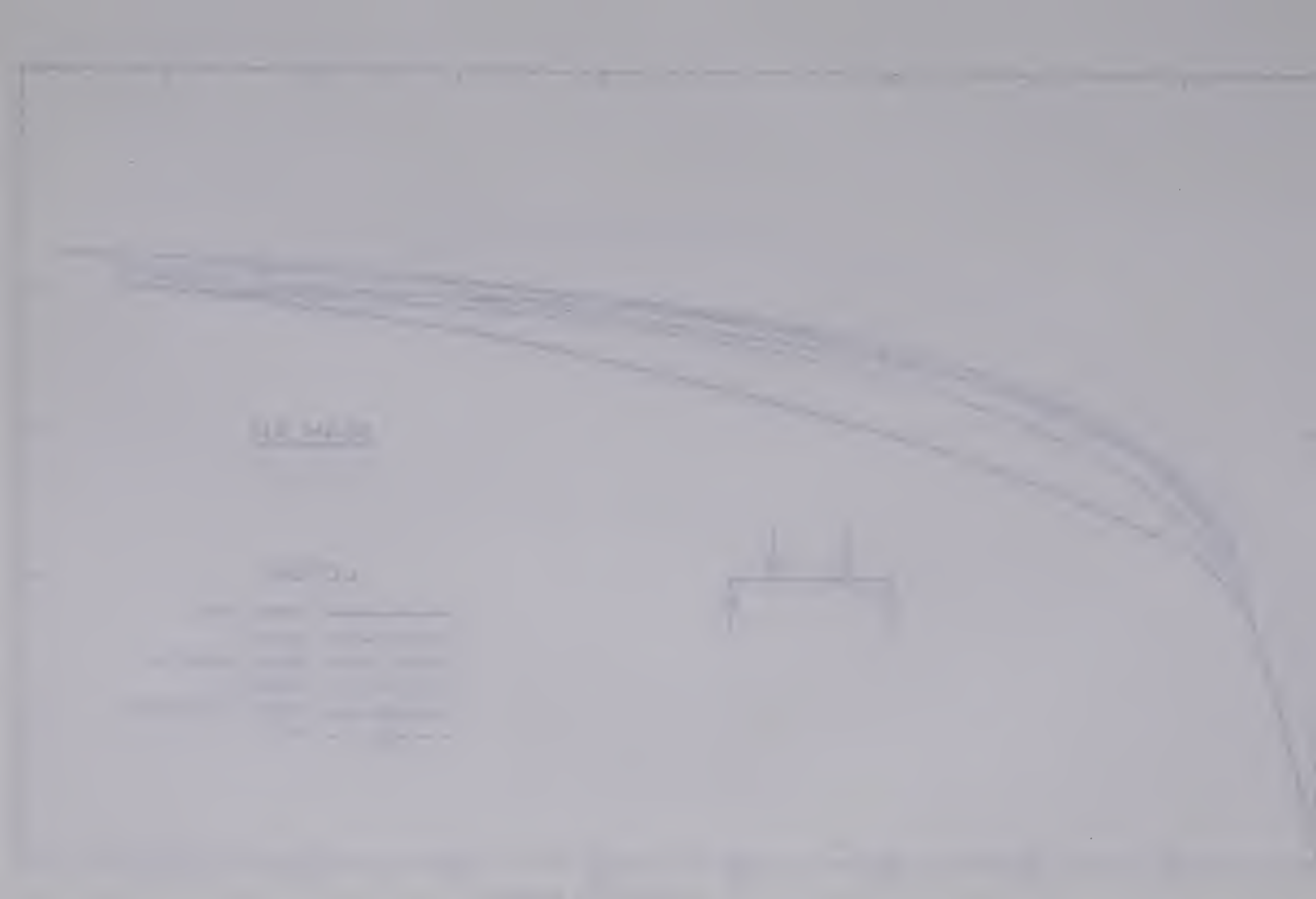

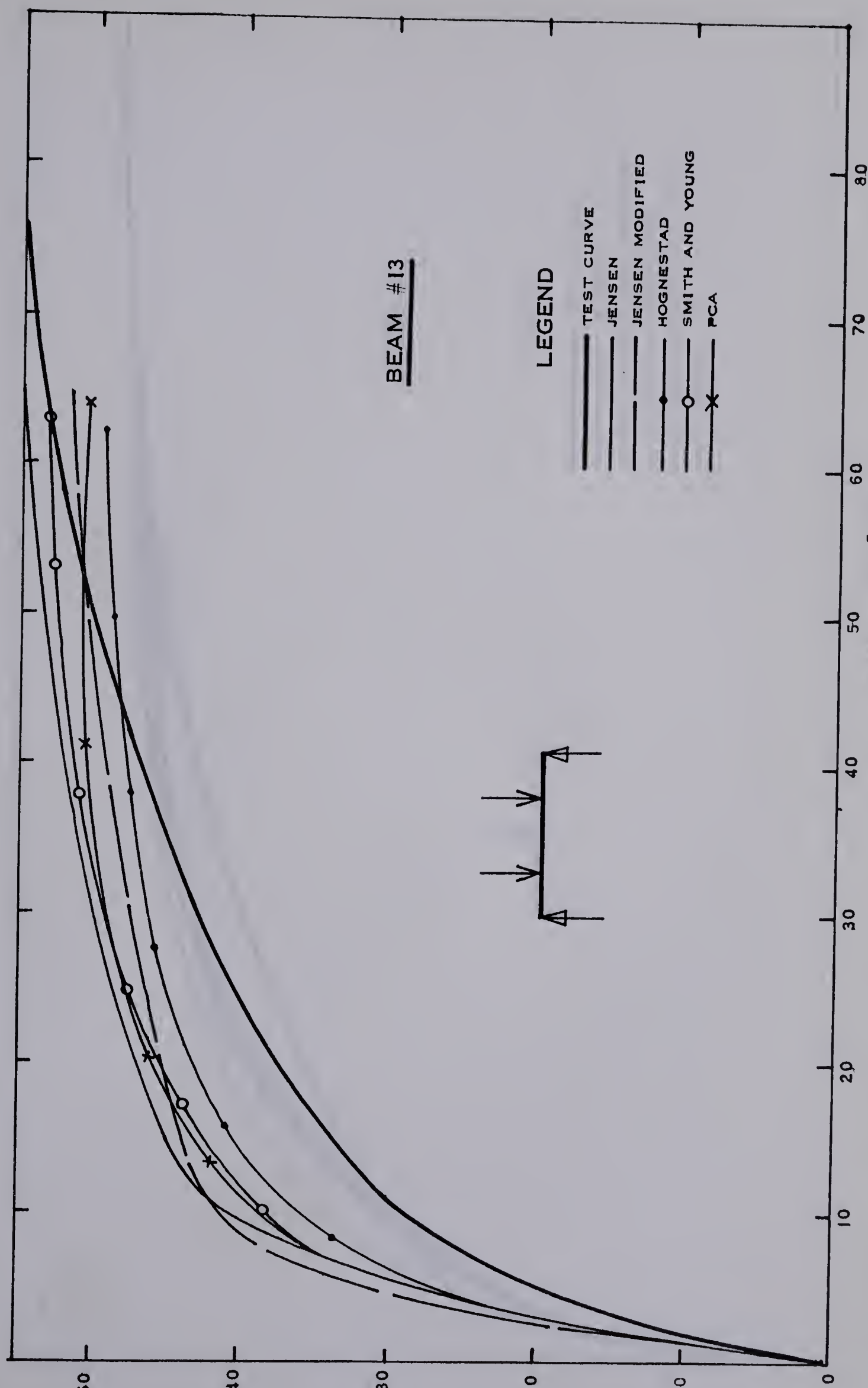

FIGURE 3.9 MOMENT VS. CURVATURE

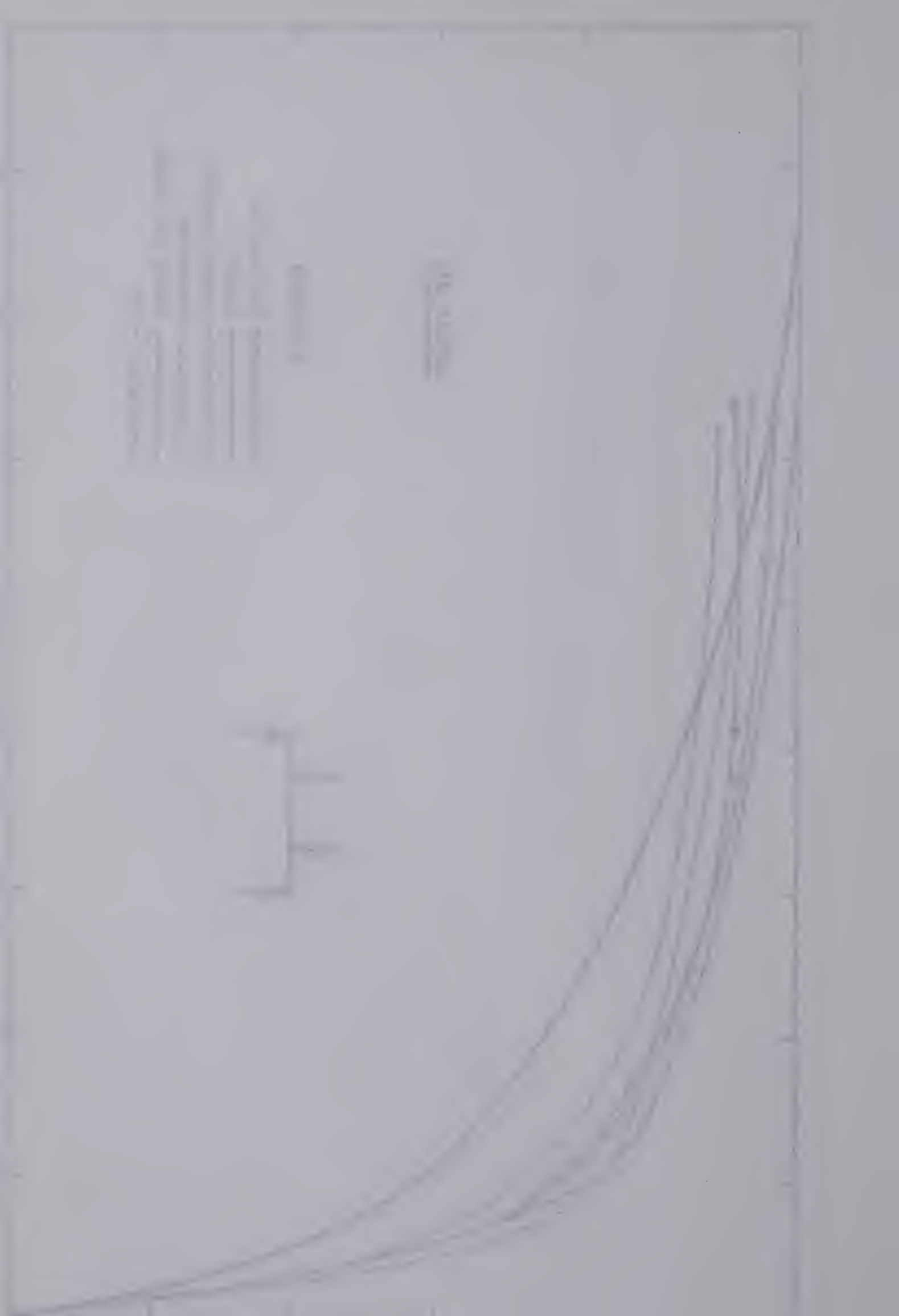

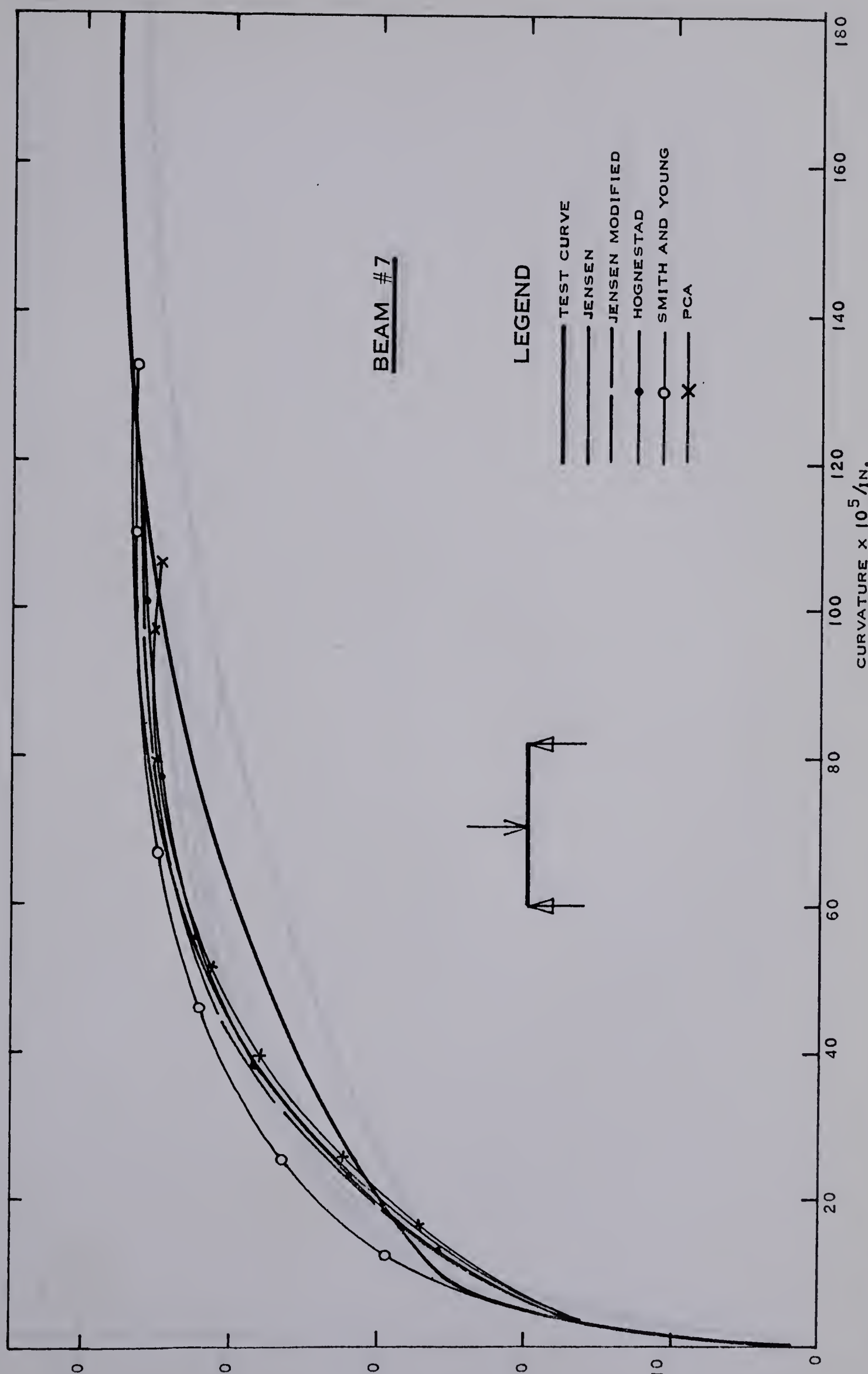

FIGURE 3.10 MOMENT VS. CURVATURE

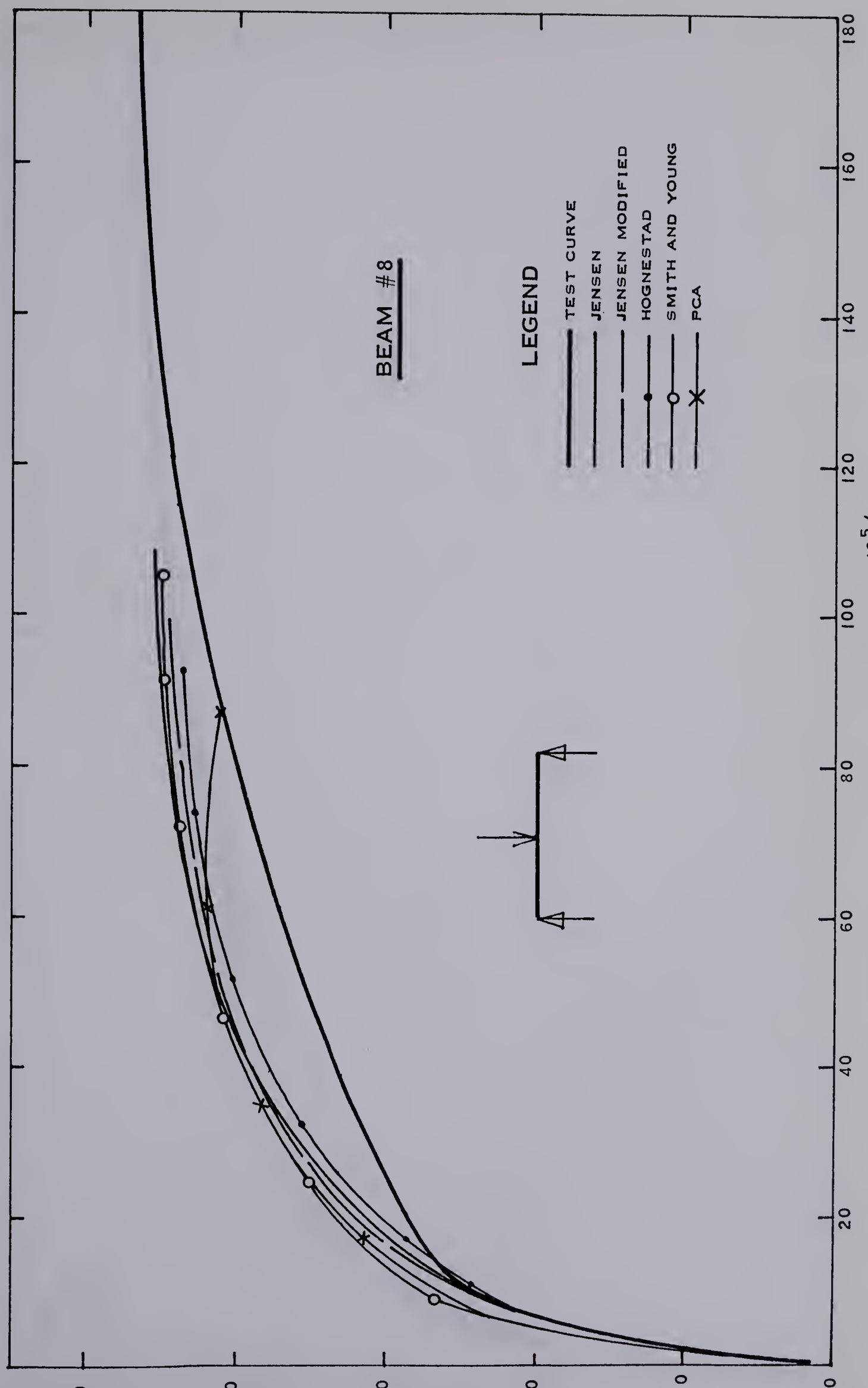

FIGURE 3.11 MOMENT VS. CURVATURE

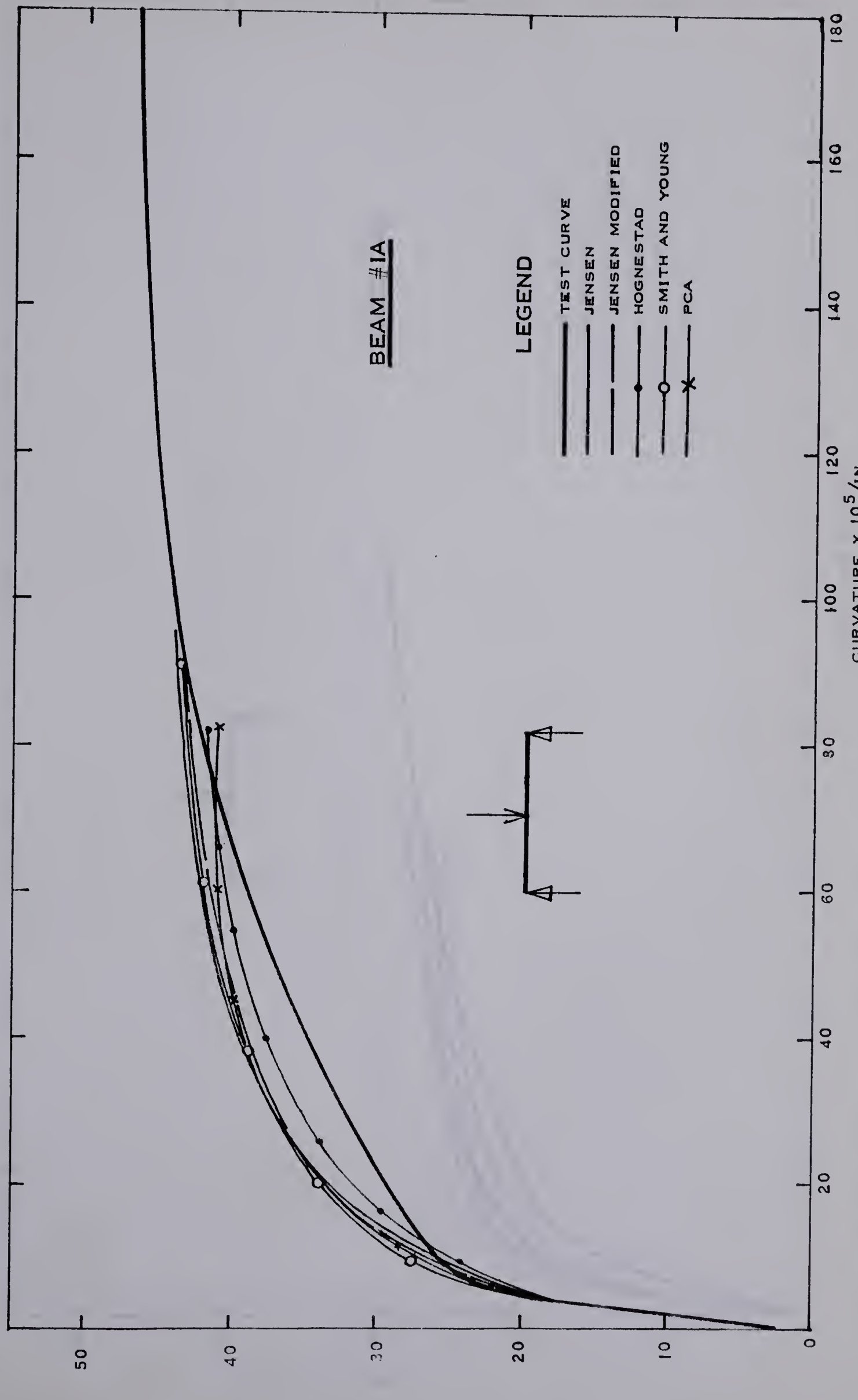

FIGURE 3.12 MOMENT VS. CURVATURE

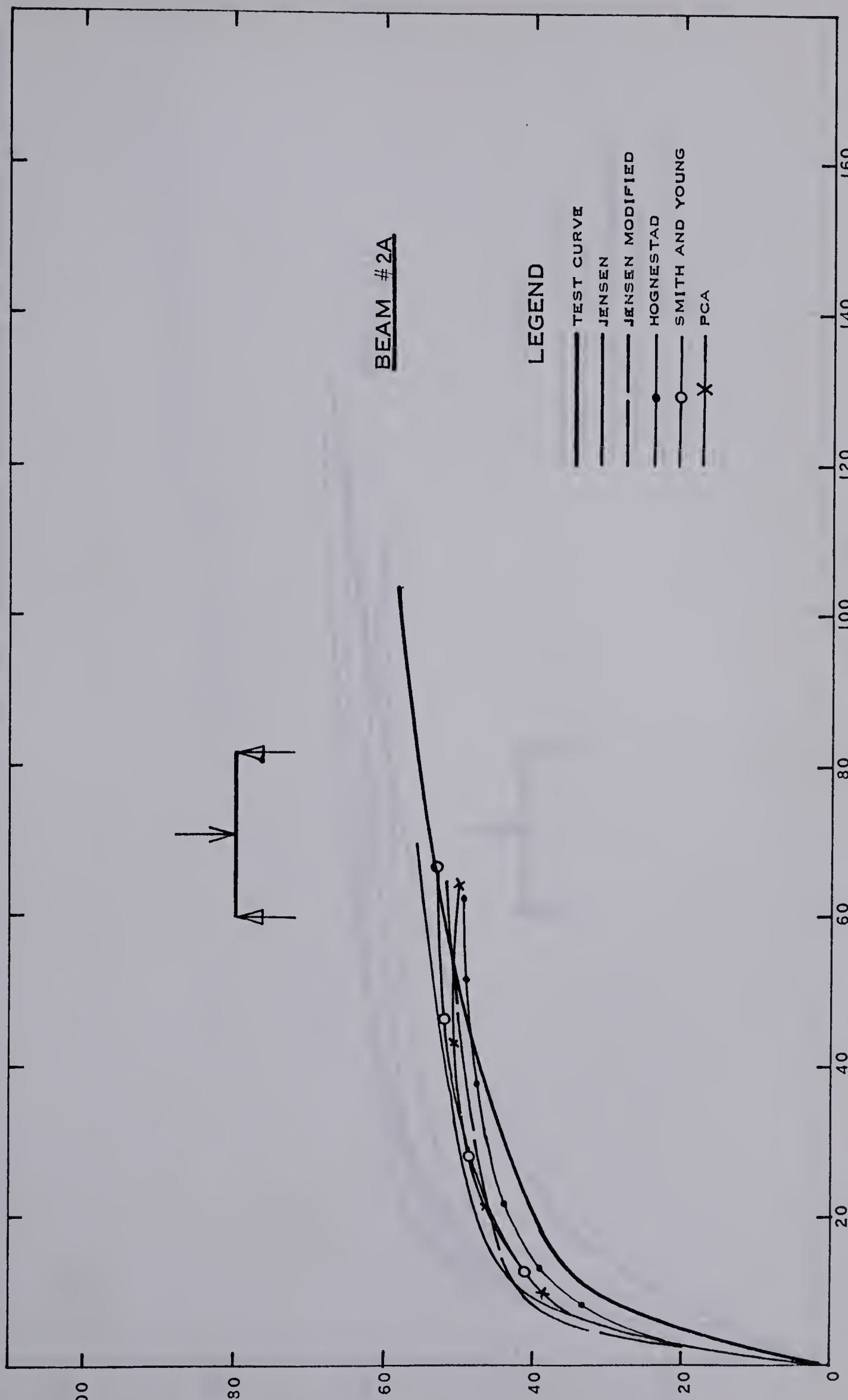

FIGURE 3.13 MOMENT VS. CURVATURE

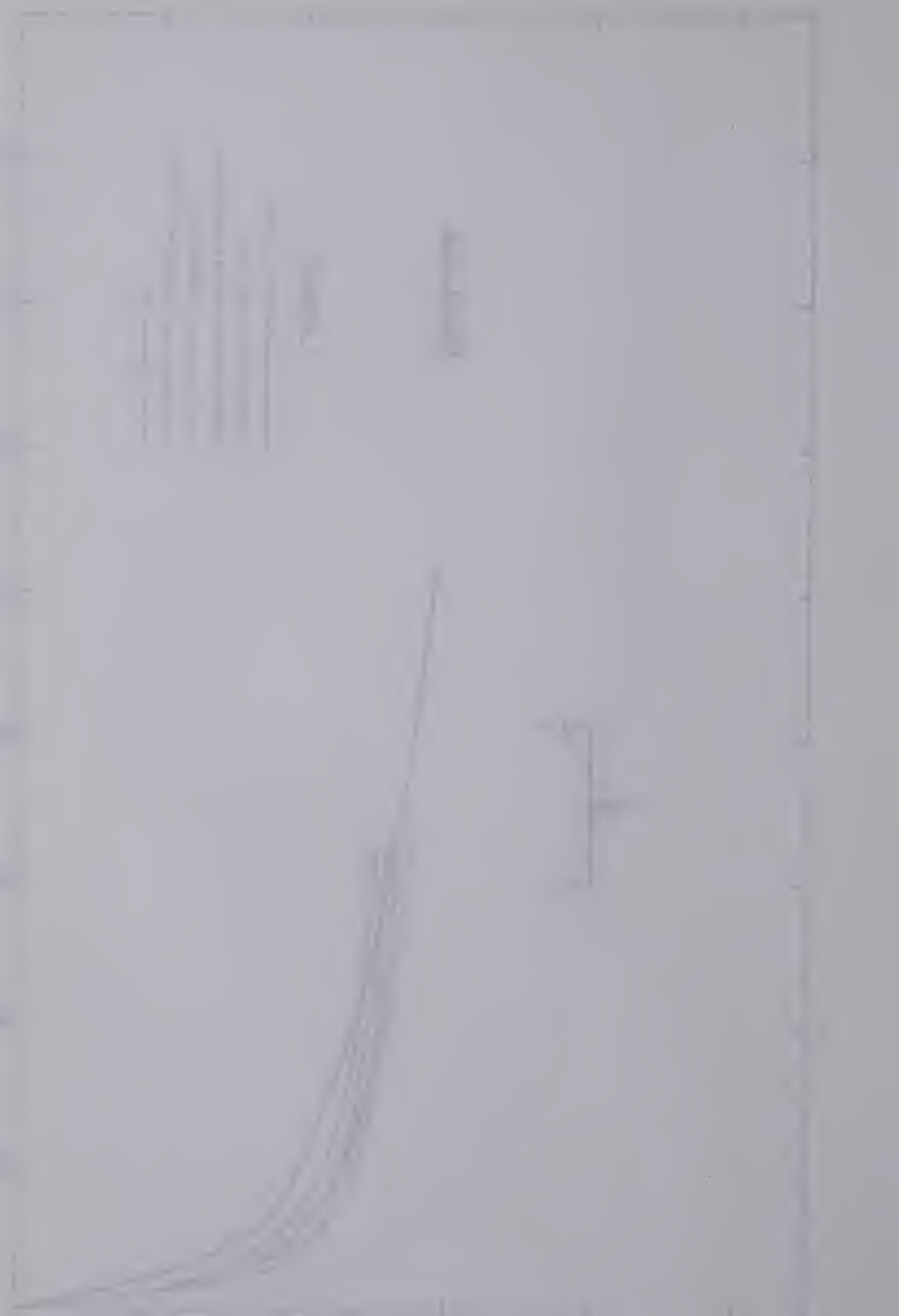

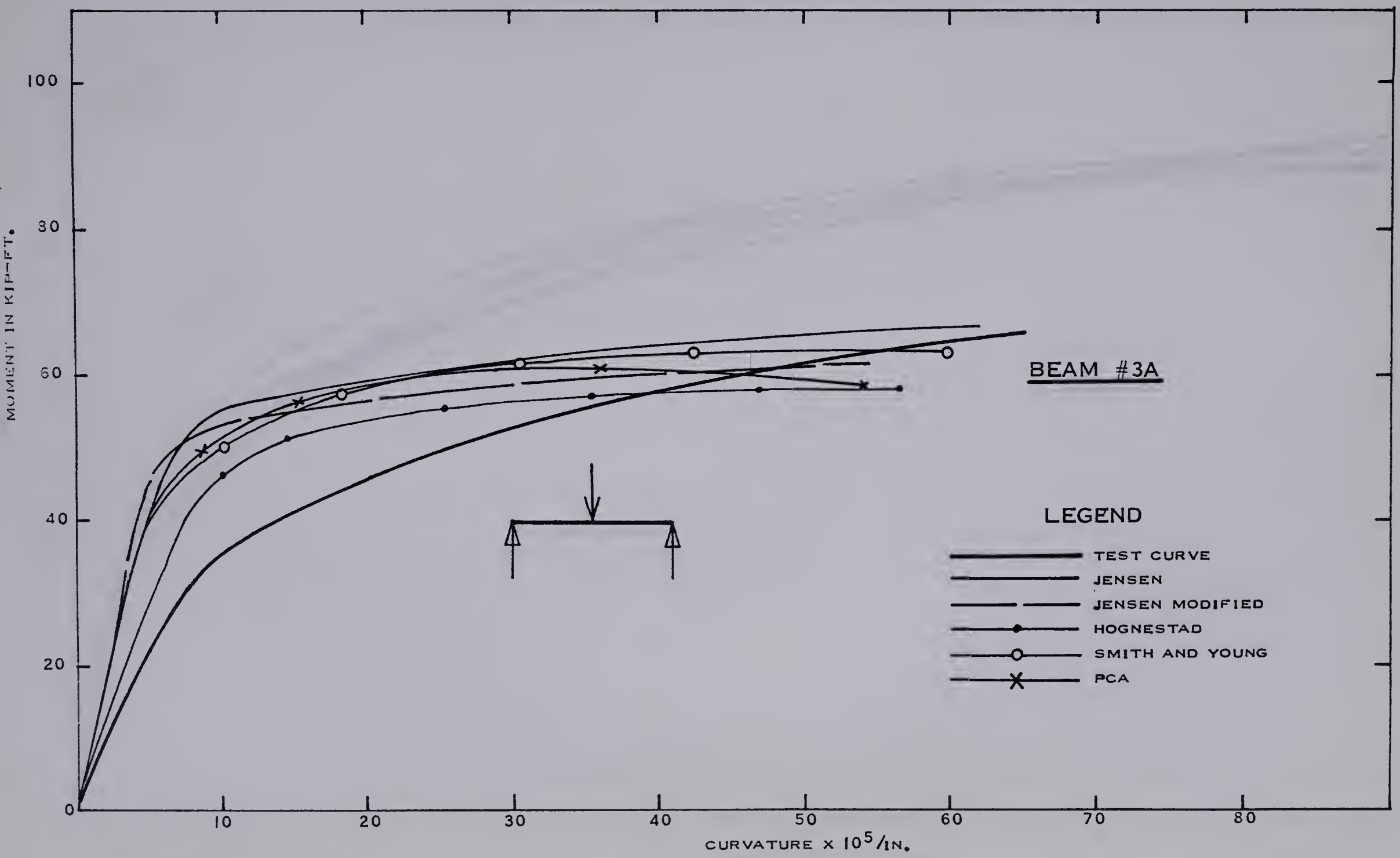

FIGURE 3.14 MOMENT VS. CURVATURE

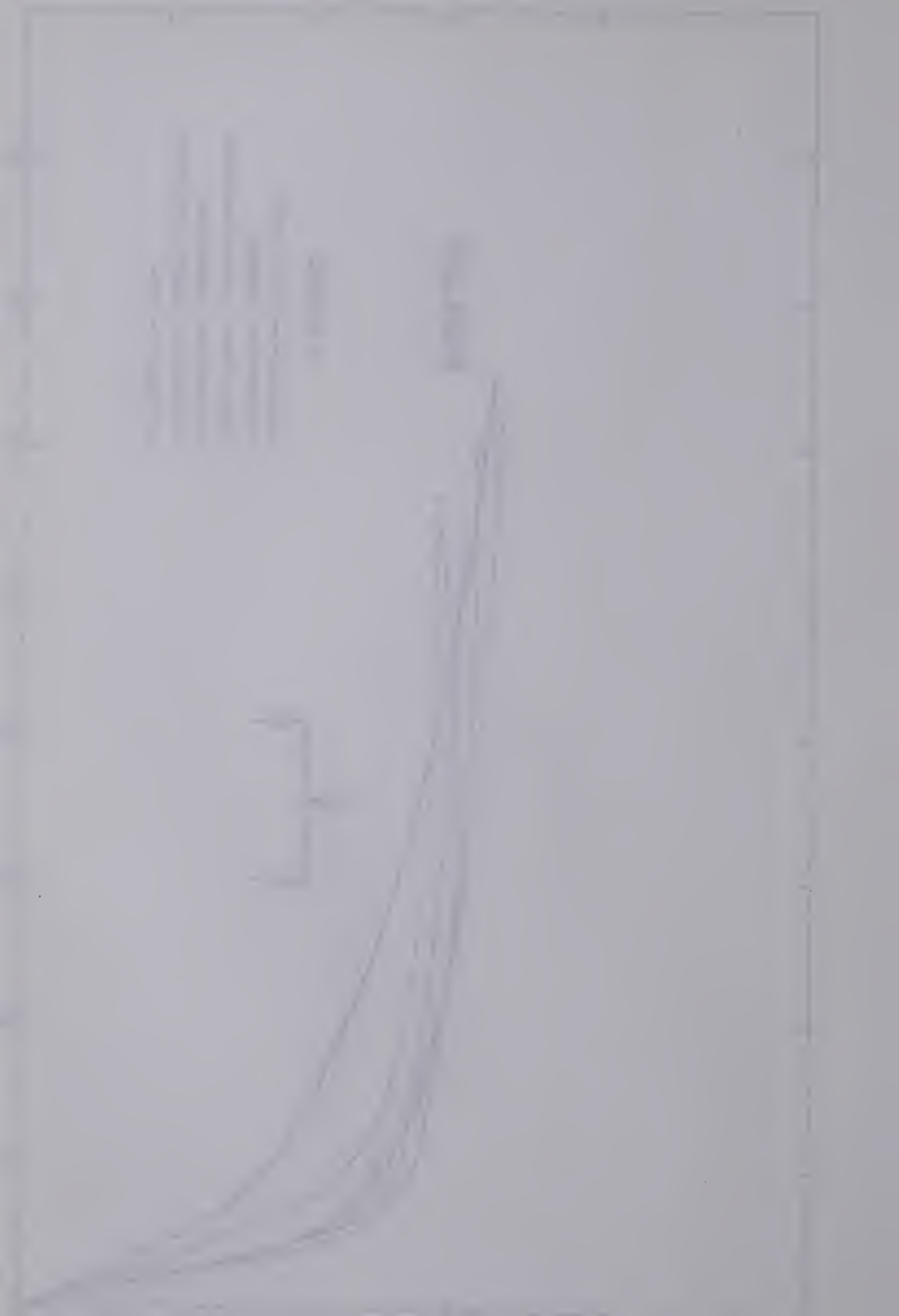

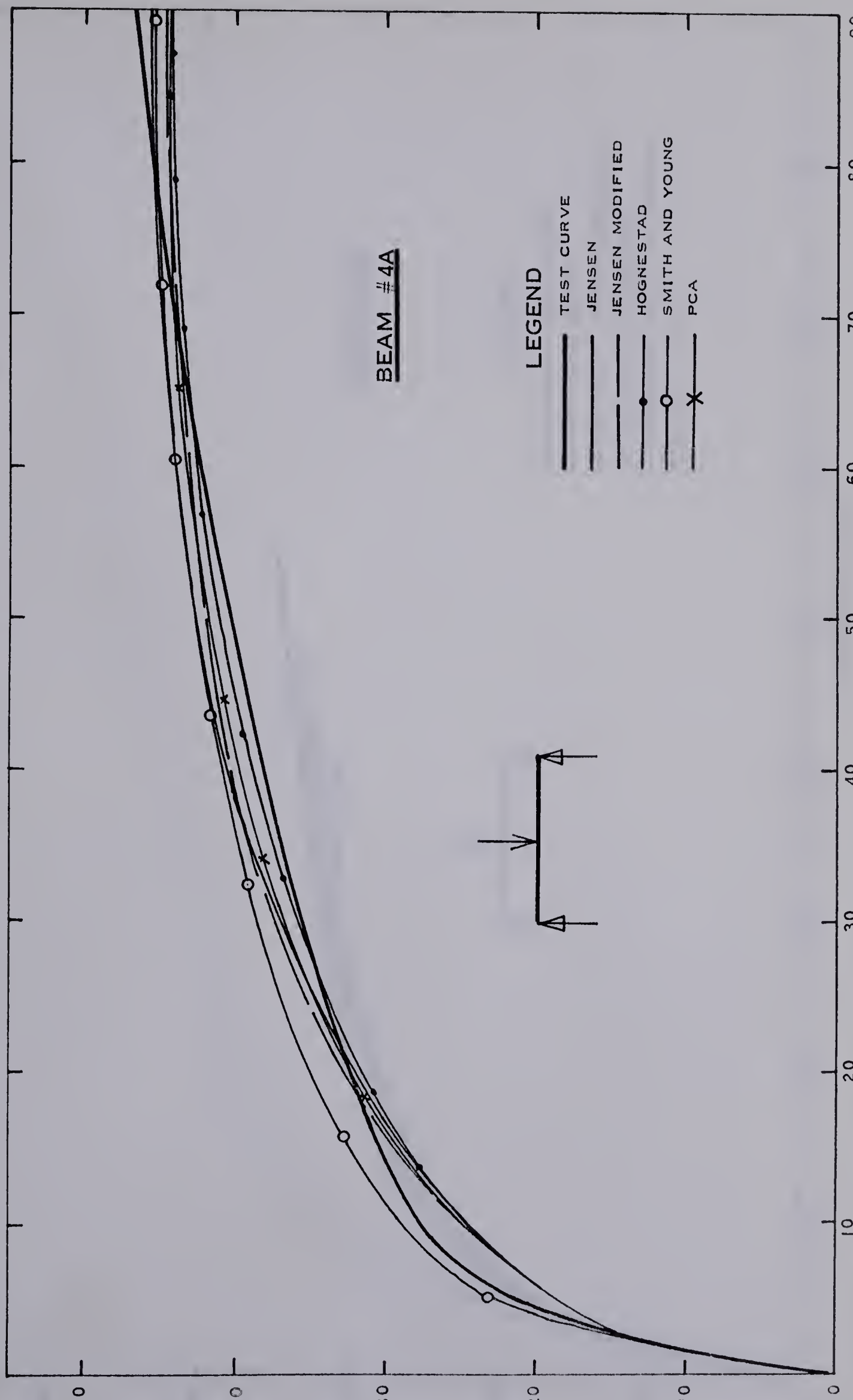

FIGURE 3.15 MOMENT VS. CURVATURE

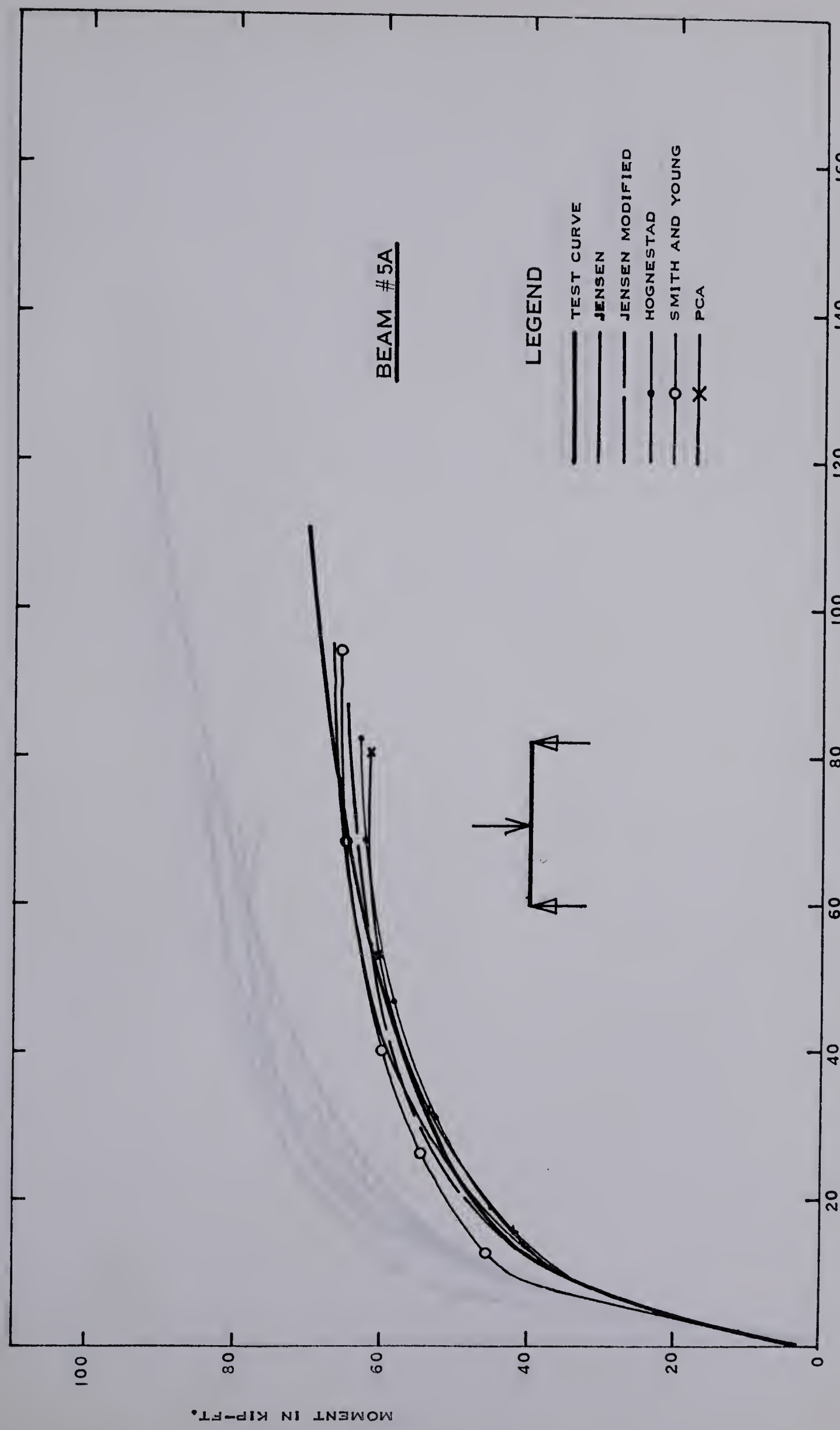

FIGURE 3.16 MOMENT VS. CURVATURE

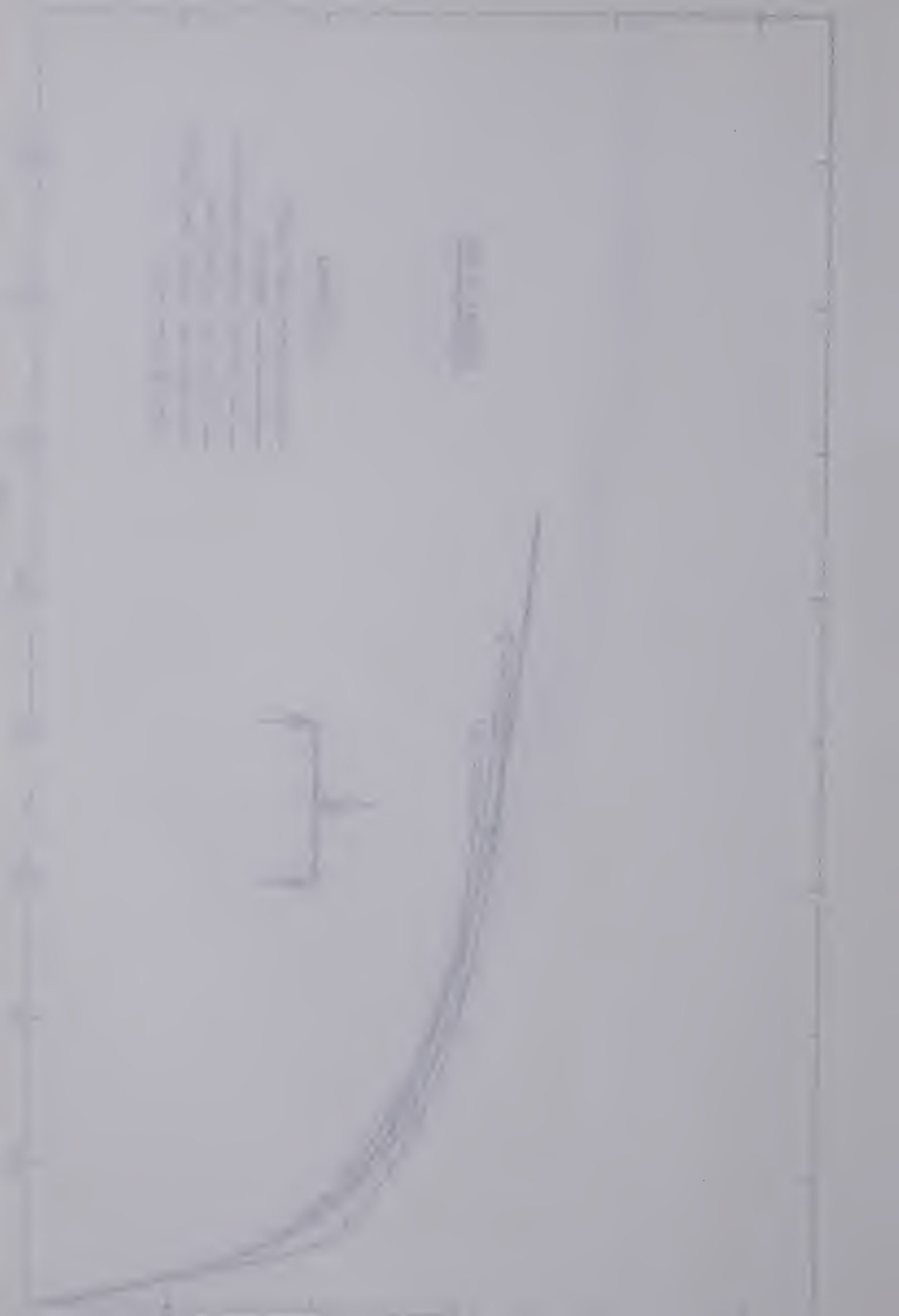

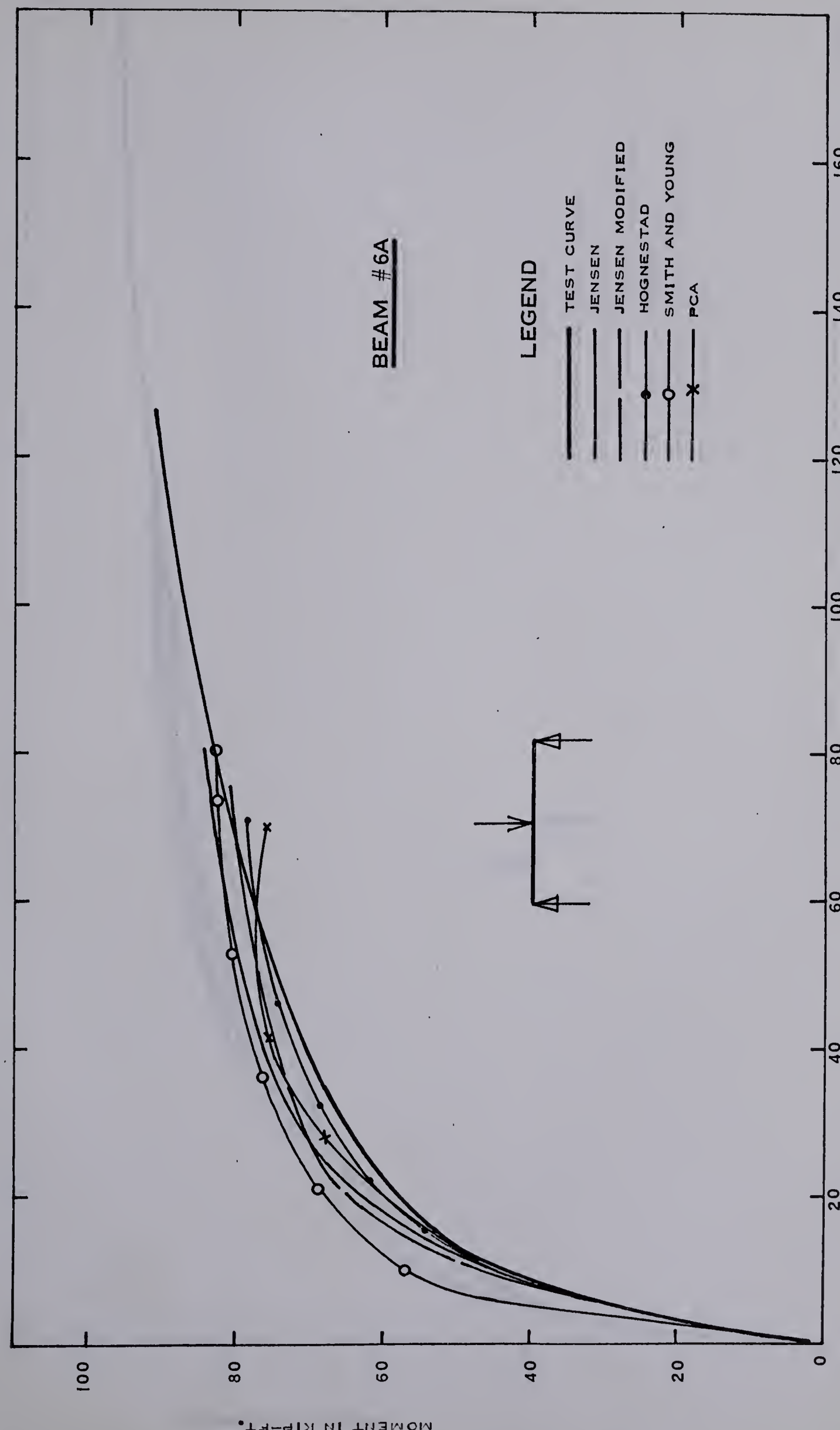

FIGURE 3.17 MOMENT VS. CURVATURE

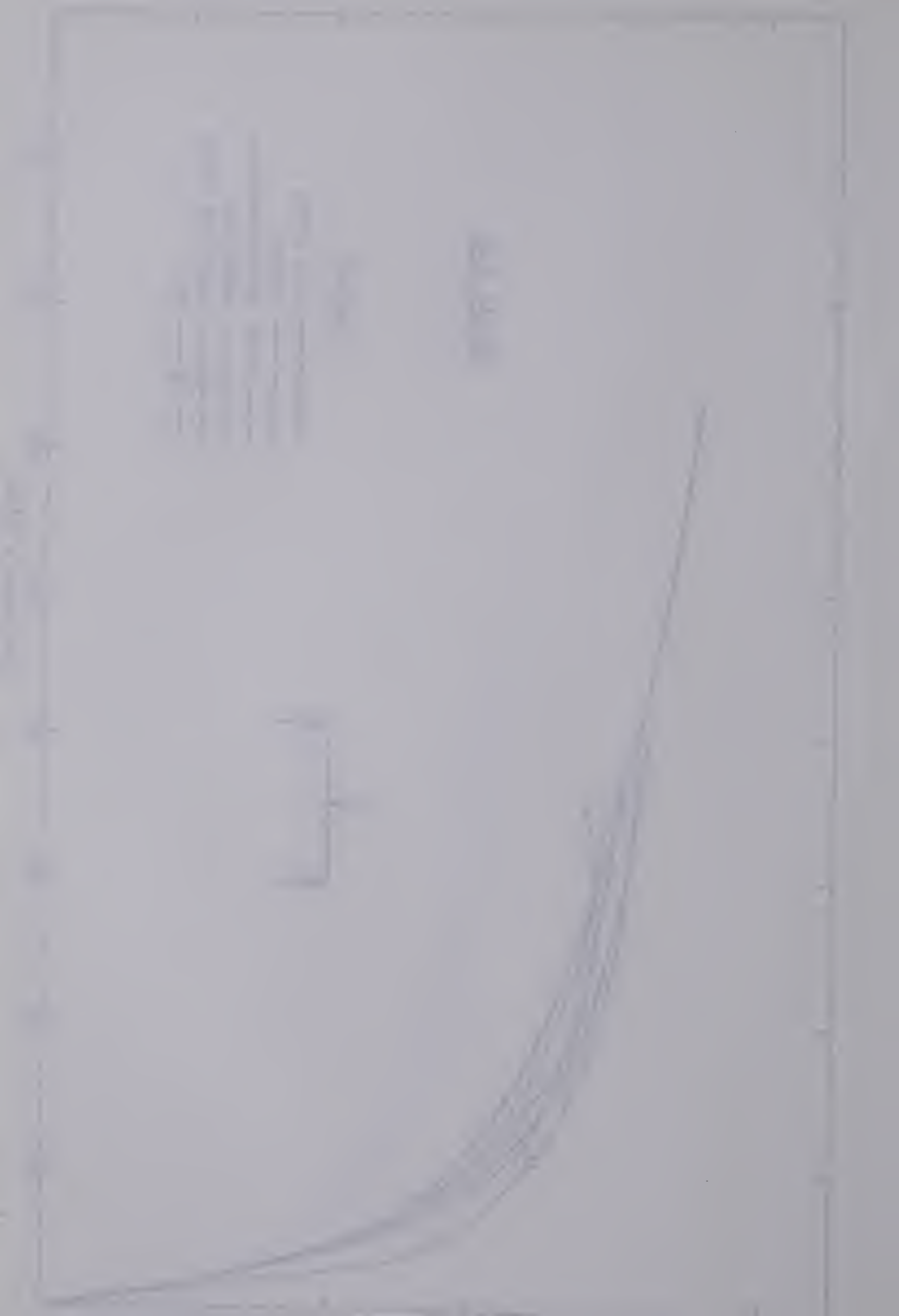

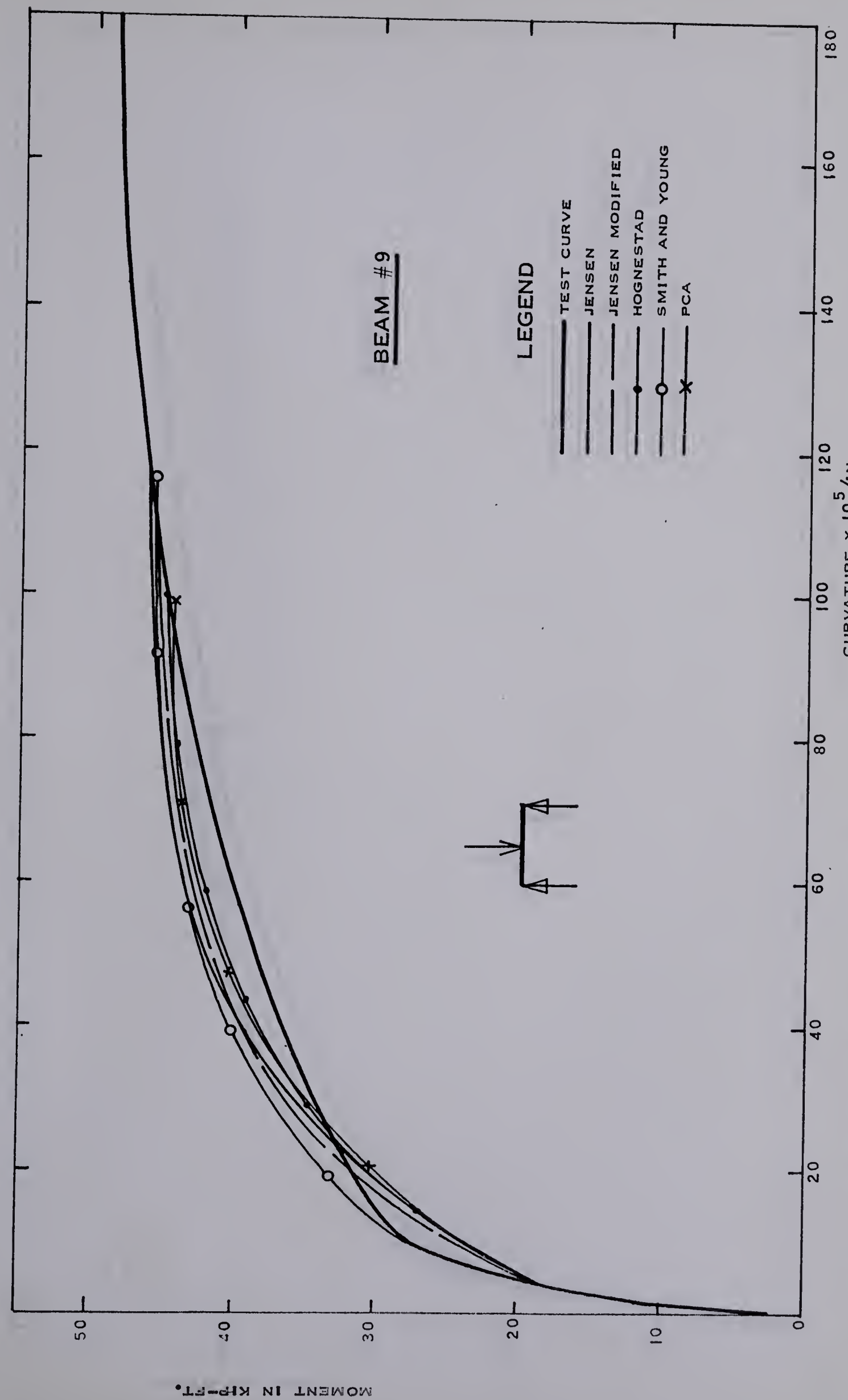

FIGURE 3.18 MOMENT VS. CURVATURE

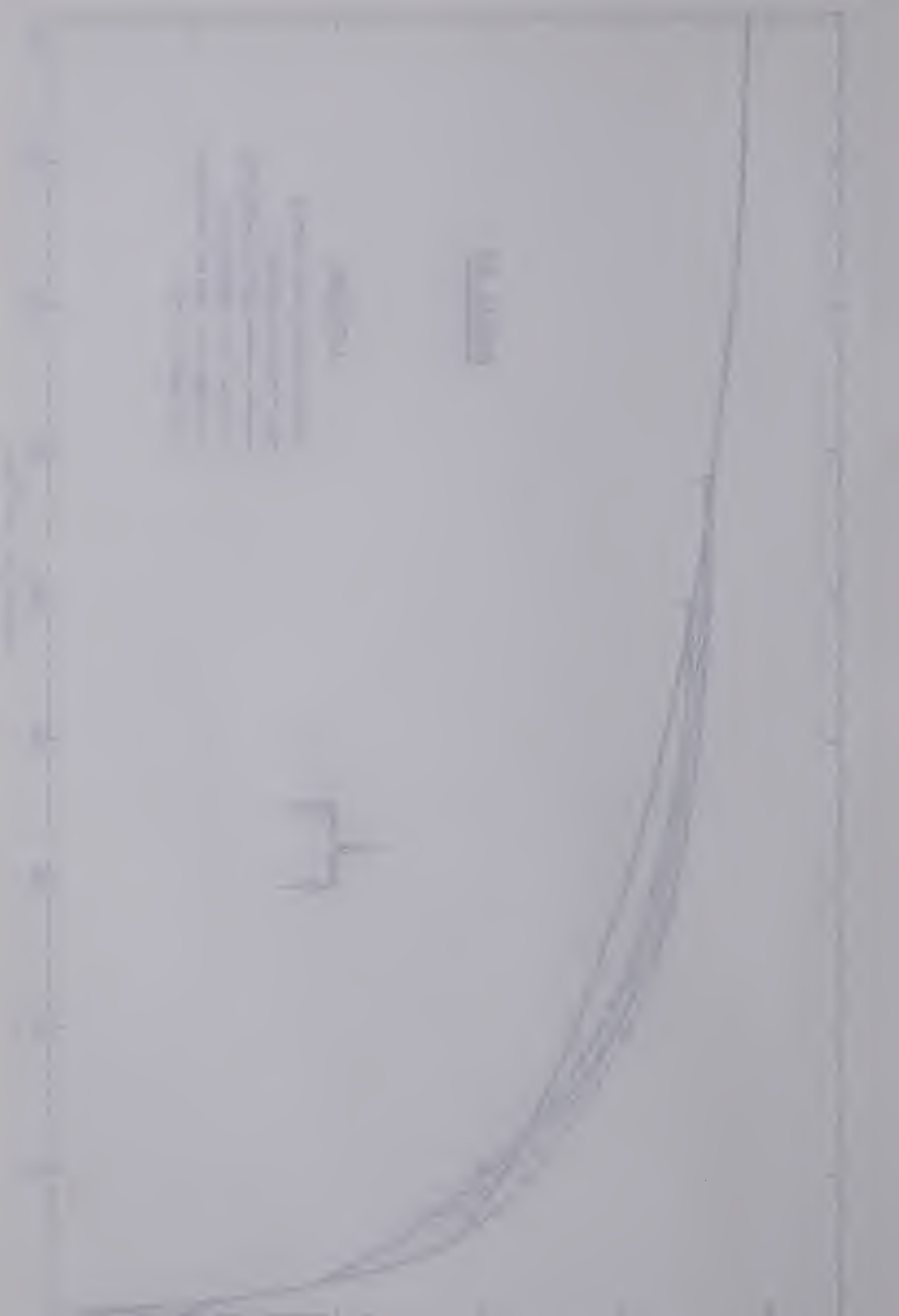

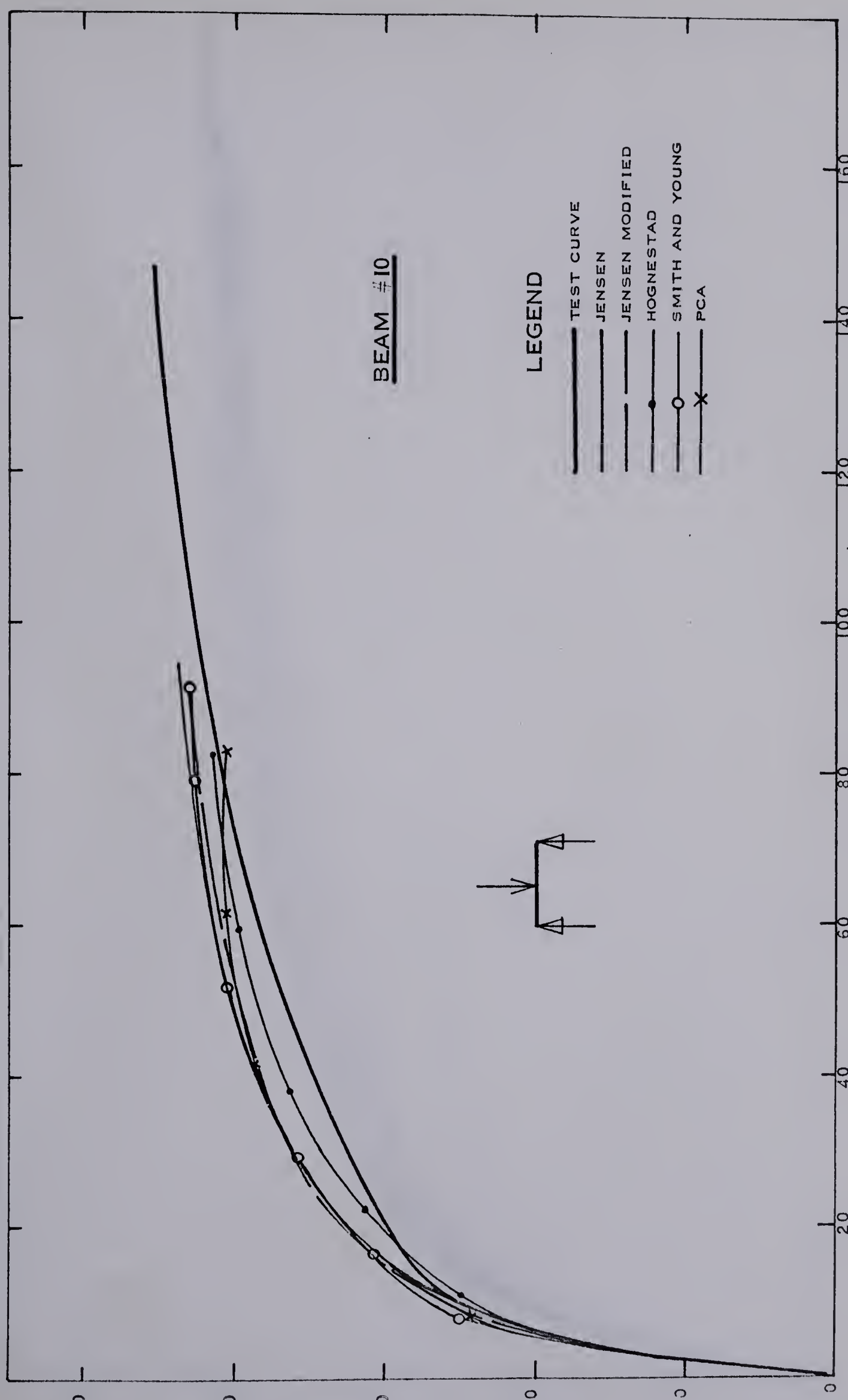

FIGURE 3.19 MOMENT VS. CURVATURE

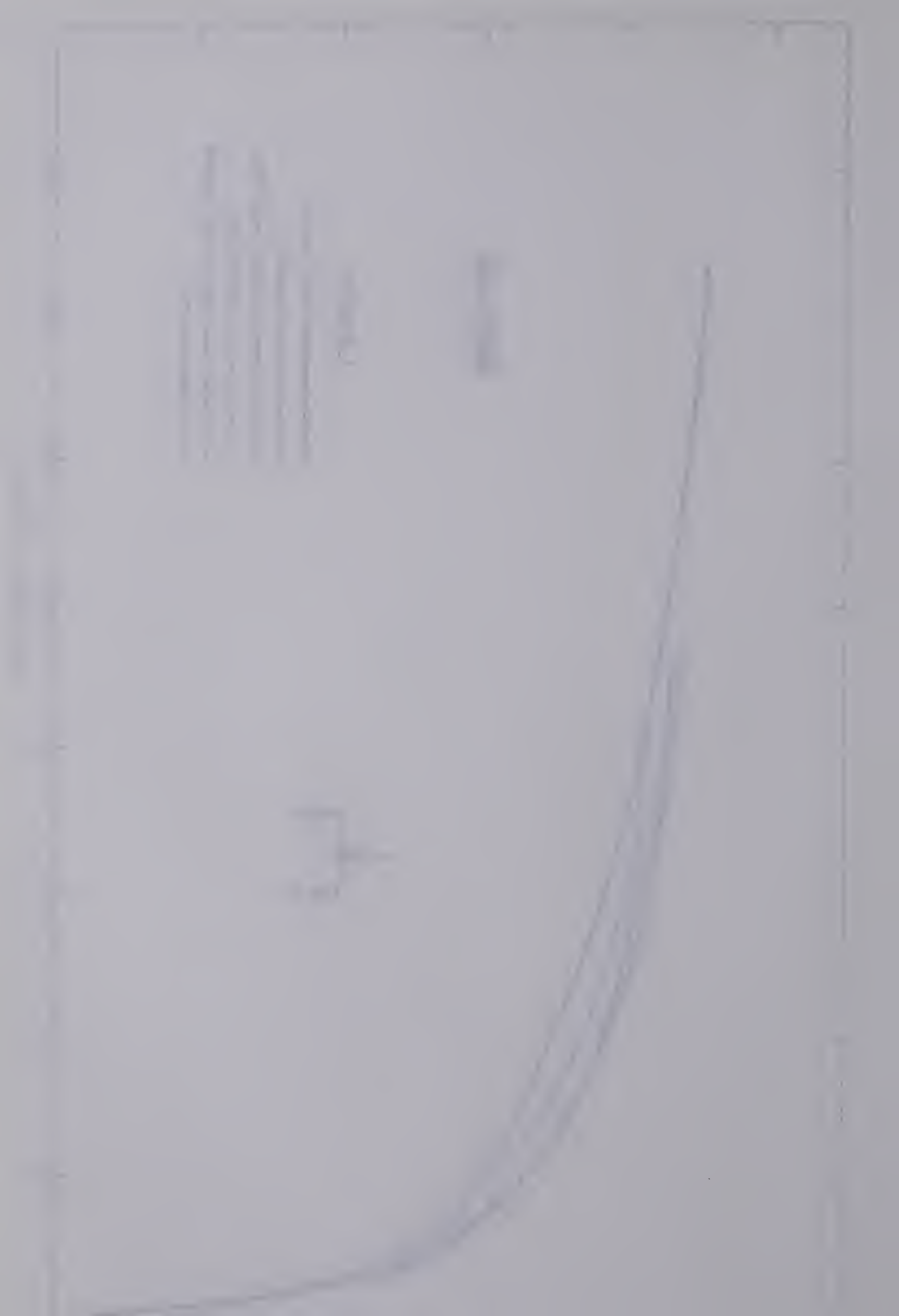

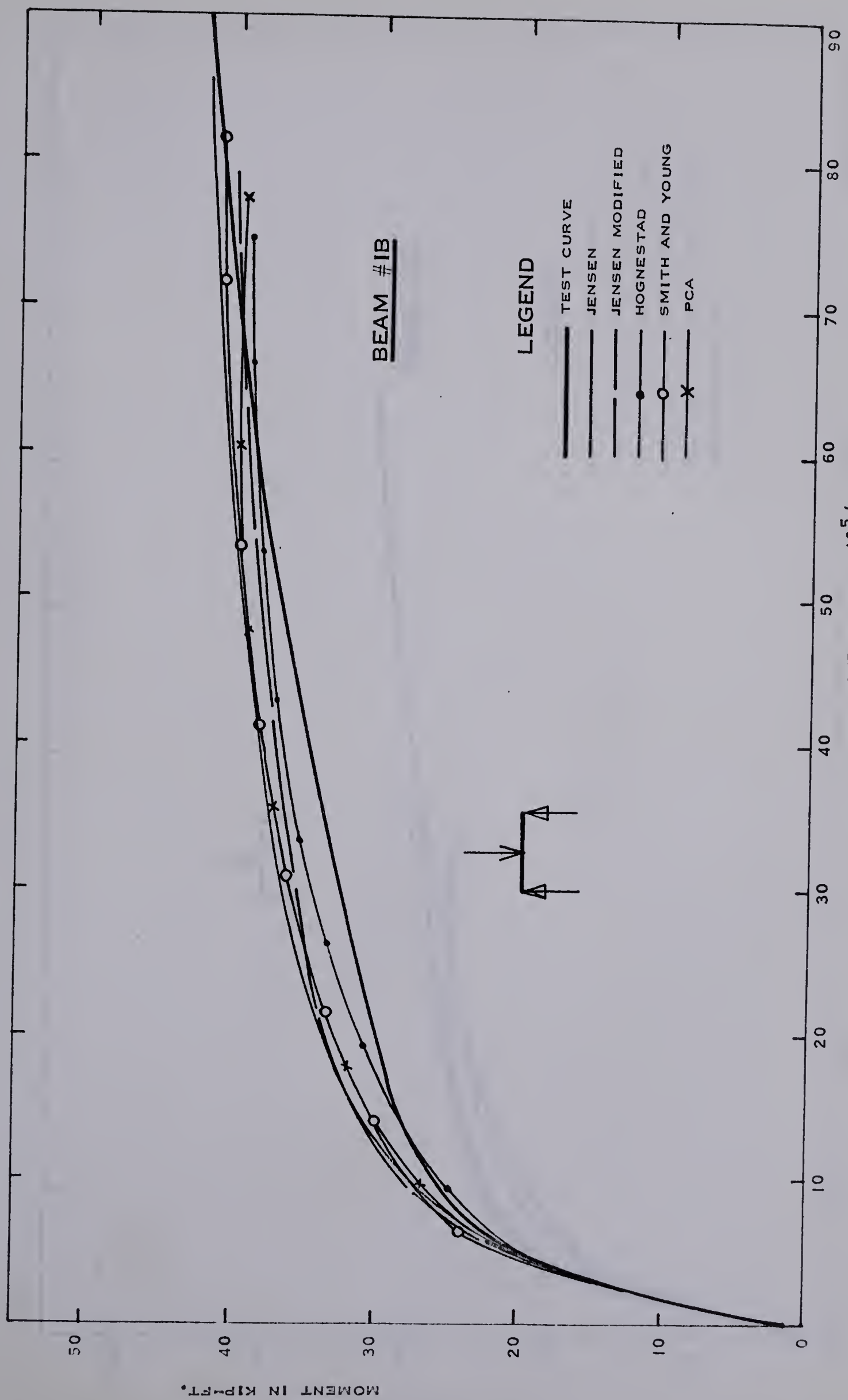

FIGURE 3.20 MOMENT VS. CURVATURE

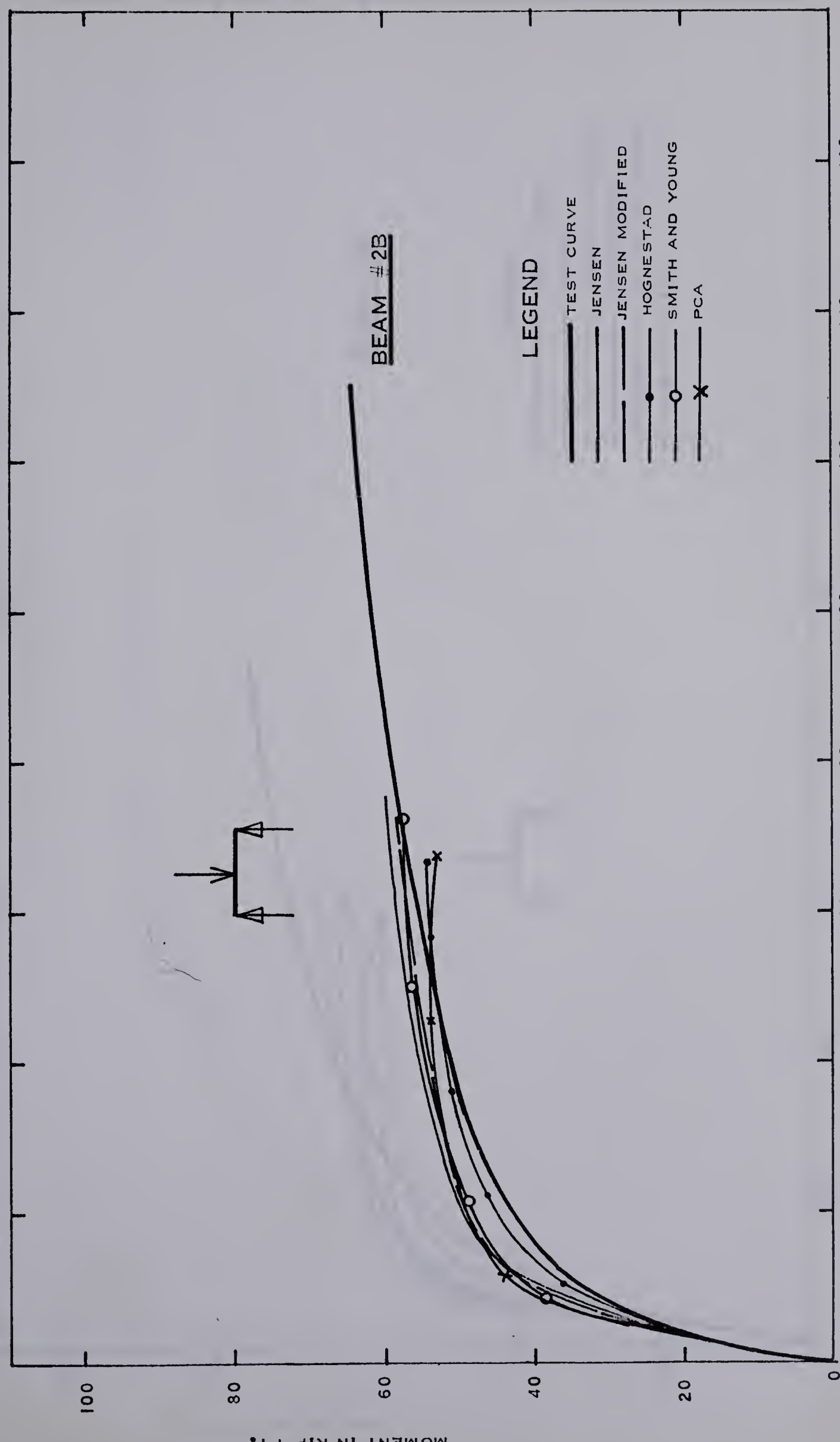

FIGURE 3.21 MOMENT VS. CURVATURE

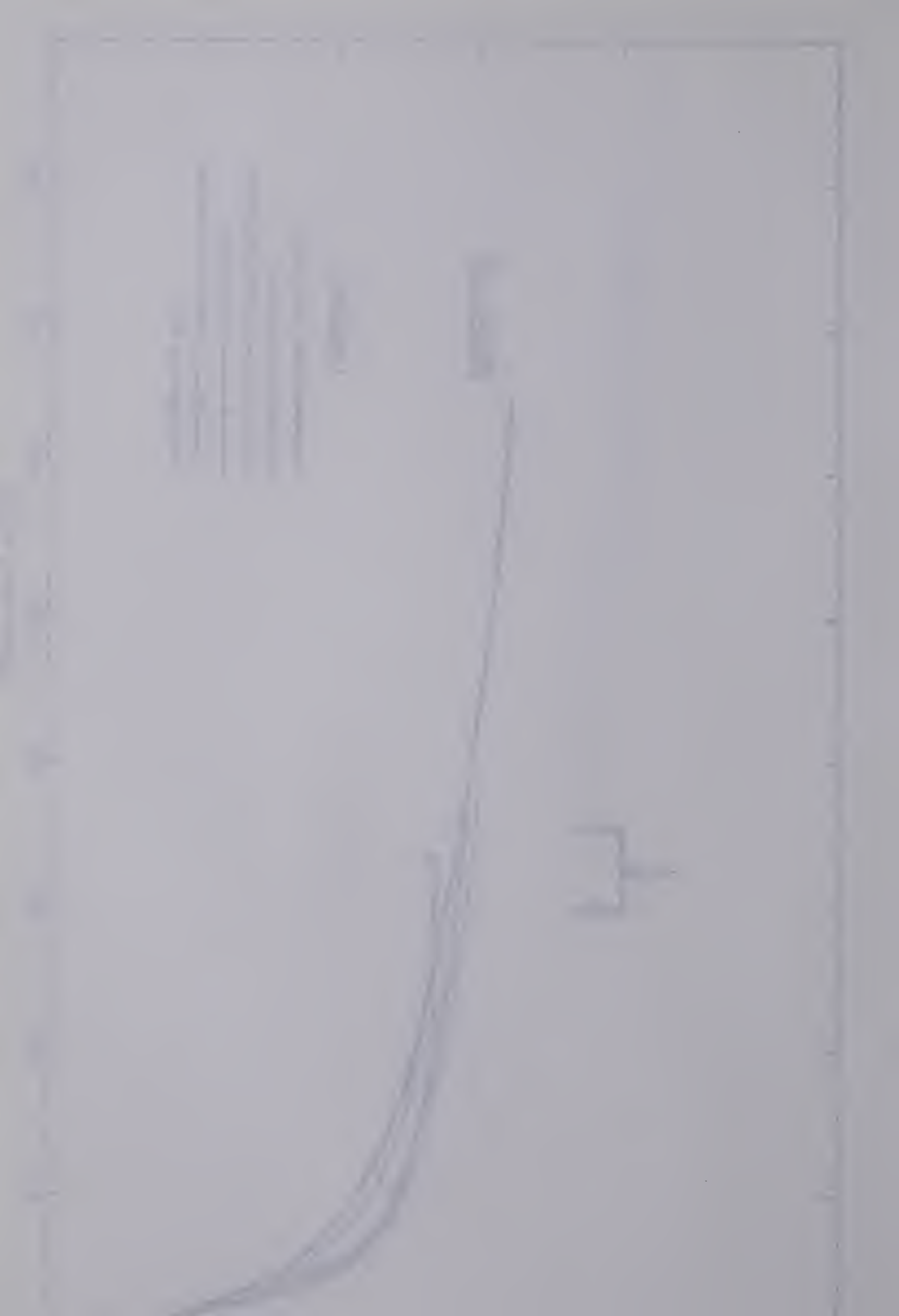

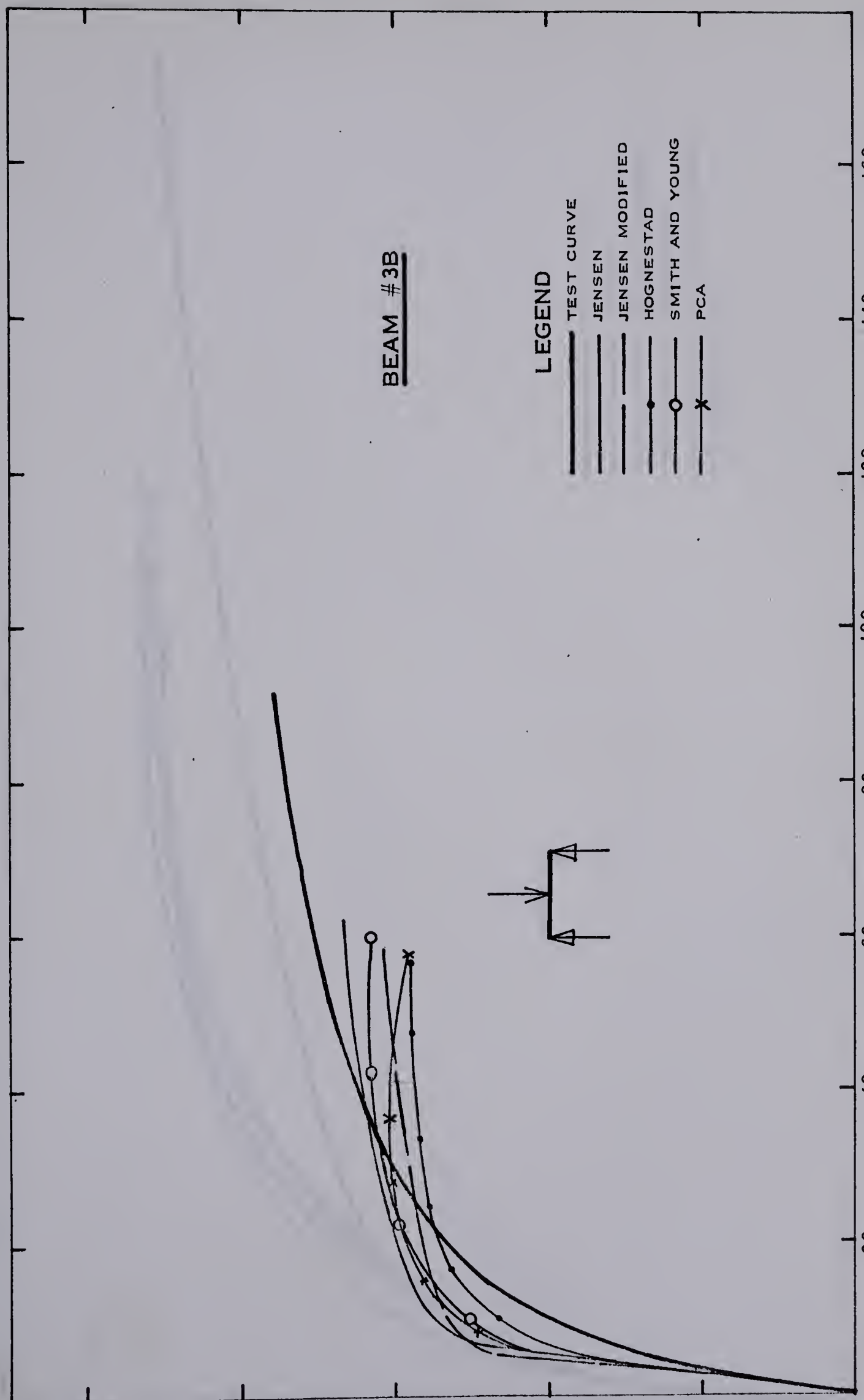

FIGURE 3.22 MOMENT VS. CURVATURE

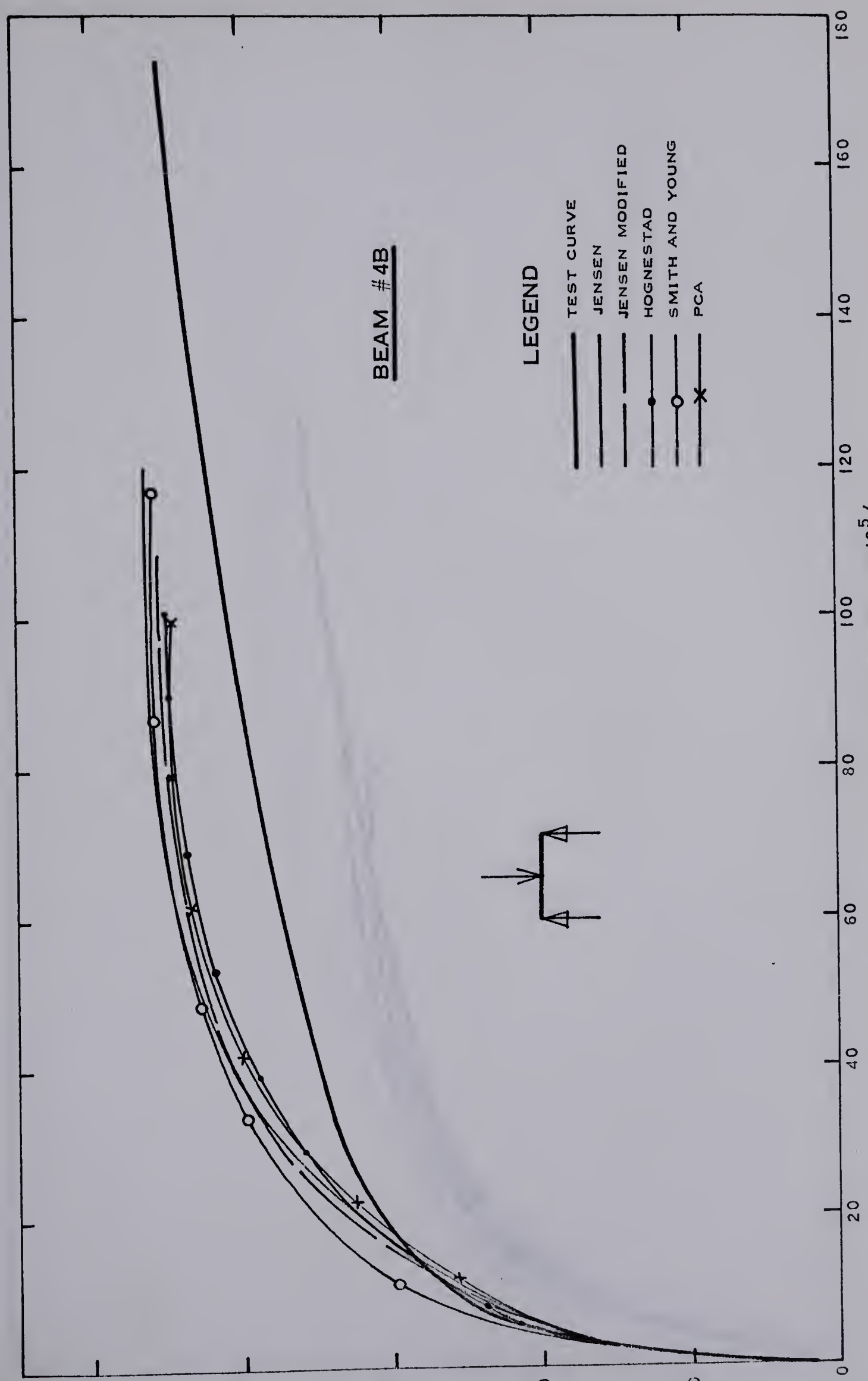

FIGURE 3.23 MOMENT VS. CURVATURE

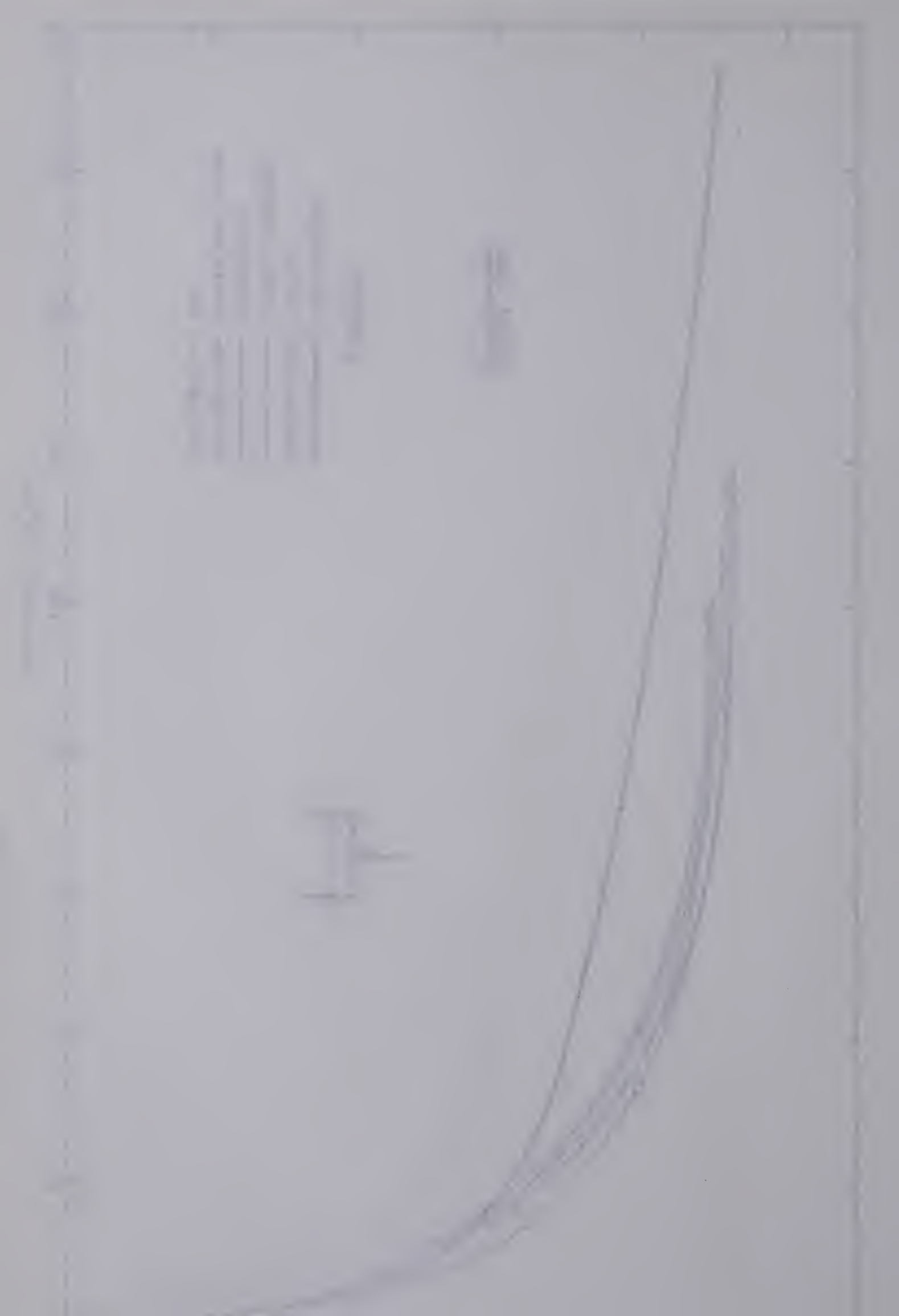

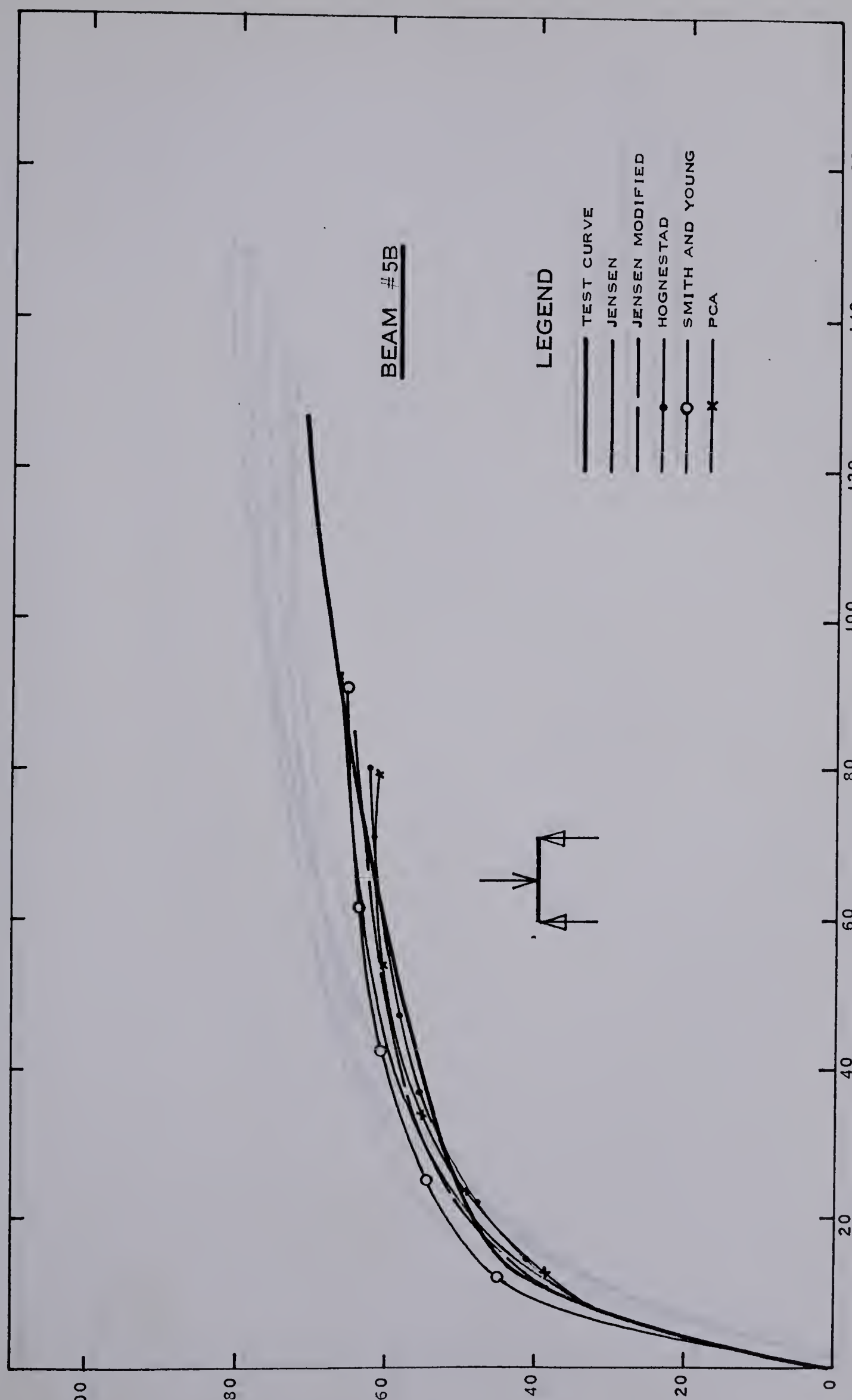

FIGURE 3.24 MOMENT VS. CURVATURE

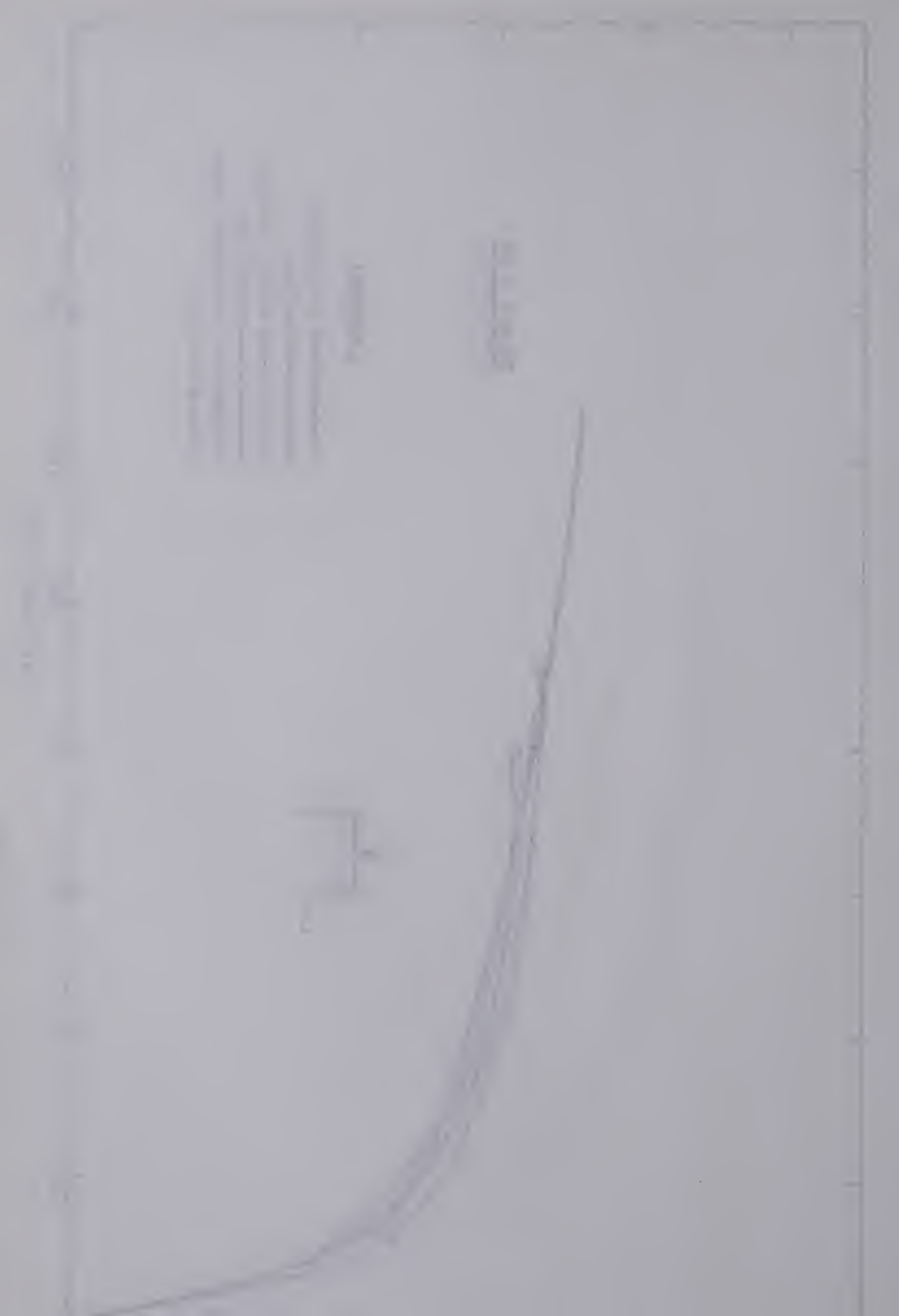

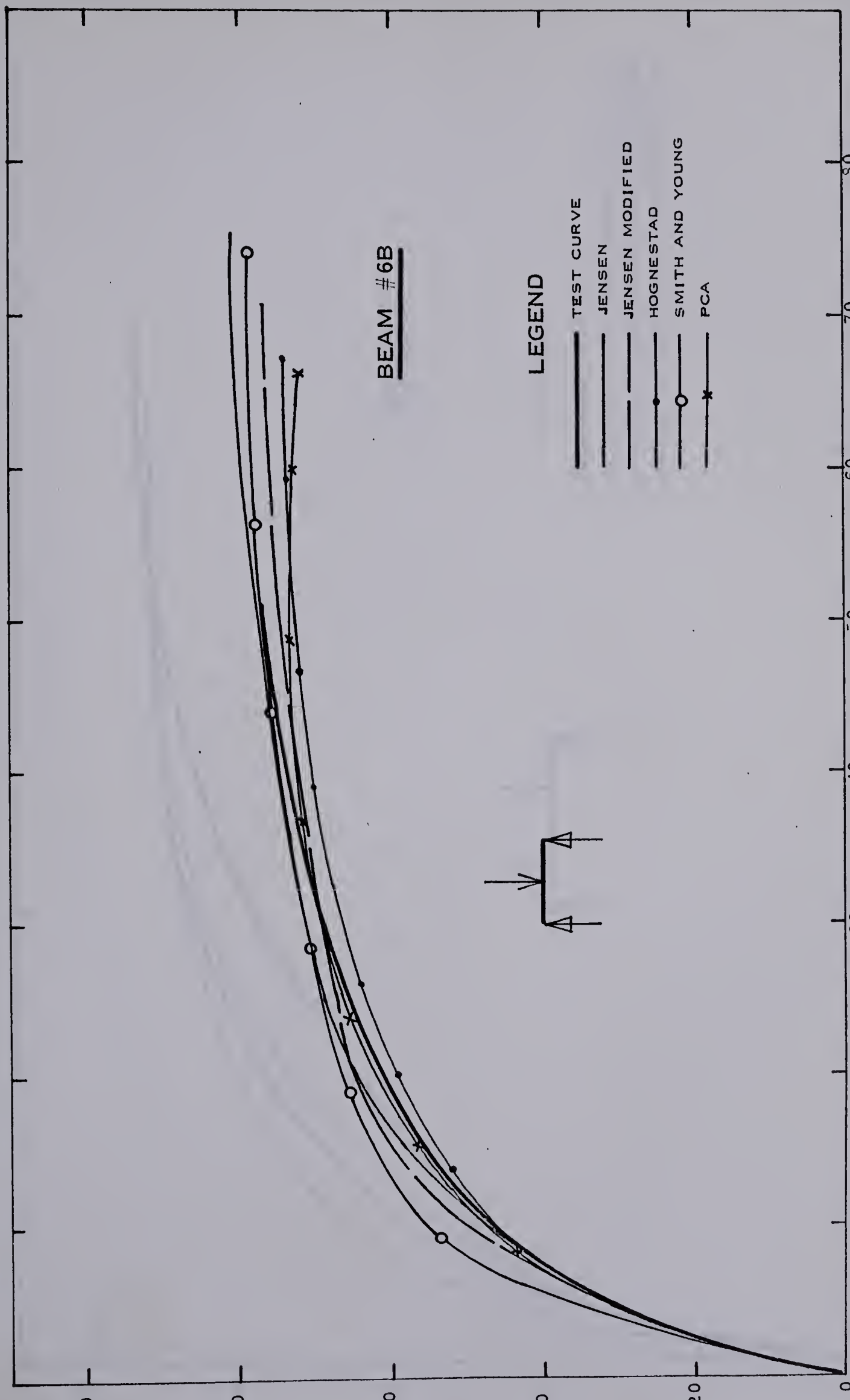

FIGURE 3.25 MOMENT VS. CURVATURE

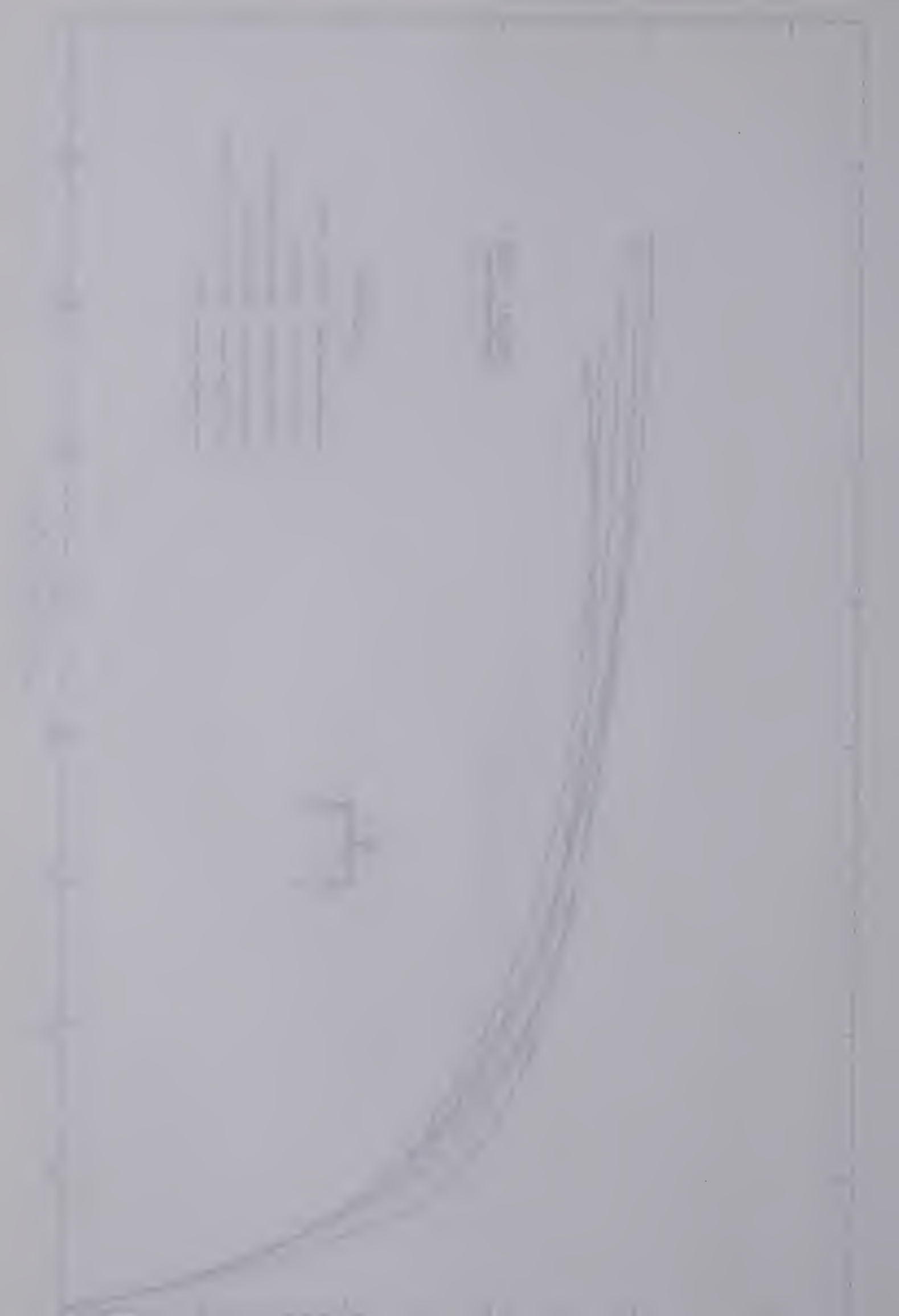

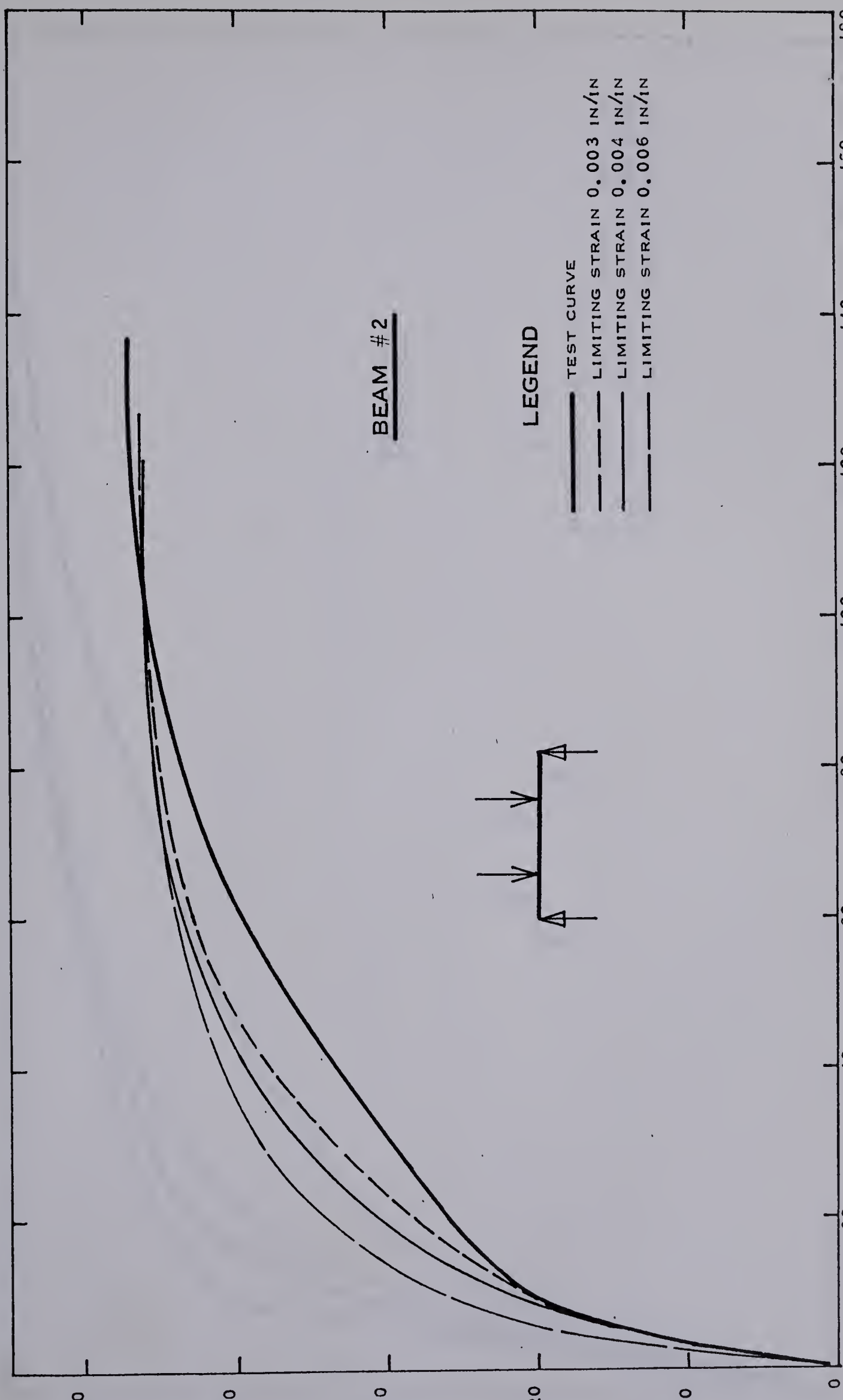

FIGURE 3.26 MOMENT VS. CURVATURE

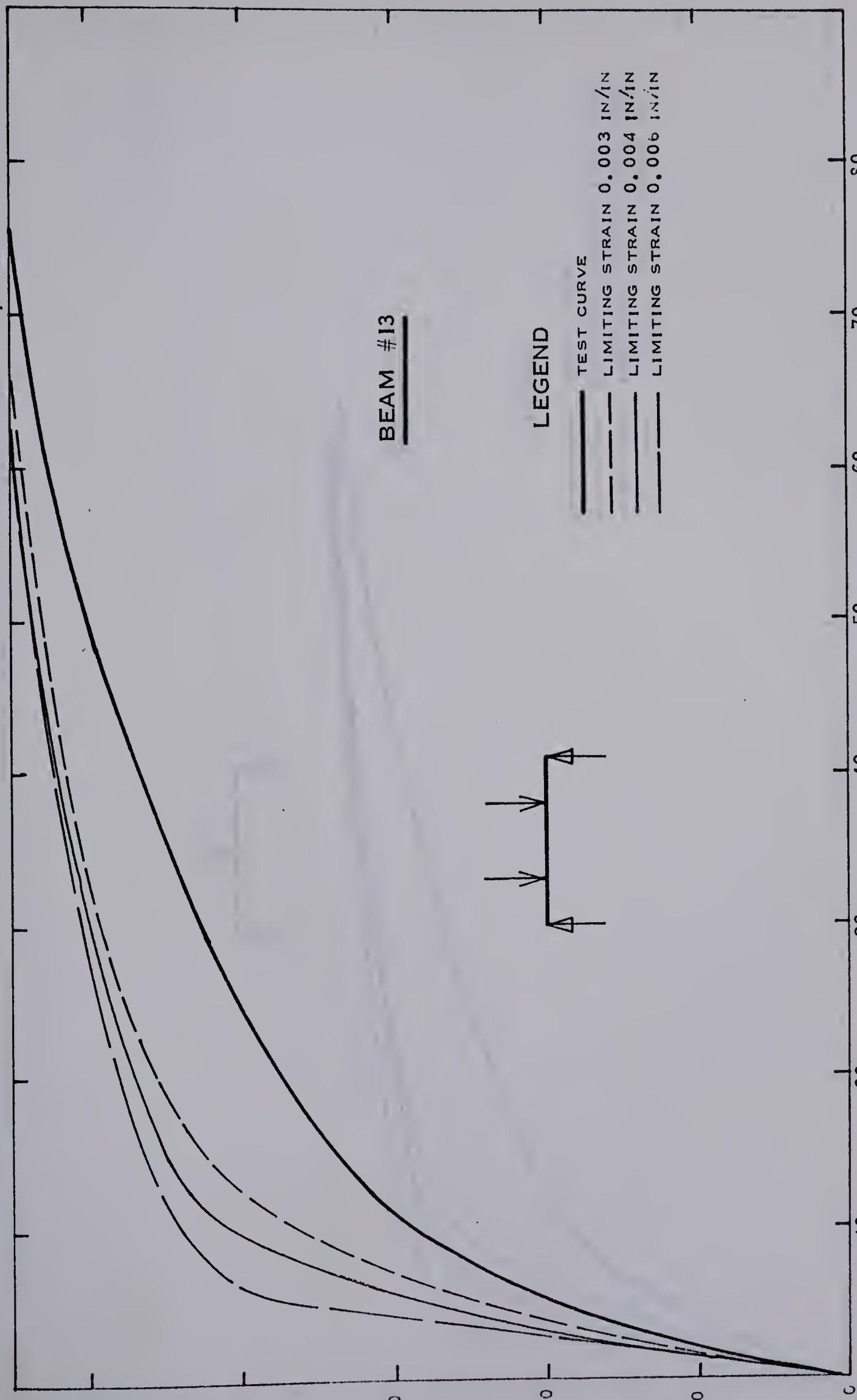

FIGURE 3.27 MOMENT VS. CURVATURE

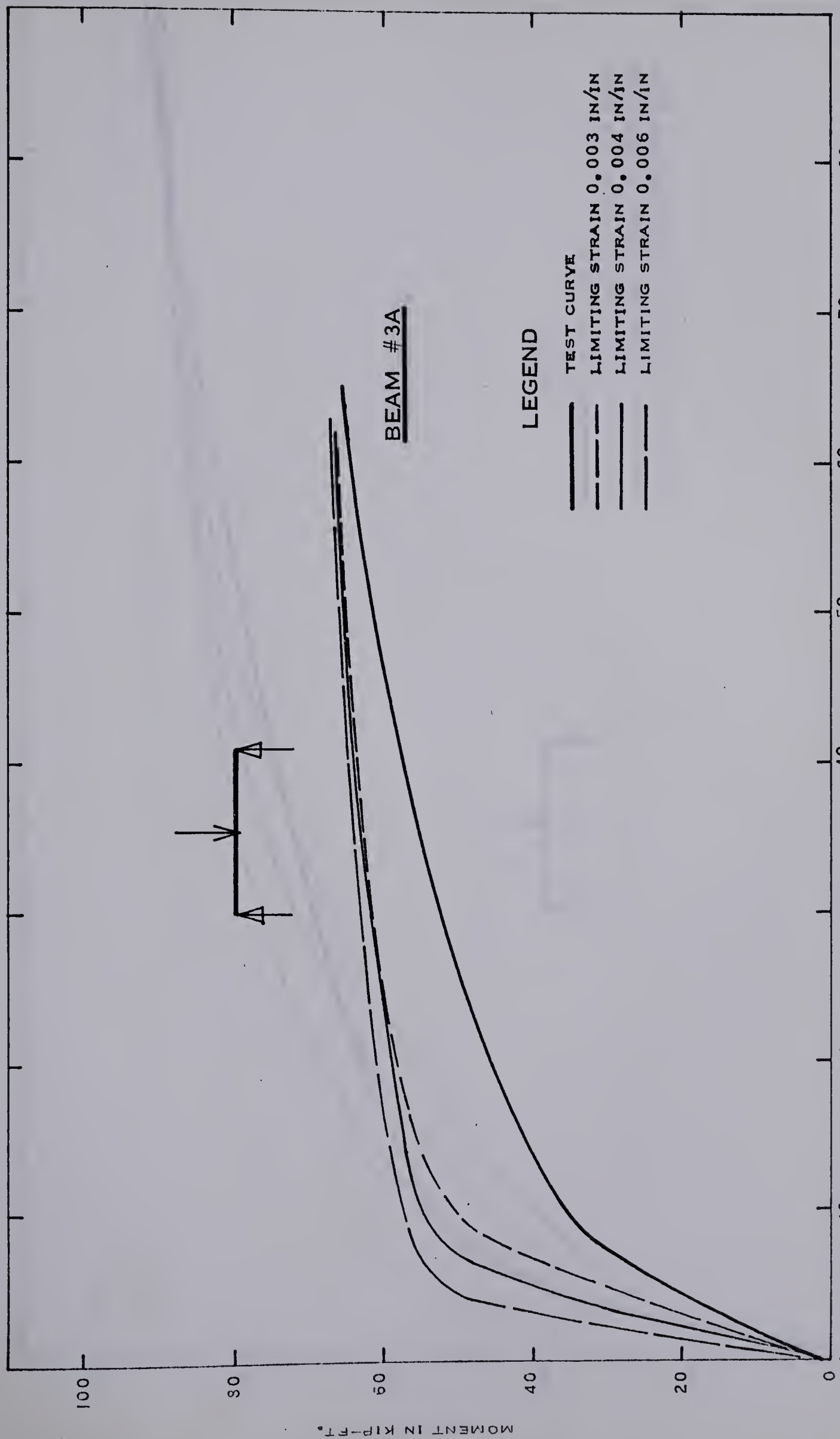

FIGURE 3.28 MOMENT VS. CURVATURE

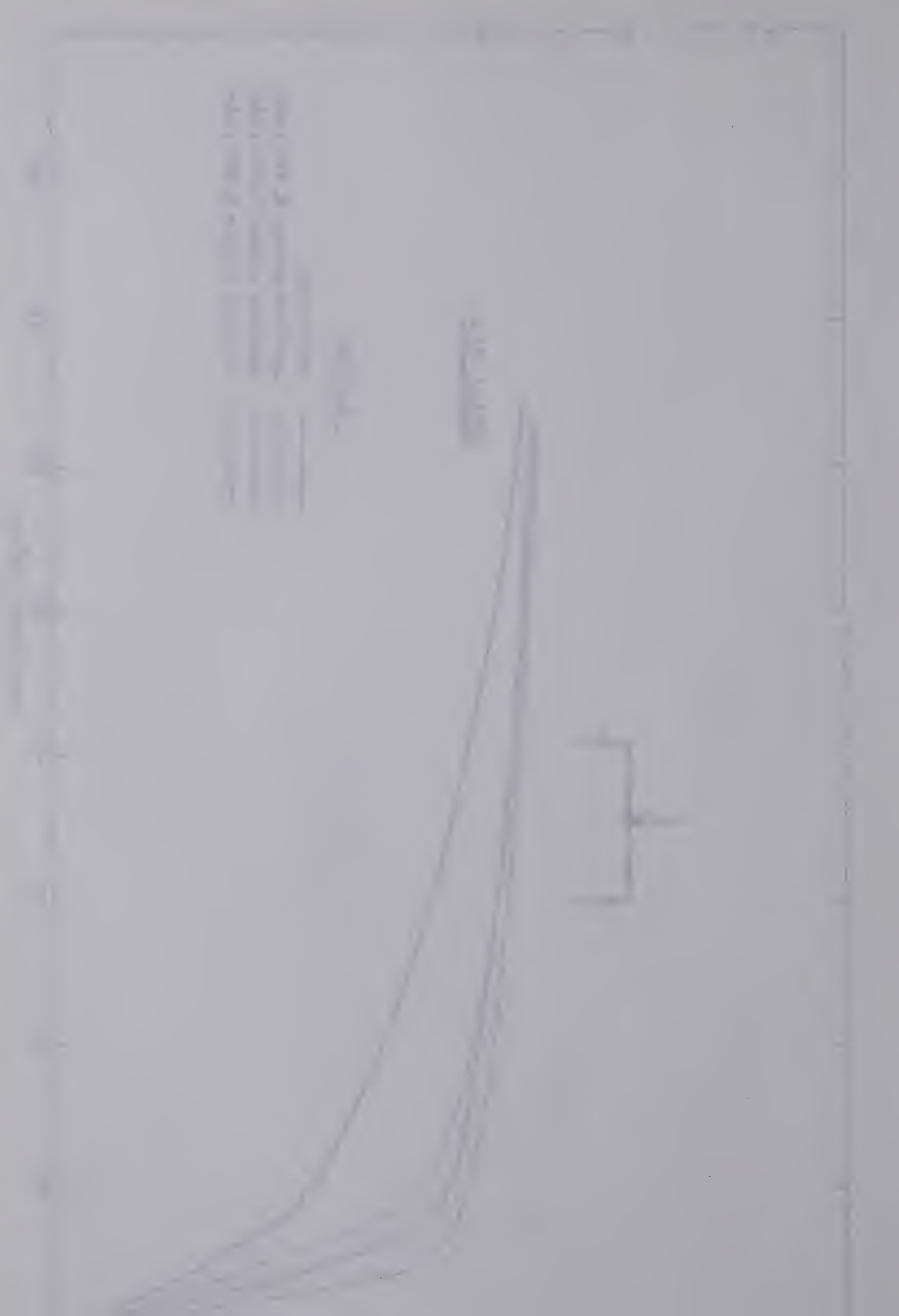

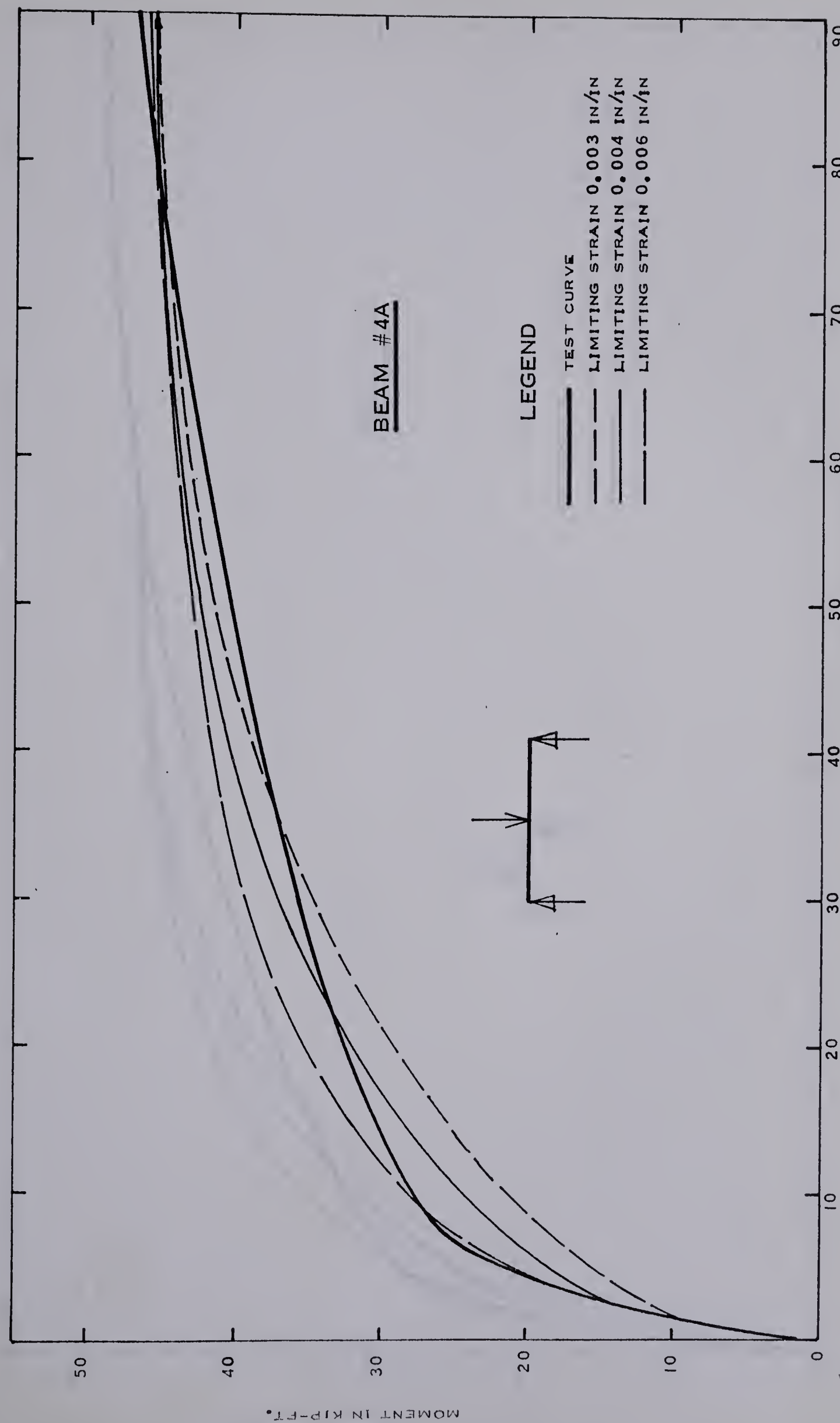

FIGURE 3.29 MOMENT VS. CURVATURE

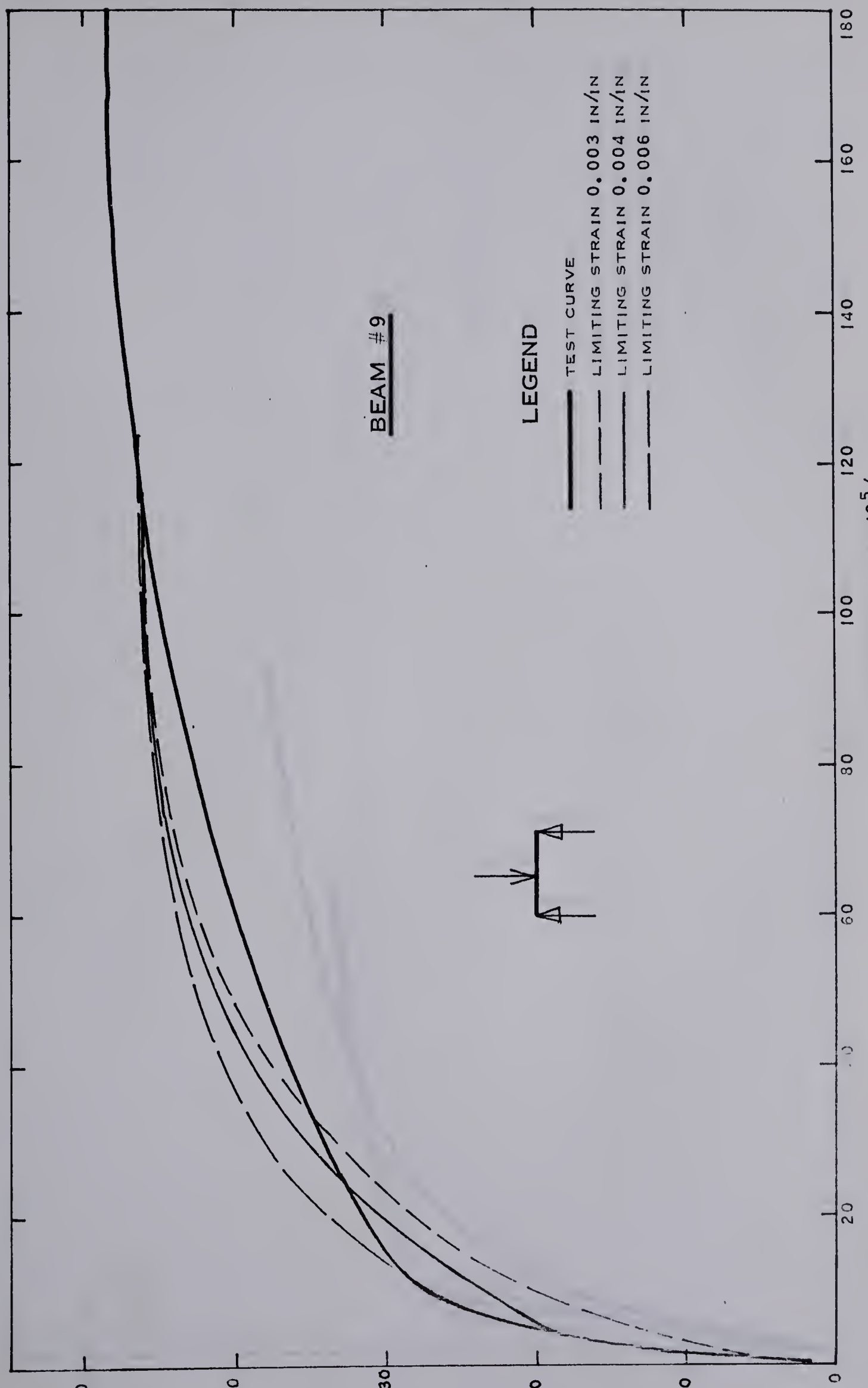

FIGURE 3.30 MOMENT VS. CURVATURE

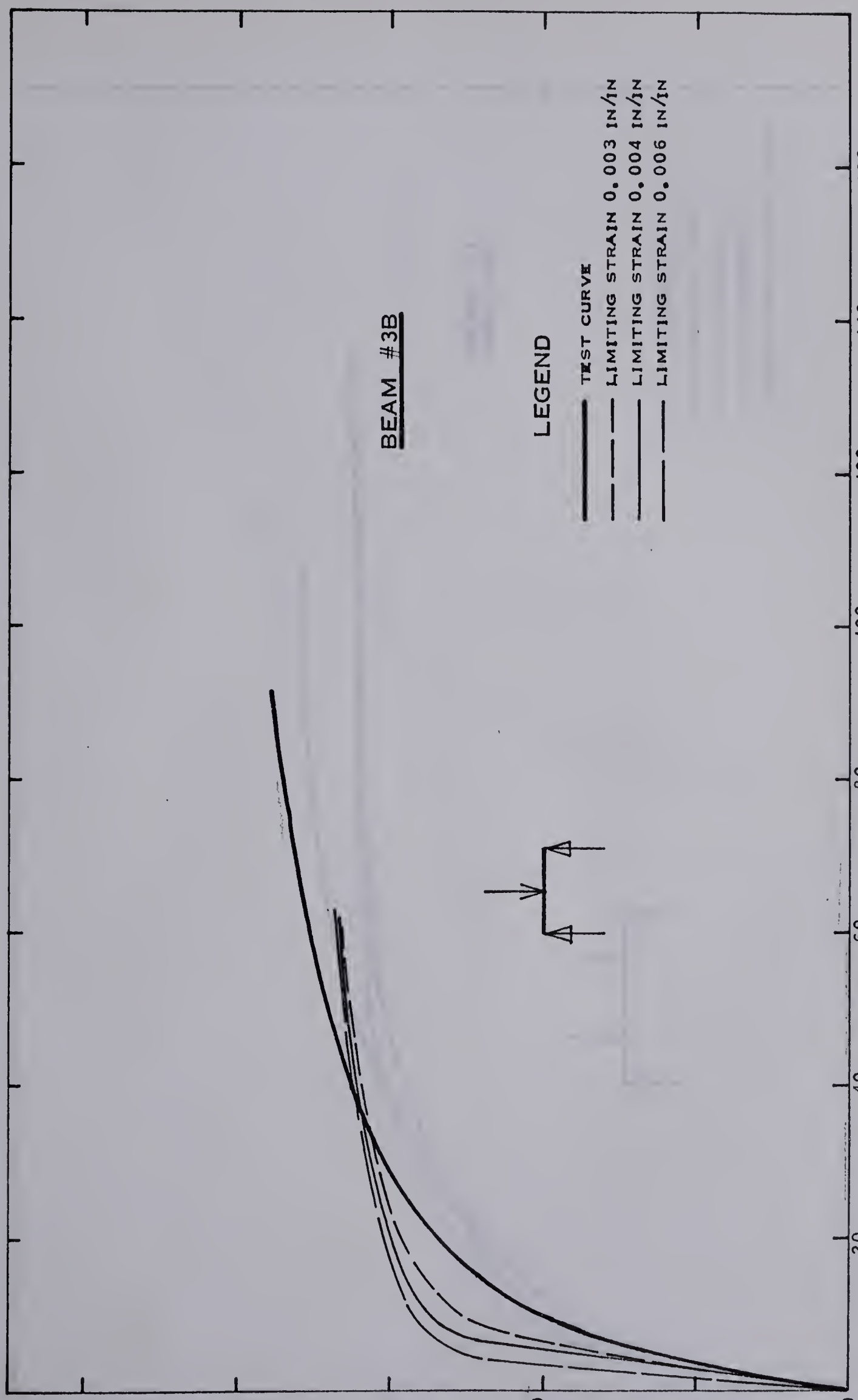

FIGURE 3.31 MOMENT VS. CURVATURE

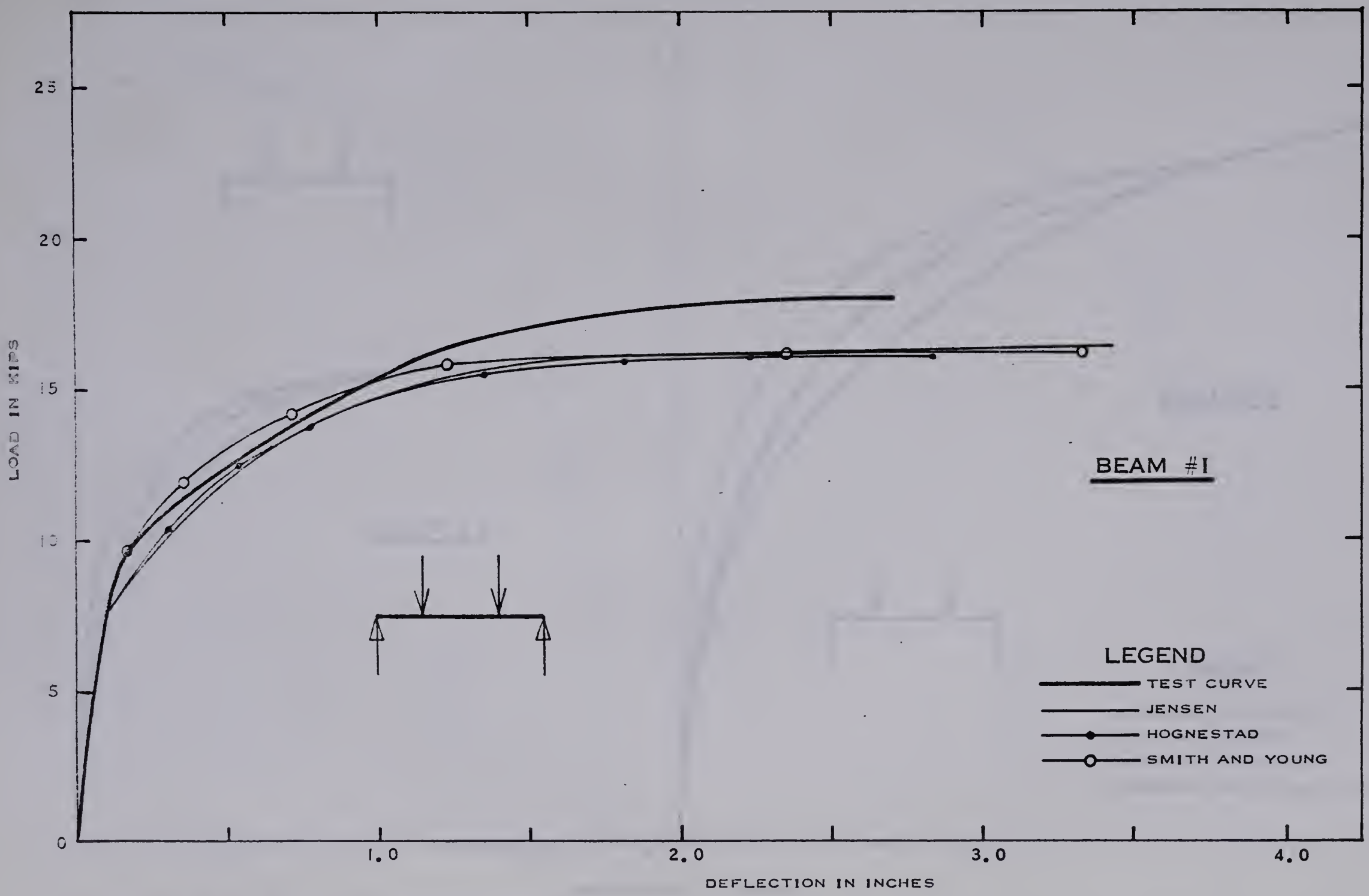

FIGURE 3.32 LOAD VS. MIDSPAN DEFLECTION

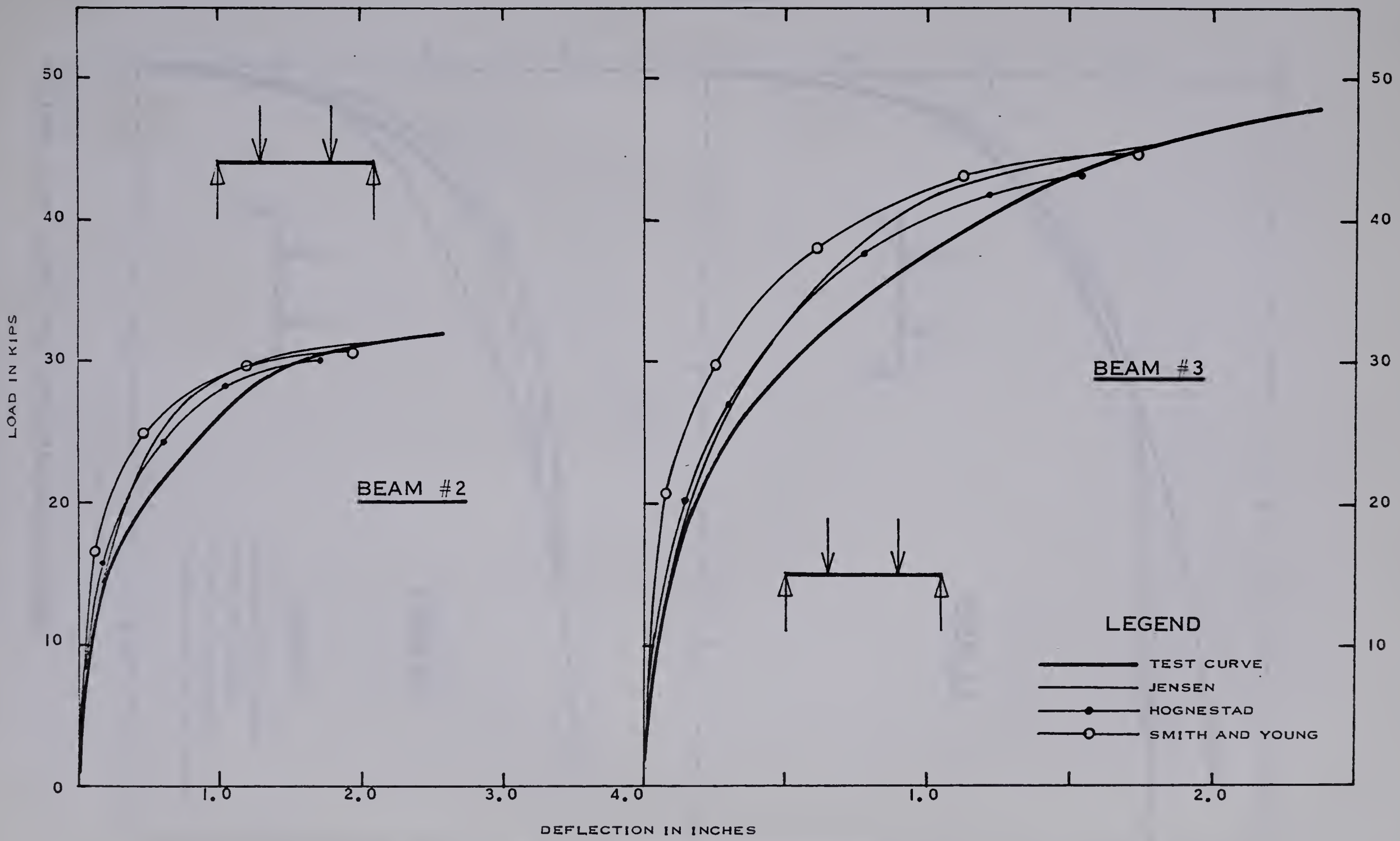

FIGURE 3.33 LOAD VS. MIDSPAN DEFLECTION

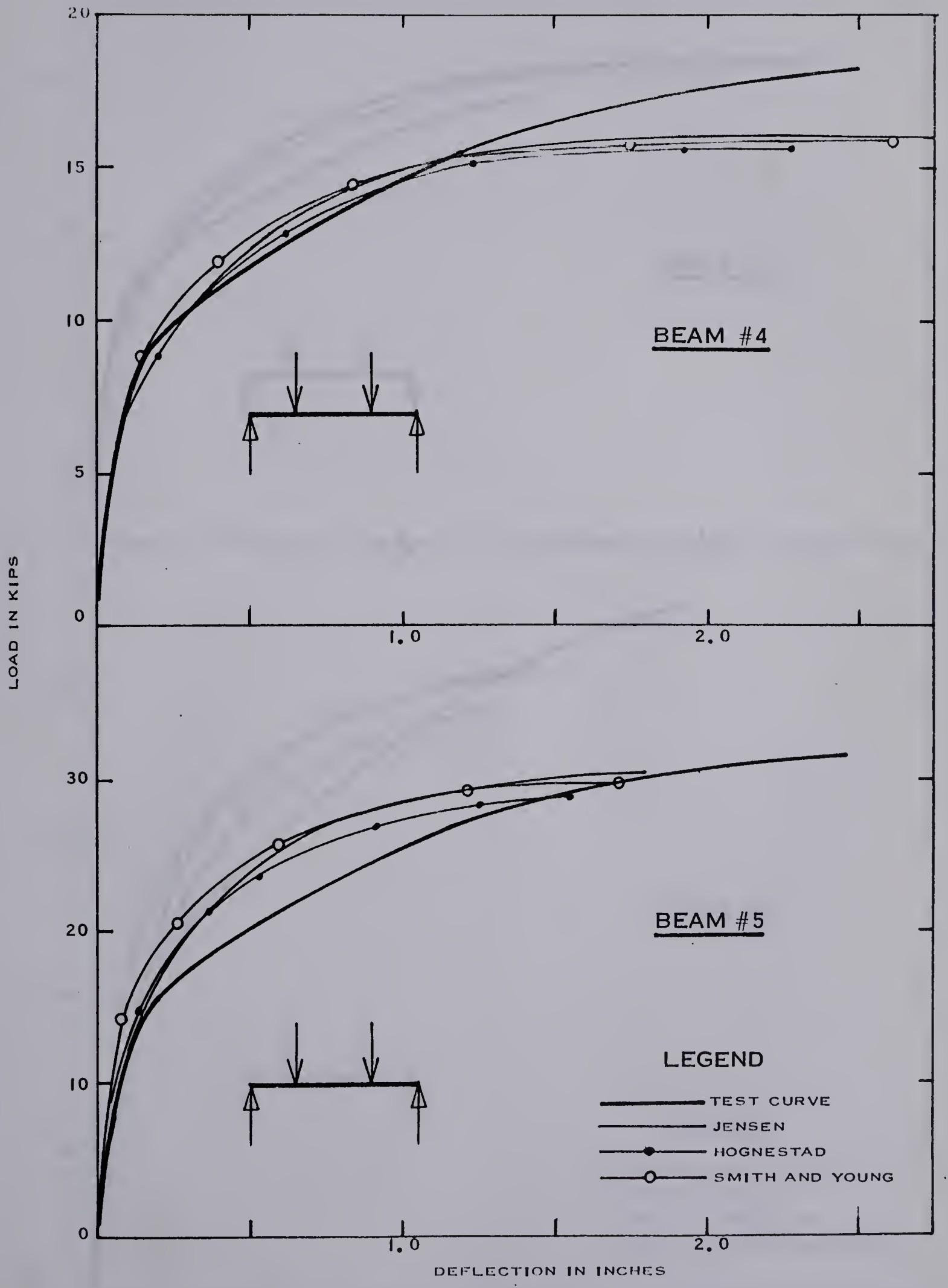

FIGURE 3.34 LOAD VS. MIDSPAN DEFLECTION

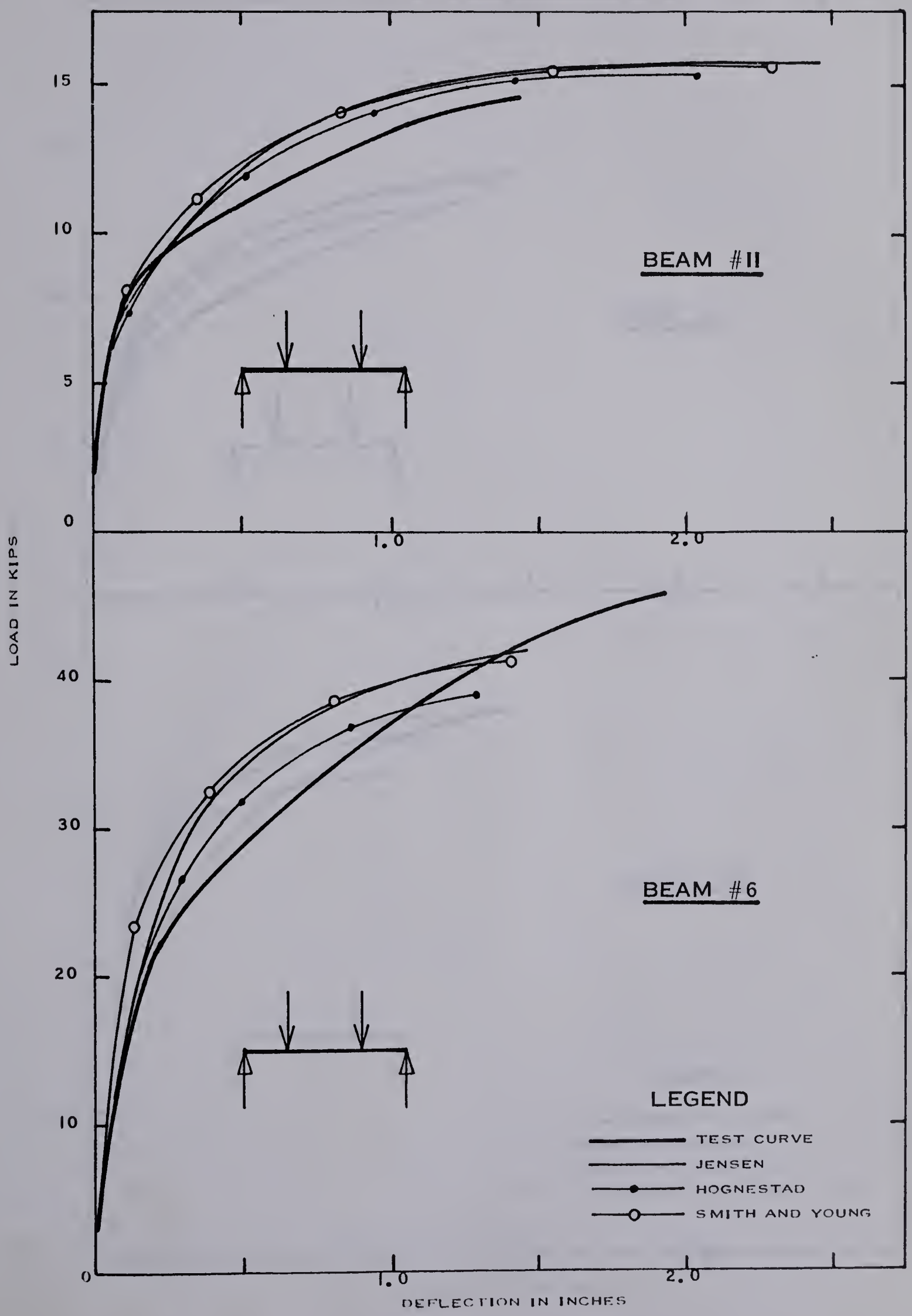

FIGURE 3.35 LOAD VS. MIDSPAN DEFLECTION

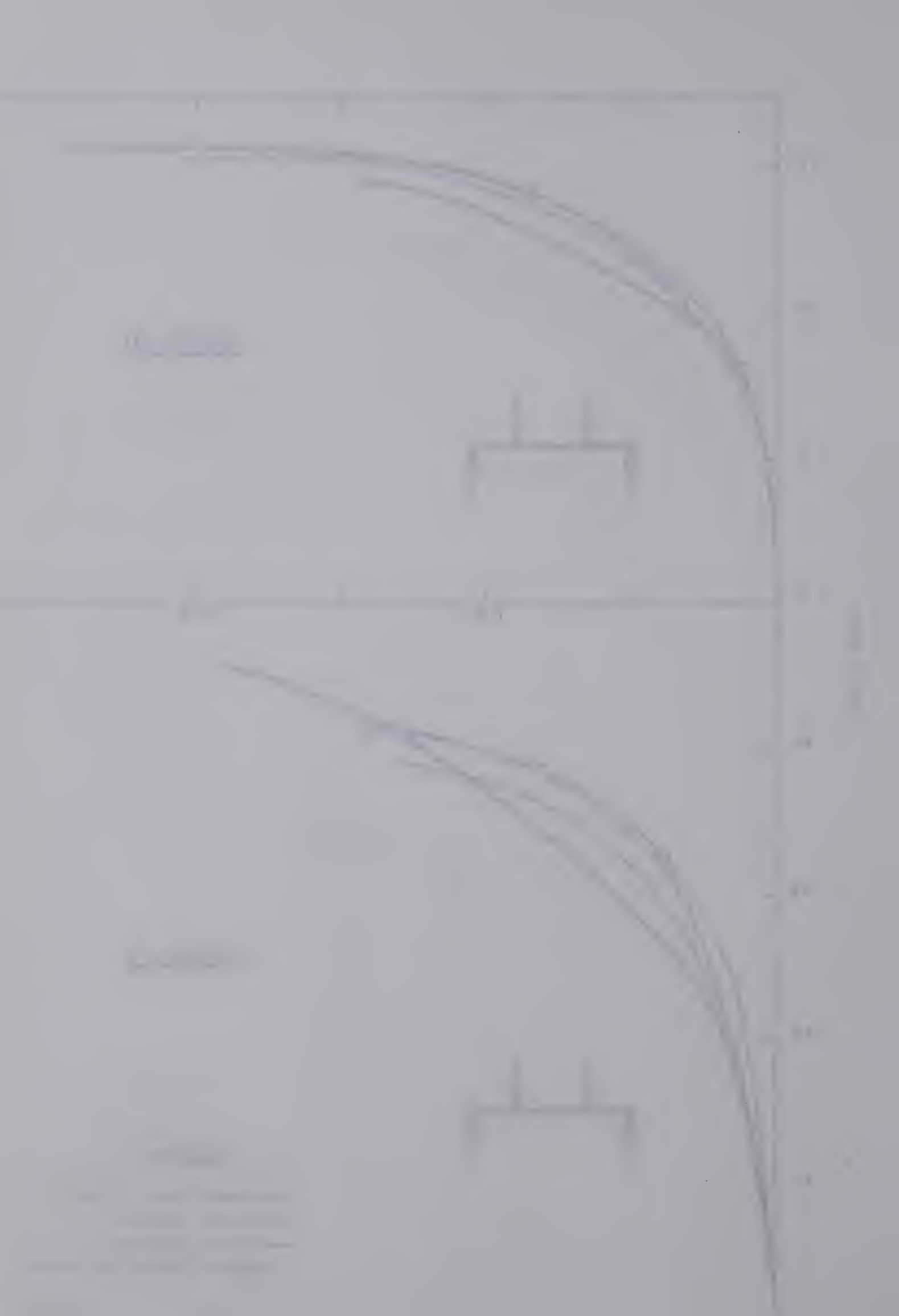

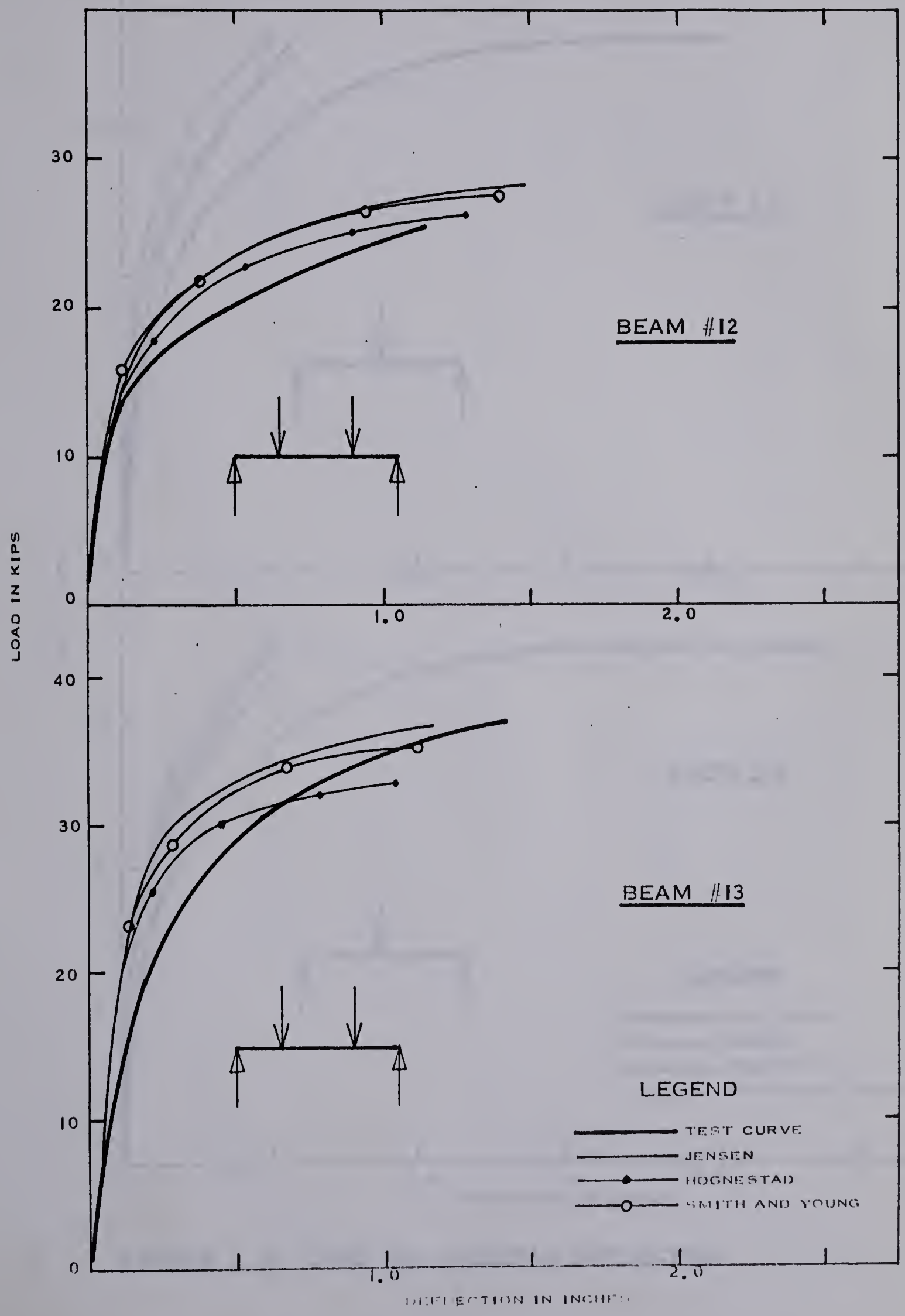

FIGURE 3.36 LOAD VS. MIDSPAN DEFLECTION

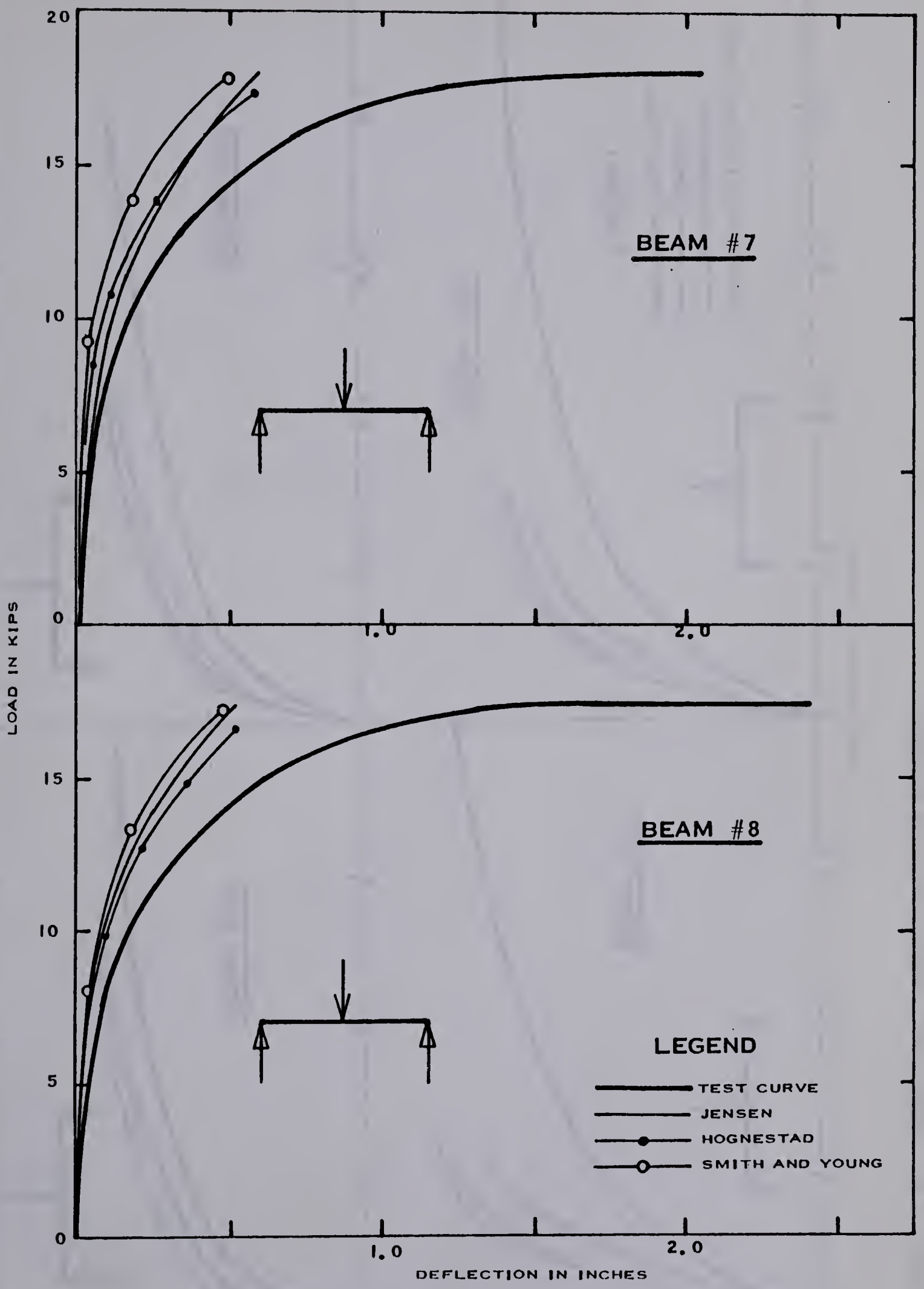

FIGURE 3.37 LOAD VS. MIDSPAN DEFLECTION

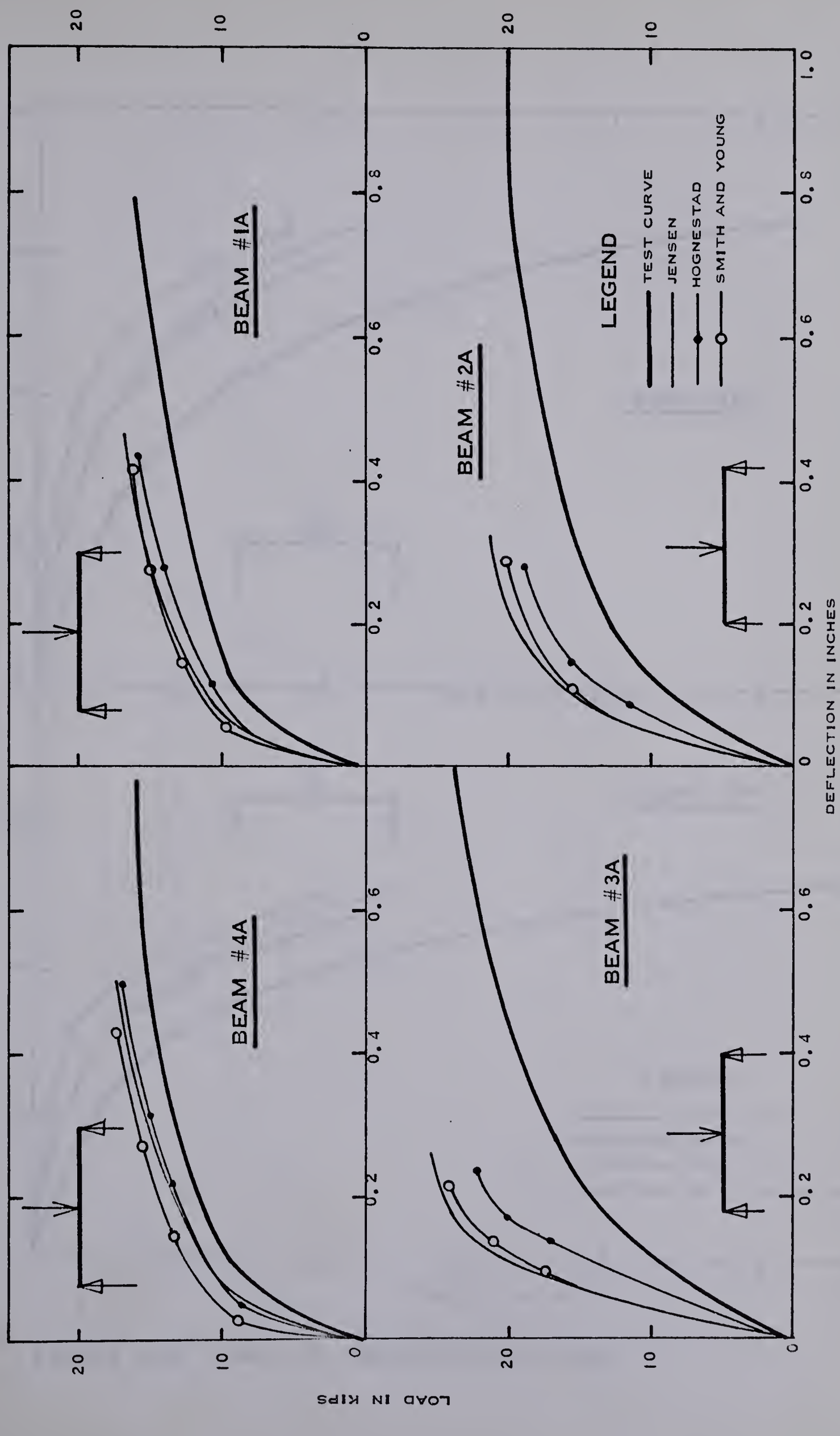

FIGURE 3.38 LOAD VS. MIDSPAN DEFLECTION

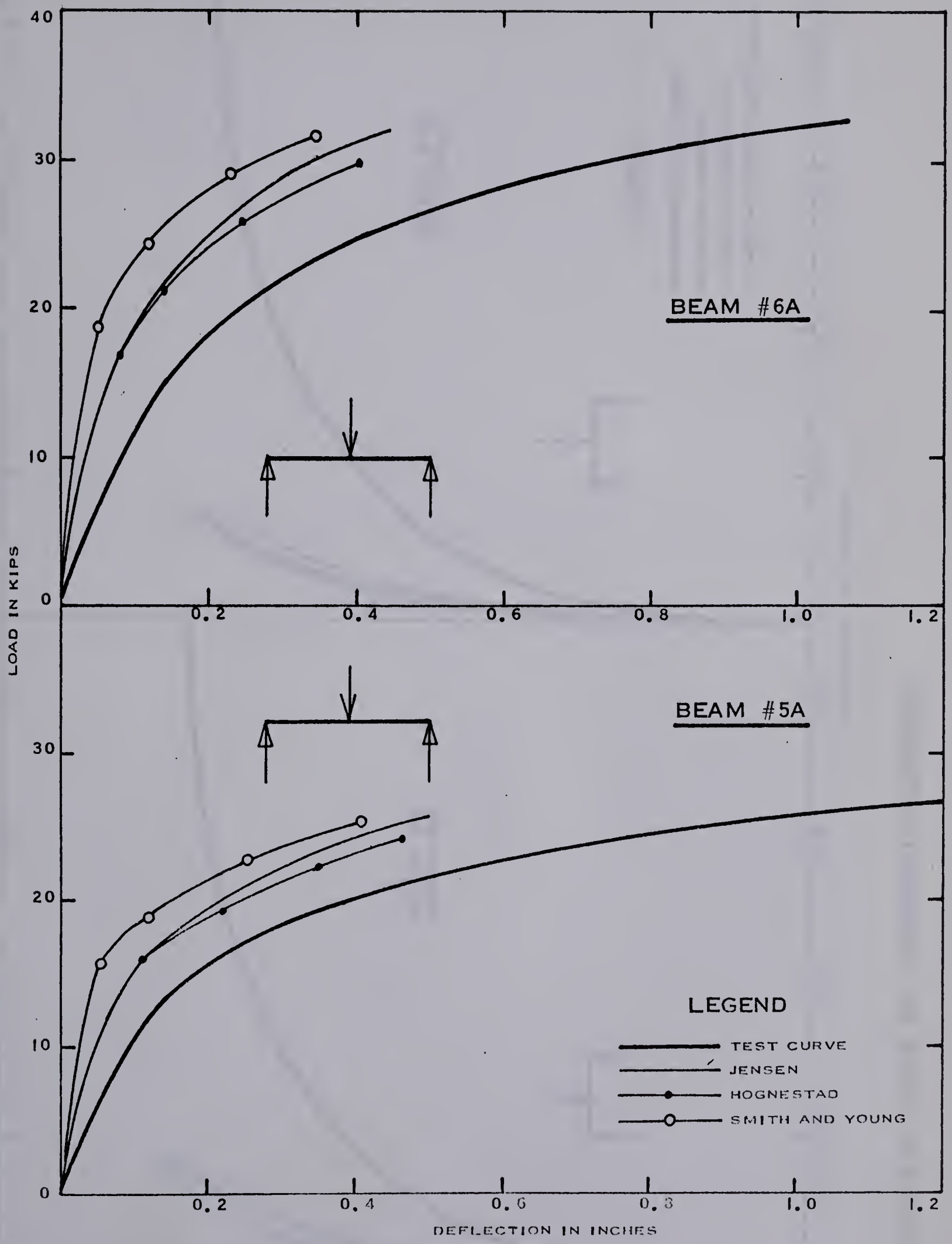

FIGURE 3.39 LOAD VS. MIDSPAN DEFLECTION

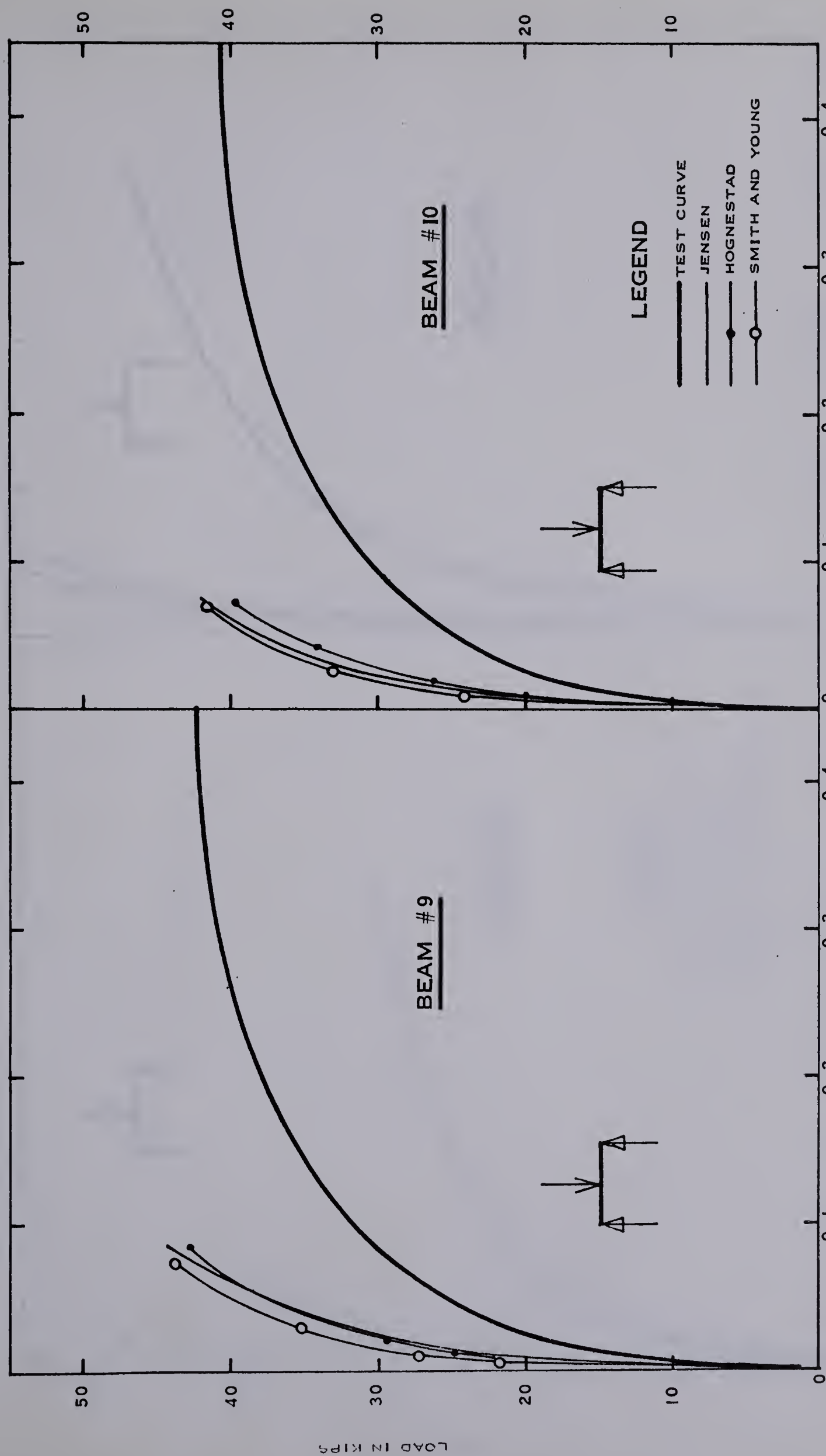

FIGURE 3.40 LOAD VS. MIDSPAN DEFLECTION

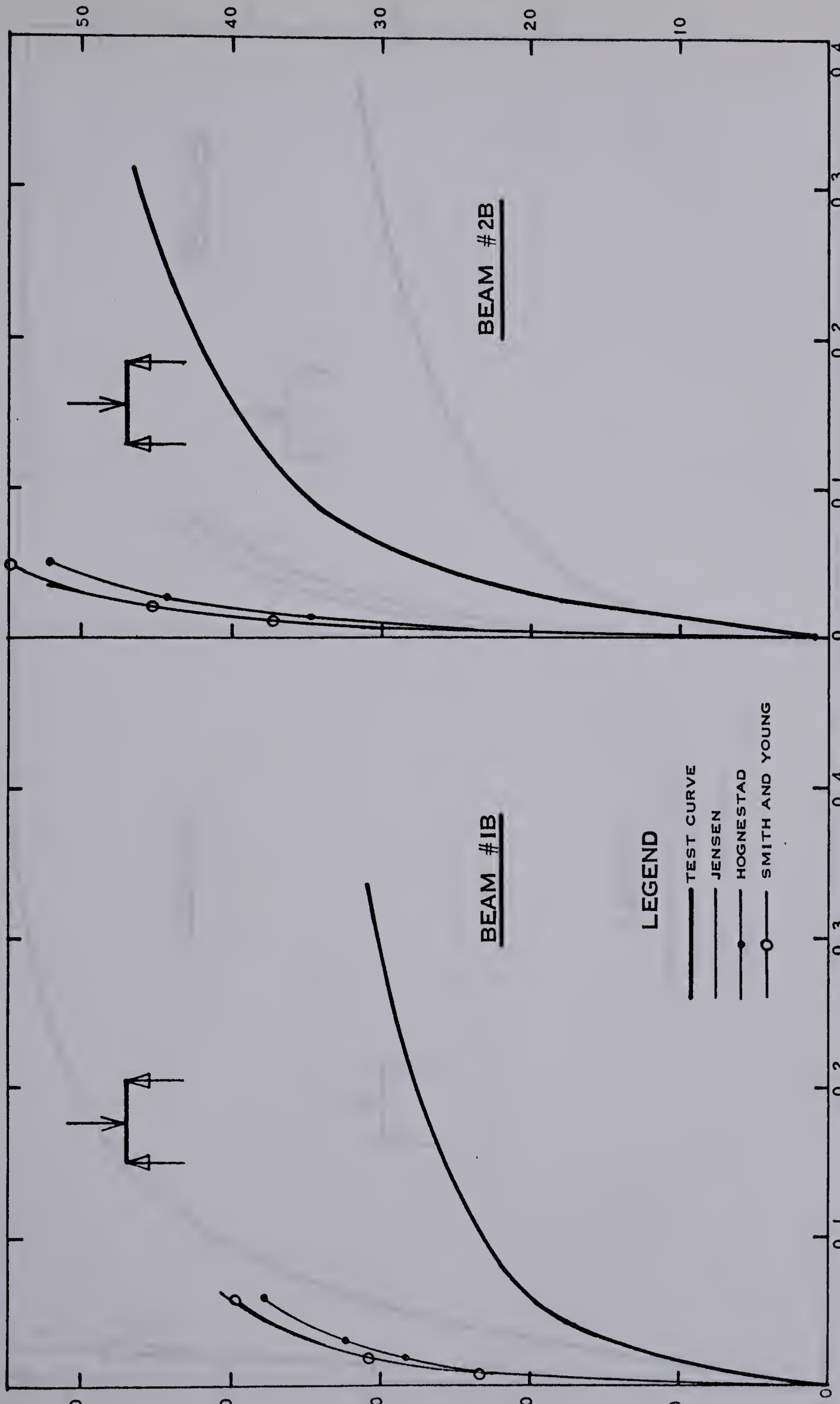

FIGURE 3.41 LOAD VS. MIDSPAN DEFLECTION

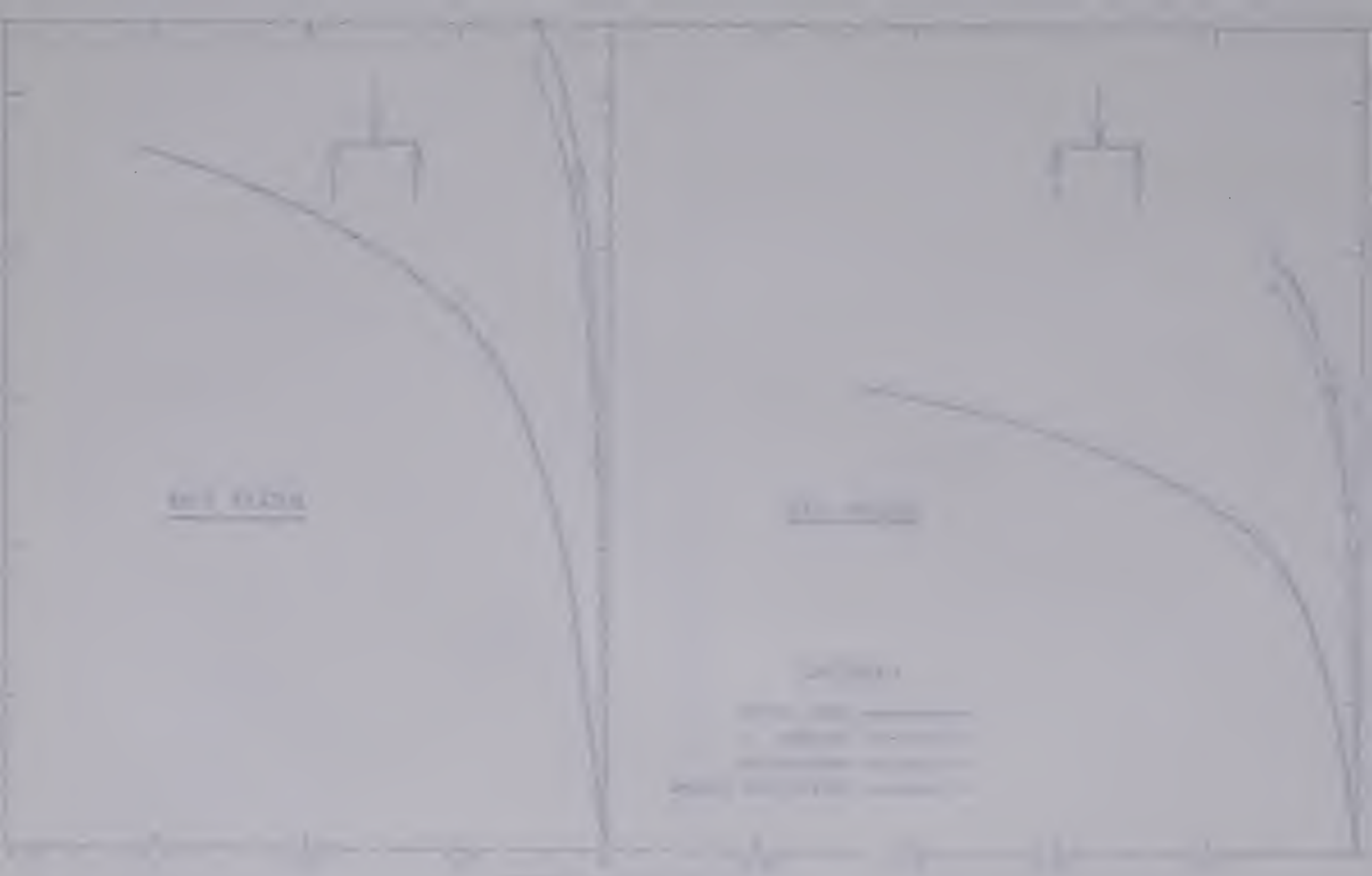

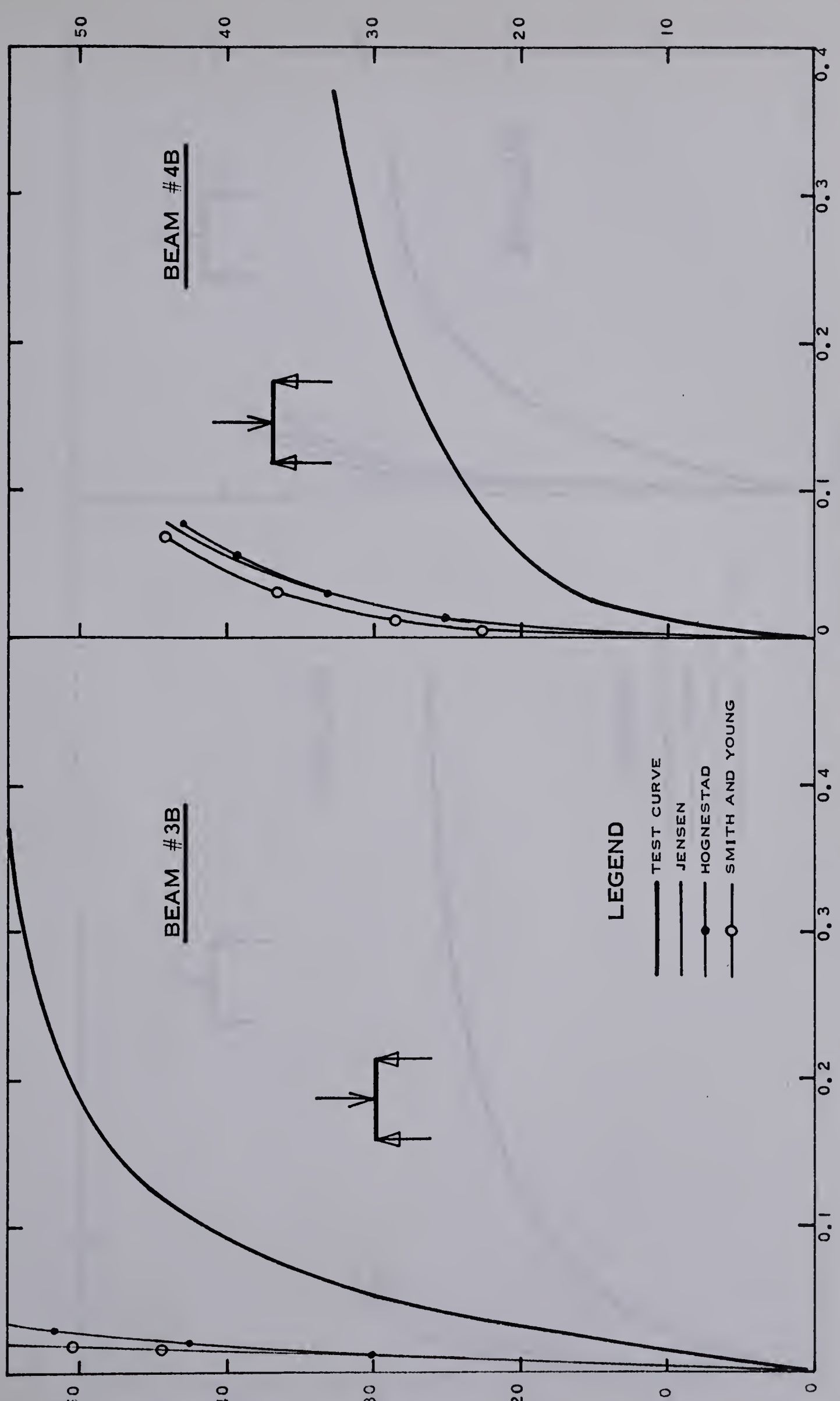

FIGURE 3.42 LOAD VS. MIDSPAN DEFLECTION

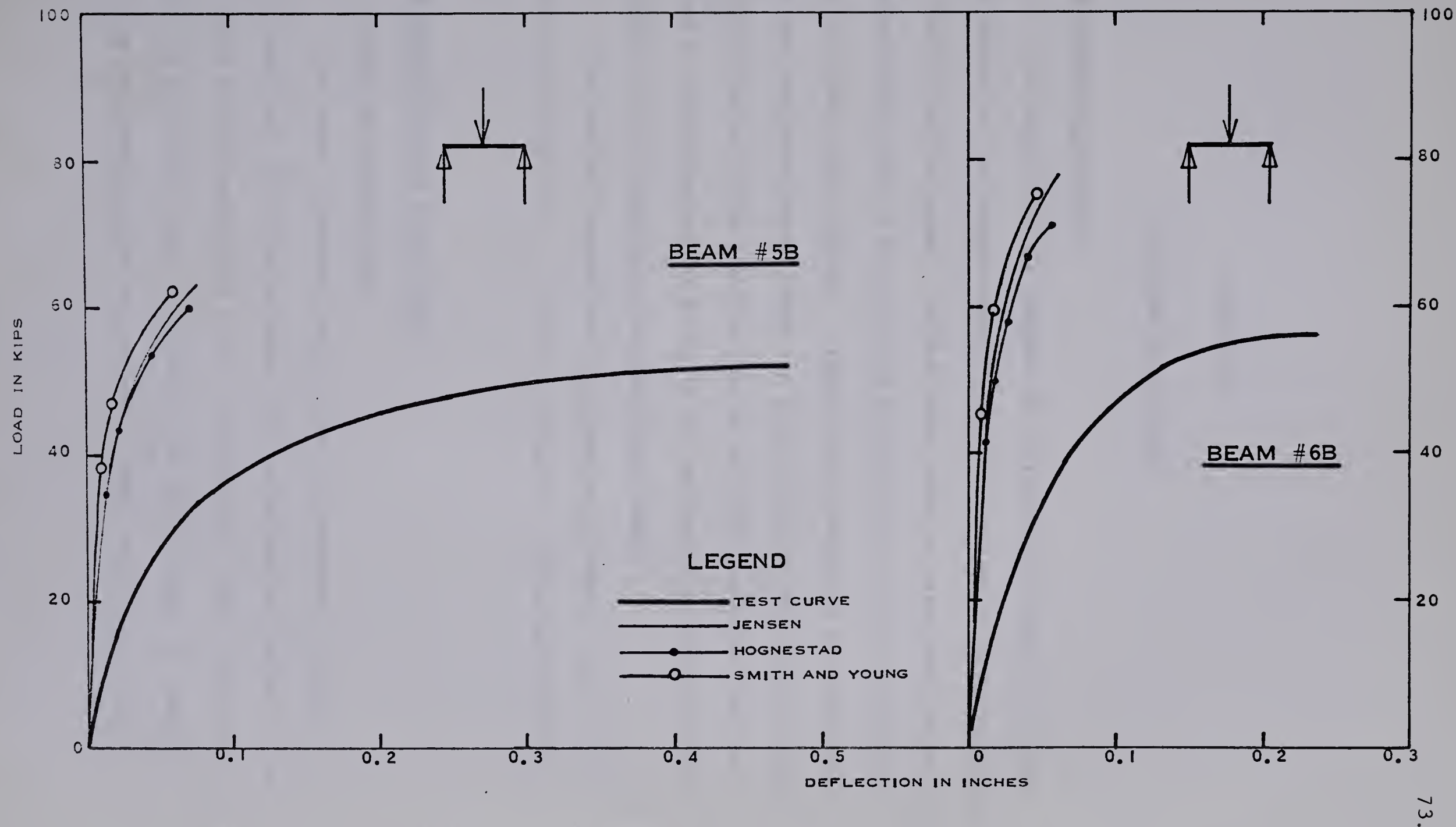

FIGURE 3.43 LOAD VS. MIDSPAN DEFLECTION

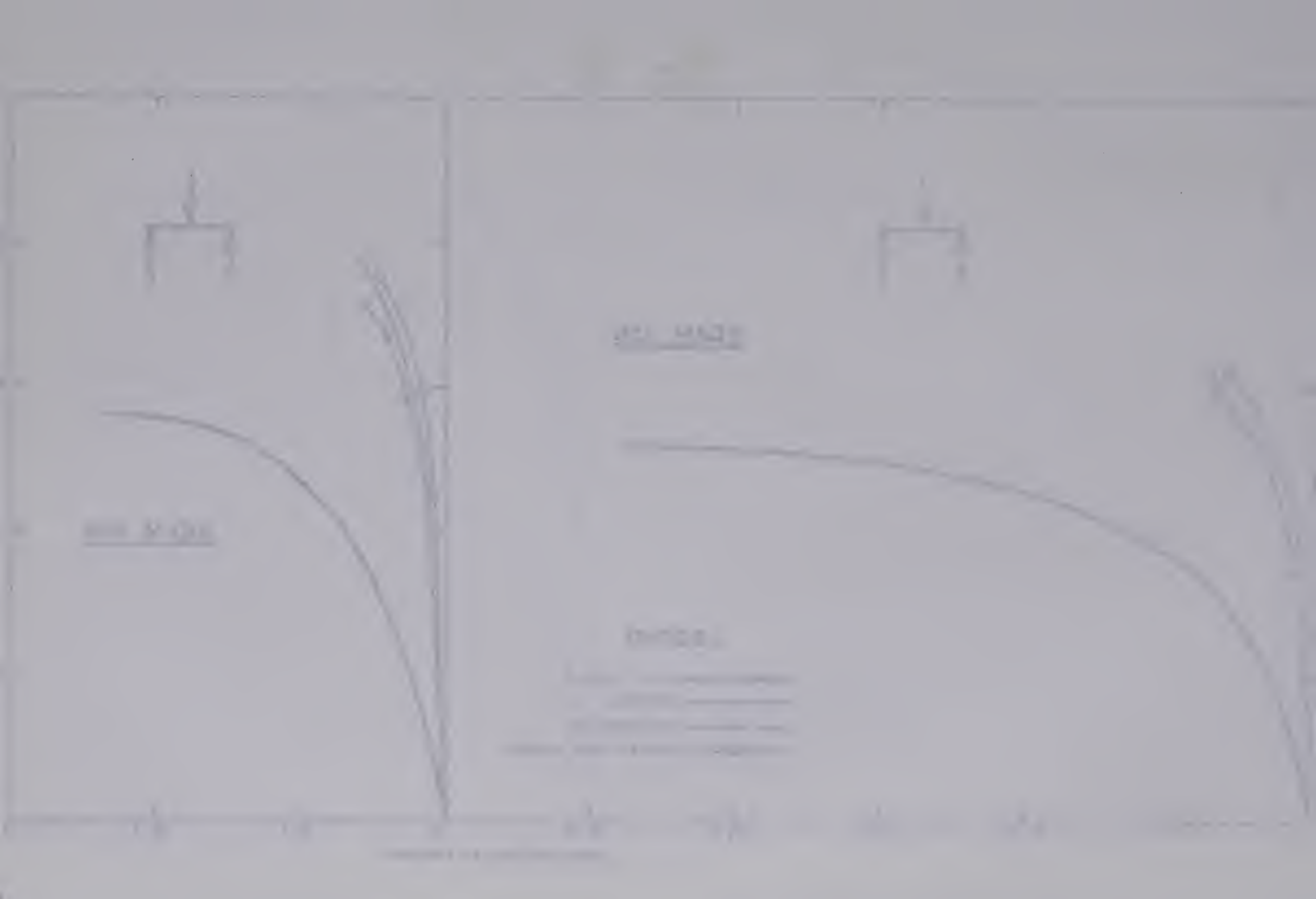

CHAPTER IV

DISCUSSION OF ANALYSIS

4.1 Introductory Remarks

The object of this chapter is to discuss the effect of five stress blocks on the moment-curvature and load-deflection relationships of prestressed concrete beams. The M-Ø curve obtained using each stress block is compared with that of test results and also with the curves obtained using the other stress blocks. A comparison is made for both two-point loaded and one-point loaded beams. A sub-section of this chapter deals with the effect of using limiting strains of 0.003 and 0.006 inch per inch and a Jensen type stress block in the determination of the M-Ø relationship for six representative prestressed beams.

The derived load-deflection curves using three stress blocks are discussed in relation to the load-deflection curves obtained from tests.

4.2 Moment-Curvature Relationship

4.2.1 Effect of Stress Blocks

The moment-curvature relationship illustrated in Figures 3.1 to 3.25 show that the ultimate moments and curvatures predicted by the five stress blocks were within a very narrow band. Most of the variation between the predicted curves occurred in the early stages of loading, just after the cracking load was reached. These variations could be

attributed mainly to the shape of the stress block, and, to a minor extent, to the compatibility factor F, which is described in Appendix A.

The compatibility factor could not greatly affect the shape of the M-Ø curve at the intermediate stages of loading, since the compressive force in the concrete was adjusted to the value of the tensile force in the reinforcement. This condition of equilibrium was attained by varying the depth of the compression face of the concrete. Also, at the cracking load and loads close to the cracking load, the value of F was unity.

The shape of each stress block had a very distinct effect on the initial portion of the M-Ø curve. It has been shown in Chapter II that, for high concrete strength, the stress block proposed by Smith and Young gave a compressive force which was 10 per cent greater than that of a standard cylinder test. This effect is reflected in the M-Ø curves shown in Figures 3.2, 3.3 and 3.10 in which the Smith and Young's curves were well above the other curves, including the actual test curves.

The Hognestad's curves were always below the Jensen's curves, as a result of the difference in the shape of the proposed stress-strain curves. In Reference (3), a maximum stress of 0.85 f'_c was assumed. This value was based on the results of tests of vertically-cast, concentrically loaded columns. Such columns had varying concrete strengths from the top to the bottom because of the difference in the degree of compaction during casting. In the case of beams in flexure only, it is possible that sufficient redistribution could occur to allow the attainment of the maximum concrete stress f'_c . Thus, it would appear that the Jensen's curves are a closer approximation of the true M-Ø curves for the reasons mentioned above.

The PCA curves followed Hognestad's curves in the intermediate stages for high f'_c . For low f'_c , the curves predicted by the PCA stress block followed the M-Ø curves of Smith and Young. This characteristic could again be attributed to the shape of the stress-strain curve. The PCA equations for stress-strain curves provided a maximum stress of about 0.85 f'_c for high concrete strength and a maximum stress equal to f'_c for concrete strength of 3500 psi and lower.

4.2.2 Two-Point Loaded Beams

Figures 3.1 and 3.4 show that the predicted ultimate moments for beams 1 and 4 were only about 90 per cent of the actual ultimate moments and the predicted $Ø_u$ were about 50 per cent greater than the actual ultimate curvature. The increase in the predicted $Ø_u$ over the actual values was a result of the beams being very under-reinforced so that failure was caused by fracture of the reinforcement. The difference between $M_u$calc and $M_u$test could be attributed to the possibility of the beam failing when the extreme fibre strain in the concrete was less than 0.004 inch per inch. The strain distribution may have been such that the stress block in the concrete at the time of failure was almost triangular in shape. This condition would provide a larger moment arm and, in turn, a larger moment. The predicted M_u for beam 11 (Figure 3.7), which failed by fracture of the reinforcement, was 5 per cent greater than the actual M_u from the test. The reason for this difference could be that individual strands of the cable broke prematurely, thus reducing the effective area of steel in the beam.

On all the M-Ø curves for the two-point loaded beams, there was a definite flattening of the test curves in excess of that of the theo-

retical curves, just after cracking was initiated. The flattening of the derived curves was due to a reduction in the stiffness of the beam. The excess flattening of the test curves could have been caused either by creep or by unbonding of the reinforcement. Since the beams were tested to failure within a three-hour period, it is unlikely that creep would affect the curvature except at stages near the ultimate condition. Thus, it would seem that unbonding was the major cause of the excess flattening effect of the M-Ø curve obtained from tests. This argument can be substantiated by examining Figures 4.17 and 4.20 in Reference (1). Figure 4.17 illustrates horizontal cracks occurring outside the flexure span on beam 13 at the level of the reinforcement. The load at which the horizontal cracks occurred was 9 kips and the failure load was 38.3 kips. Similarly on beam 12 in Figure 4.20 (1), horizontal cracks occurred at loads of 11 to 13 kips whereas the actual failure load was 28.3 kips. Thus, horizontal cracking at the level of the reinforcement initiated unbonding, which in turn caused the strain in the reinforcement to be distributed over the unbonded length. In order to maintain equilibrium in the flexure span, the beam deflected further so that a tensile force was established which was compatible with the concrete compressive force and the external loads.

4.2.3 One-Point Loaded Beams

For the one-point loaded beams having an eleven foot span, the ultimate moment could be predicted accurately but the corresponding $\emptyset_u$ was always smaller than those of the actual beam tests. The only exception was beam 4A which failed by fracture of the reinforcement. For

the five and one-half foot beams, the predicted $\emptyset_u$ were much smaller than the ultimate curvatures obtained from test results. The excess curvature of the test beams could have been caused by unbonding, shear deflection and possibly creep at higher loads.

Unbonding was probably the major cause of the increased curvature for all the one-point loaded beams. In the case of the short beams, as soon as inclined cracks were formed, there was hardly enough anchorage length available to prevent unbonding of the reinforcement. Thus, an unstable condition was reached at an early stage. For the long beams, horizontal cracks developed along the level of the reinforcement at loads which were about 50 per cent of the ultimate load. For example, Figure 4.16 in Reference (1) shows beam 1A with horizontal cracks occurring at a load of 8 to 10 kips. This beam eventually failed at a load of 17.6 kips. Thus, it appears that the excess curvature exhibited by the M-Ø curves obtained from test data was caused by the beam deflecting to maintain equilibrium after horizontal cracking occurred. Shear deflection was difficult to measure because the occurrence of flexure cracks changed the stiffness and cross-sectional area of the beam. Shear deflection is appreciable only in cases of beams with small L/d ratios (less than 5). When cracking takes place, the L/d ratio tends to increase. Thus, the curvature due to shear deflection was probably less than 10 per cent. Additional curvature due to creep could have occurred only at a stage approaching the ultimate load, since the tests were performed at a fast rate.

4.2.4 Effect of Limiting Strain

The effect of varying the limiting strain ϵ_u , on the predicted ultimate moment and curvature was not appreciable. Three different ultimate conditions were assumed; these corresponded to limiting strains of 0.003, 0.004 and 0.006 inch per inch in the extreme compression fibre of the concrete. The ultimate moments and corresponding curvatures obtained from using these three limiting conditions were essentially the same. The M-Ø curve obtained using a limiting strain of 0.006 inch per inch was much flatter in the intermediate stage than the curves obtained using limiting strains of 0.003 or 0.004 inch per inch. This phenomenon seems to indicate that the maximum moment corresponding to a limiting strain of 0.006 inch per inch was attained at a strain less than the limiting strain. The difference between the ultimate curvatures corresponding to limiting strains of 0.004 and 0.006 inch per inch was very small, because the compatibility factor, F , at the ultimate condition decreased as the ultimate strain increased. It should be noted that the ultimate strain ϵ_u implies a concentrated strain in the extreme concrete fibre above a crack. The strains in the top fibre between cracks are usually smaller than this strain. Thus, the average strain along the compression face of the concrete tends to remain constant, being defined as $F\epsilon_u$.

In all cases, it appears that an ultimate strain of 0.004 inch per inch is a good average value for the purpose of analysis. Such an average value of ϵ_u can be chosen because some beams may have a high concrete strength and a low value of p/f'_c . These beams would behave in a ductile manner, yet it is doubtful whether an ϵ_u greater than 0.004

inch per inch would be realized. In the case of a beam with a high p/f'_c value and low concrete strength, the behaviour is less ductile than that of a beam with low p/f'_c . Thus, although concrete strains in excess of 0.004 inch per inch are possible, failure will be a compression type with the maximum moment occurring at a strain of about 0.004 inch per inch. The amount of strain which the beam can carry beyond 0.004 inch per inch depends partly on the rate of strain and partly on the amount of stress redistribution which takes place in the compression zone of the concrete.

4.3 Load vs Midspan Deflection

4.3.1 Two-Point Loaded Beams

For the two-point loaded beams, the load-midspan deflection curves had the same shapes as those of the corresponding M-Ø curves. Again it was noted in Figures 3.32 to 3.36 that there was some excess flattening of the test curves just after cracking occurred. The reasons for the flattening have already been discussed in section 4.2.2.

The ratio of $\emptyset_u calc/\emptyset_u test$ were always slightly higher than the corresponding ratios of $\triangle_{calc}/\triangle_{test}$, but were still within the same range of values. This difference could be a result of rounding-off in the $\emptyset_u$ test values (1), which were not obtained from the results of this investigation. Table 3.4(a) shows beams 11 and 12 with ratios $\triangle_{calc}/\triangle_{test}$ higher than the corresponding ratios $\emptyset_u calc/\emptyset_u test$. This discrepancy appears because the last deflection readings corresponding to $\emptyset_u test$ were not recorded during the tests since an unstable condition was reached when the deflection was increasing under a constant load.

4.3.2 One-Point Loaded Beams

For the long one-point loaded beams (Figures 3.37 to 3.39), the predicted deflections at midspan using any one of the five stress blocks were always smaller than the actual deflections. The ratios $\Delta_{calc}/\Delta_{test}$ shown in Table 3.4(b) were always smaller than the values of $\phi_u calc/\phi_u test$ shown in Table 3.3(b), except in the case of beam 1A in which the last deflection corresponding to $\phi_u test$ was not recorded.

For the short one-point loaded beams, the ratios of $\Delta_{calc}/\Delta_{test}$ obtained were very much smaller than the corresponding $\phi_u calc/\phi_u test$. This difference was a result of additional deflection induced by unbonding together with the development of shear and diagonal tension cracks.

It was difficult to predict the midspan deflection for the one-point loaded beams since there was no definite point-at the centre of the beam where the maximum curvature could be assumed. The maximum curvature for the two-point loaded beams was assumed constant across the flexure span. On the other hand, for the one-point loaded beams, crushing of the concrete was assumed to take place just outside the edge of the 6 x 6-in. loading plate because of the biaxial stress condition under the plate where stresses higher than f'_c were possible. Thus, at ultimate condition, the curvature was derived for a point just at the edge of the loading plate. It would be unrealistic to assume that the beam was homogeneous and apply a concentrated curvature value over the portion of the beam under the loading plate, since the formation of flexure-shear cracks close to the loading plate would disrupt this condition. However, even if the ultimate curvature were applied over the 6-inch length occupied by the

loading plate, the ultimate deflection obtained at midspan would still be less than the measured value because of unbonding.

CHAPTER V

SUMMARY, CONCLUSIONS AND RECOMMENDATIONS

5.1 Summary

Six proposed stress blocks were used to derive the moment-curvature (M-Ø) relationship of prestressed concrete beams, using the method described in Reference (12). The results of the analysis were compared with the results of tests on twenty-five prestressed beams at the University of Alberta (1), (9). The load-midspan relationship was obtained using the conjugate beam method. This derived relationship was also compared with the measured load-midspan deflection relationship.

Instead of the cracking moment proposed in Reference (12), a moment corresponding to the stage at which the neutral axis was at the level of the reinforcement was used. With this modification, more consistent moment-curvature relationships were obtained for points just beyond cracking.

5.2 Conclusions

The method of analysis proposed in Reference (12) predicted the moment-curvature (M-Ø) relationship at all stages of loading for the two-point loaded beams. At the stage near the ultimate condition, the M-Ø curves using all six stress blocks converged into a narrow band, such that the predicted ultimate moments were virtually the same.

For the one-point loaded beams, the ultimate moment could be

predicted accurately; the corresponding curvature predicted was always much less than the curvature obtained from strain measurements in the actual tests. Unbonding of the reinforcement was the major cause of the increased deflection which, in turn, influenced the increased curvature.

The load-midspan deflection obtained from this analysis for the two-point loaded beams showed close agreement with the measured load-midspan deflection relationship. In the case of the one-point loaded beams, the predicted deflection was always smaller than the observed deflection. This effect was amplified on the short one-point loaded beams.

An ultimate strain of 0.004 inch per inch can be considered to be a good average value for purposes of analysis. The test curves were best approximated using this value of ϵ_u together with the compatibility factor, F, given in Reference (12). The product $F\epsilon_u$ is an essential factor in predicting the ultimate moments and curvatures. All other points on the M-Ø curves between the cracking and ultimate stages of loading depend on the use of a compatibility factor varying from unity at cracking to some known value less than one at the ultimate condition.

For all the predicted M-Ø curves there was a smooth transition from the cracking moment to the ultimate moment. In the initial and intermediate stages of loading, the shape of the predicted M-Ø curves was directly related to the shape of the assumed stress block.

5.3 Recommendations

From the results obtained in this study, it appears that a Jensen type stress block is best suited for moment-curvature analysis

of prestressed beams because of its close prediction of the test curve and also because of its simplicity. For design purposes, Hognestad's stress block may be employed since the moment and curvature predicted would be slightly more conservative than those derived using the Jensen stress block.

The ultimate moments predicted in all cases, assuming a limiting strain of 0.004 inch per inch, were within 10% of those obtained from the tests. The corresponding curvatures at ultimate condition can be predicted only in the case of two-point loaded beams.

It is recommended that tests be conducted on one-point loaded prestressed beams with some type of mechanical device attached to the prestressing cables. The object should be to study the shape of the M-Ø curves when unbonding of the cables is reduced.

REFERENCES

1. Belke, T. 1965
   Deformation characteristics of pretensioned concrete beams subjected to bending and shear
   M.Sc. Thesis, University of Alberta (Edmonton)

2. Desayi, P. and Krishnan, S. 1964
   Equation for the stress-strain curve of concrete
   J. Am. Concr. Inst. 61: 345

3. Hognestad, E. 1951
   A study of combined bending and axial load in reinforced concrete members
   Bull. Ill. Univ. Engng Exp. Stn. 399

4. Hognestad, E., Hanson, N.W. and McHenry, D. 1955
   Concrete stress distribution in ultimate strength design
   PCA Research and Development Lab. Bull. D6

5. Jensen, V.P. 1943
   Ultimate strength of reinforced concrete beams as related to the plasticity ratio of concrete
   Bull. Ill. Univ. Engng Exp. Stn. 345

6. Kriz, L.B. and Lee, S.L. 1960
   Ultimate strength of over-reinforced beams
   PCA Research and Development Lab. Bull. D36

7. Lee, L.H.N. 1953
   Inelastic behavior of reinforced concrete members subjected to short time static loads
   Proc. ASCE 79: Separate No. 286

8. Neville, A.M. 1963
   Properties of concrete, London, Pitman

9. Raffa, G. 1964
   Deformation characteristics of pretensioned concrete beams in flexure
   M.Sc. Thesis, University of Alberta (Edmonton)

10. Smith, G.M. and Young, L.E. 1956
    Ultimate flexural analysis based on stress-strain curves of cylinders
    J. Am. Concr. Inst. 53: 597

11. Smith, R.G. 1960
Determination of the compressive stress-strain properties of concrete in flexure
Mag. Concr. Res. 12: 165

12. Warwaruk, J., Sozen, M.A. and Siess, C.P. 1962
Strength and behaviour in flexure of prestressed concrete beams
Bull. Ill. Univ. Engng Exp. Stn. 464

Appendix A

NOTATIONS AND METHOD OF ANALYSIS

NOTATIONS

Cross-Sectional Constants and Dimensions

A_s - total area of prestressing reinforcement

b - width of rectangular beam

d - effective depth from the top of the beam to the centroid of the reinforcement

I - gross moment of inertia of the concrete cross-section about the centroidal axis

y_b - the distance from the centroidal axis to the extreme fibre in tension

e - the distance from the centroidal axis to the centroid of the reinforcement

Moments and Forces Acting on the Cross-Section

C - the total compressive force in the concrete

T - the total tensile force in the prestressing reinforcement

P_{eff} - the effective prestress

P - the total prestressing force

M_{cr} - the resisting moment at flexural cracking

M_u - the resisting moment at failure

Stresses and Strain in Concrete

E - the modulus of elasticity of concrete

ϵ_c - the concrete strain

ϵ_{ce} - concrete strain at the level of the reinforcement due to the effective prestress

NOTATIONS (Continued)

ϵ_u - the limiting strain in compressed concrete

f - concrete stress at any strain

f'_c - compressive strength of concrete determined from a standard 6 x 12-in. cylinder

f_r - modulus of rupture of concrete

C_f - the equivalent uniform stress in the compression zone of the concrete beam

Stresses and Strains in Steel

E_s - modulus of elasticity of the prestressing reinforcement

ϵ_s - strain in the reinforcement

ϵ_{se} - effective prestrain in reinforcement due to the effective prestress

ϵ_{sa} - the increase in strain in the prestressed reinforcement between cracking and failure

ϵ_{su} - the total strain in the reinforcement at failure

f_s - the stress in the reinforcement

f_{su} - the prestressing reinforcement stress at ultimate condition

Factors Related to the Beam Cross-Section

k - the ratio of the depth of the compression face to the effective depth of the beam

k_u - the ratio of the depth of the compression face to the effective depth at failure

k_2 - the ratio of the depth of the resultant compressive force to the depth of the neutral axis

p - the reinforcement ratio, A_s/bd

F - the strain compatibility factor

NOTATIONS (Continued)

External Loads, Moments and Deformations

M - the applied moment

$M_u calc$ - the derived ultimate moment

$M_u test$ - the measured ultimate moment

P - the applied load (in text only)

Δ - the midspan deflection

Δ_{test} - the measured deflection at midspan at ultimate load

Δ_{calc} - the midspan deflection obtained from analysis

$\emptyset$ - the curvature of the beam at any point

$\emptyset_u test$ - the curvature at ultimate condition obtained from strain measurements

$\emptyset_u calc$ - the derived curvature at ultimate condition

METHOD OF ANALYSIS

A.1 Introduction

The method of analysis (12) derives the moment-curvature relationship for prestressed concrete beams. It is based on the establishment of two points on the M-Ø curve. These points represent the ultimate condition and cracking condition of the beam. After these two points are obtained, all other points are derived by interpolation. A linear behavior is assumed for the stages of loading from zero load to cracking. Between cracking and ultimate, all moments and curvatures are obtained by assuming a linear relationship between the extreme fibre strain in the concrete and the increase in reinforcement strain ϵ_{sa}. The compatibility factor F , varies from a value of unity at cracking to a value less than one at the ultimate condition.

A.2 Assumptions

The following assumptions are made in the analysis:

(a) Strains in the compression face of the concrete are linearly distributed.

(b) The effective strength of the concrete is known, being determined beforehand from the standard 6 x 12-inch cylinder test.

(c) The resultant compressive force and its position can be determined from the shape of the assumed stress-strain curve.

(d) No tension is carried by the concrete. The tensile stress carried by concrete is usually small and unreliable, varying with the moisture content and concrete strength (3) .

(e) Failure of the beam takes place at a limiting strain of 0.004 inch per inch in the extreme fibre of the concrete in compression.

(f) The strain compatibility factor F at ultimate condition is known and is given by the equation

$$F\epsilon_u = \epsilon_{sa}\left(\frac{k_u}{1 - k_u}\right) \qquad (A.1)$$

The concrete strain in the extreme fibre varies from a maximum value above a crack to a minimum value between cracks. It is therefore convenient to use an average strain in the extreme compression fibre. This average strain is the product of the limiting strain and the compatibility factor

$$F\epsilon_u = \frac{1 + 2k_u}{600} \leqslant 0.004 \qquad (A.2)$$

(g) The stress-strain relationship of the prestressing cables was known.

A.3 Method of Analysis

A.3.1 Introduction

For any assumed stress block, the compressive force factor C_f and k_2 factor (see Notations) were derived in increments of 0.0002 inch per inch for all strains from .0002 to 0.004 inch per inch. These factors

were then used to derive the M-Ø relationship.

The moment-curvature relationship was obtained using three basic types of computations. These are as follows:

i. The ultimate moment and corresponding curvature

ii. The moment and curvature at cracking

iii. The moment and curvature at intermediate points between cracking and ultimate.

The method used in each of these computations is discussed in the following subsections. The flow diagram for the computer program is presented in Appendix B.

A.3.2 Ultimate Moment

The condition of stress and strain distribution in a prestressed beam at ultimate load is shown in Figure A.1. The steps taken in deriving the ultimate moment and corresponding curvature are as follows:

i. A value of k_u was assumed and $F\epsilon_u$ was calculated using equation A.2.

ii. With the computed $F\epsilon_u$ from step i and the use of equation A.1, the increase in reinforcement stress ϵ_{sa} , at ultimate condition was derived

iii. The total strain in the reinforcement was then obtained from the relationship

$$\epsilon_{su} = \epsilon_{sa} + \epsilon_{se} + \epsilon_{ce} \qquad (A.3)$$

iv. The tensile stress f_{su} in the reinforcement was computed using ϵ_{su} from step iii, and the relationship discussed in section A.3.5. The tensile force was then found from the

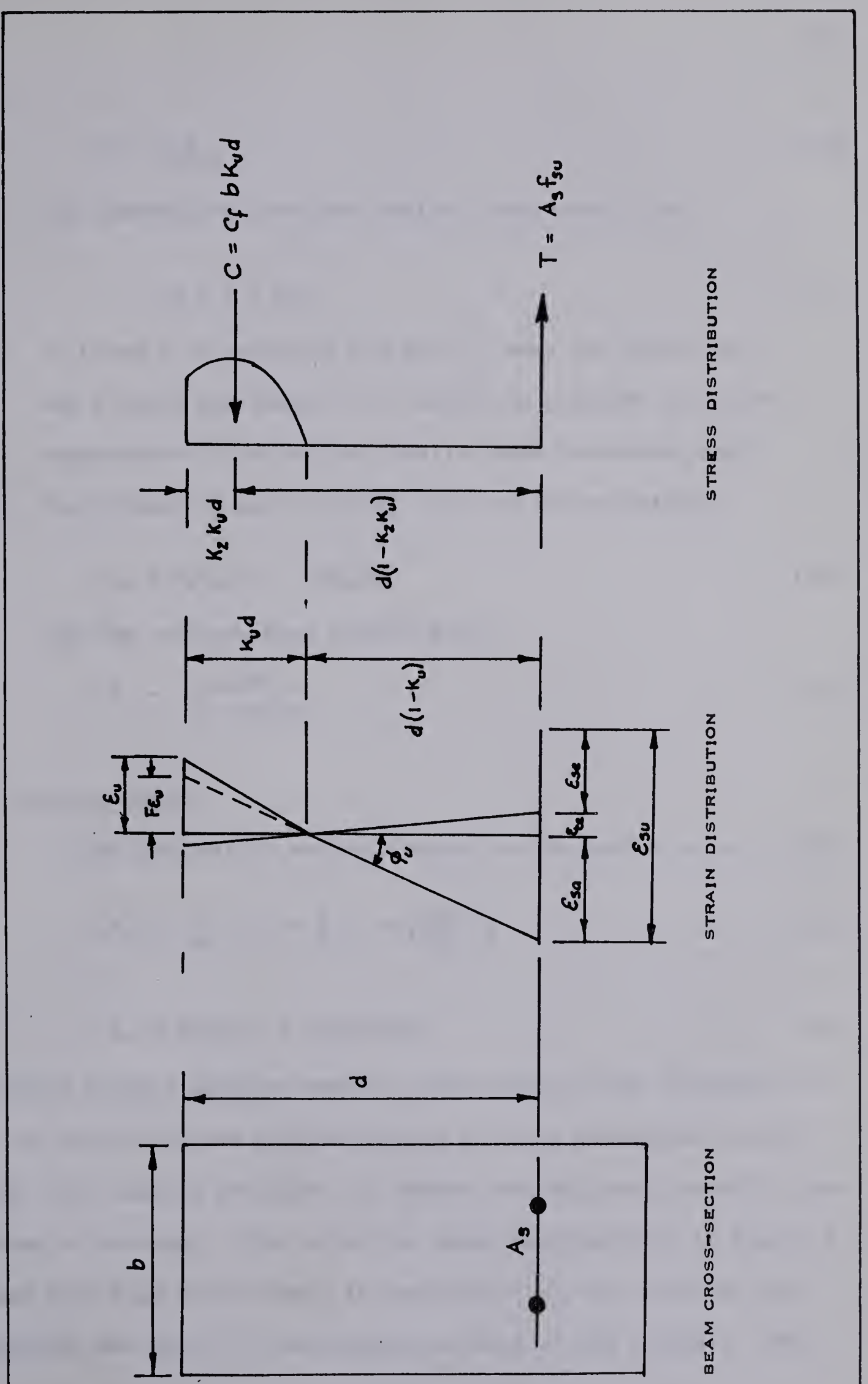

FIGURE A.1 CONDITIONS OF STRESS AND STRAIN AT FAILURE

equation

$$T = A_s f_{su} \tag{A.4}$$

v. The compressive force was derived independently as

$$C = C_f \times b \times k_u d \tag{A.5}$$

vi. If C and T of equations A.4 and A.5 were not equal, k_u was revised and steps i to v were then repeated until the compressive force and the tensile force were made equal.

vii. The ultimate moment was then given by the expression,

$$M_u = A_s f_{su}(1 - k_2 k_u) d \tag{A.6}$$

and the corresponding curvature by

$$\phi_u = \frac{\epsilon_{sa}}{(1 - k_u) d} \tag{A.7}$$

A.3.3 Cracking Moment

In the preliminary analysis using the expression given in (12)

$$M_{cr} = \frac{I}{y_b} \left[f_r + \frac{P}{A} \left(1 + \frac{eA}{I/y_b}\right) \right] \tag{A.8}$$

where

$$f_r = 3000/(3 + 12{,}000/f'_c) \tag{A.9}$$

the cracking moments obtained were in some cases low and in others too high. For beams with low p/f'_c values, the cracking moment was usually too high. The moments obtained just beyond cracking were generally less than those at cracking. This effect is shown qualitatively in Figure A.2. For beams with high p/f'_c values, it was found that, at cracking, the reinforcement was still in the compression zone of the concrete. The

moments just beyond cracking showed a corresponding curvature less than that at cracking. This effect is also shown qualitatively in Figure A.2. Since the reinforcement was in the compression zone at cracking, a negative value of ϵ_{sa} was produced on the ϵ_c vs ϵ_{sa} diagram shown in Figure A.4.

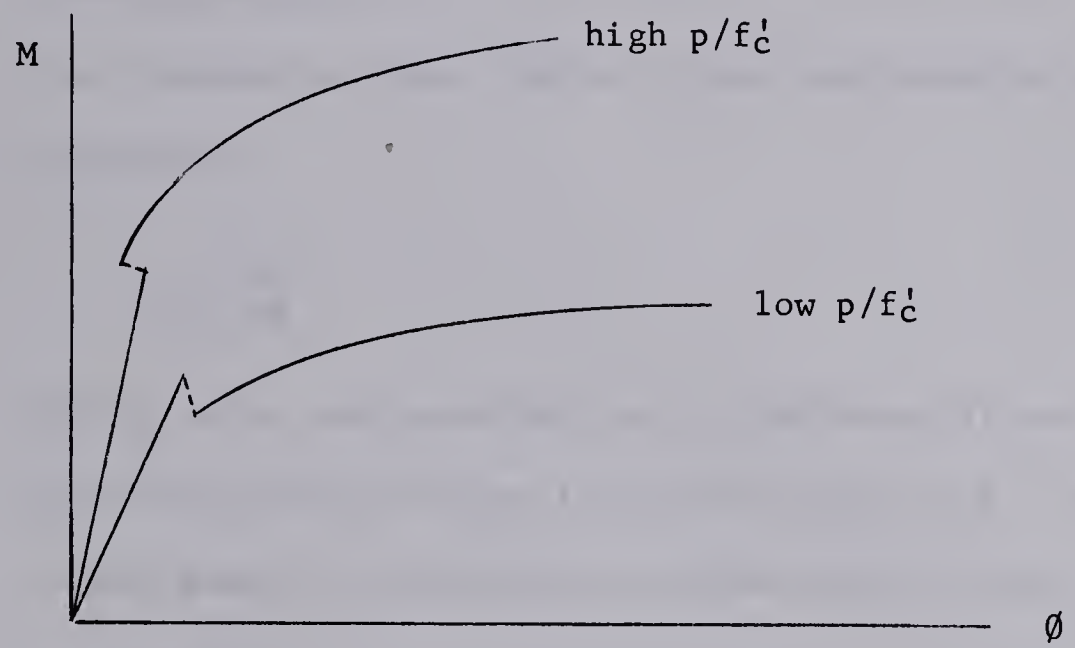

Figure A.2 M-Ø Curves for High and Low p/f'_c

These discrepancies were avoided by assuming another moment close to cracking as the second known point on the M-Ø curve. The assumed moment corresponded to the stage of loading at which a crack had progressed up to the level of the reinforcement. In the actual case, since tension was neglected, the crack had progressed to some point below the reinforcement such that the neutral axis was at the level of the reinforcement. Thus the increase in reinforcement strain was zero. With the above assumptions, the moment at this new cracking point was obtained by following the steps outlined:

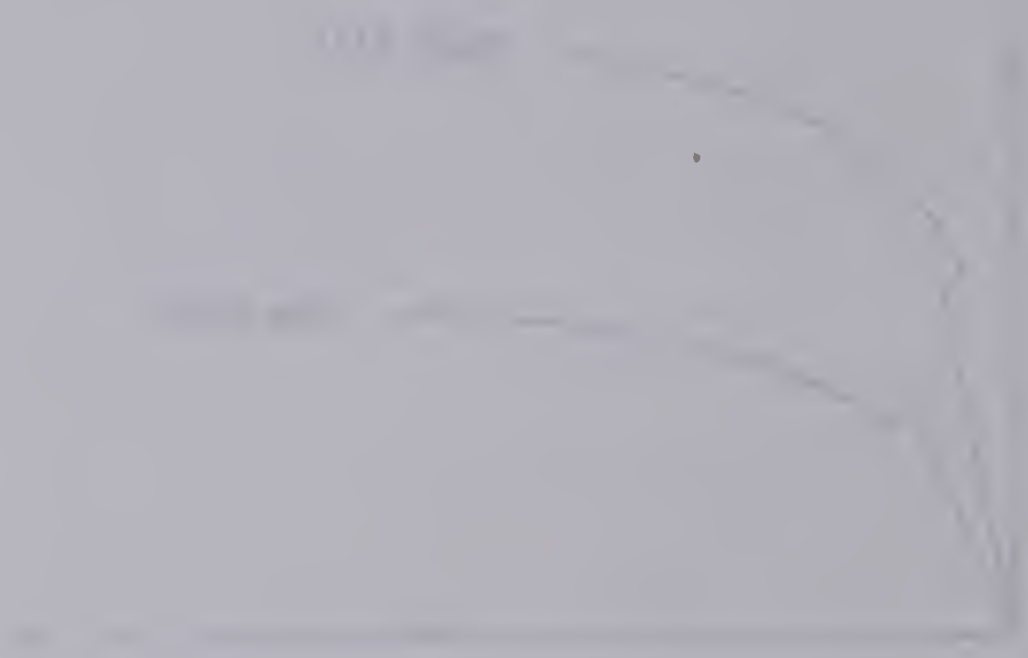

i. The total reinforcement strain was given by

$$\epsilon_s = \epsilon_{se} + \epsilon_{ce} \tag{A.10}$$

ii. The tensile stress in the reinforcement was obtained from a knowledge of ϵ_s and the tensile force T was computed from equation A.4.

iii. The compressive force factor C_f was then found using the expression

$$C_f = \frac{T}{bd} \tag{A.11}$$

iv. The k_2 value corresponding to C_f from step iii was derived by interpolating between the known values of k_2 corresponding to the known C_f increments on either side of the C_f obtained in step iii.

v. The moment was calculated using the expression

$$M = A_s f_s (1 - k_2) d \tag{A.12}$$

For purposes of comparison, the modulus of rupture for each beam was calculated using equation A.9, the expression (8)

$$f_r = 9.5 \sqrt{f'_c} \tag{A.13}$$

and by working backwards from equation A.8.

In Reference (12) the modulus of rupture was obtained from equation A.9 and the cracking moment M_{cr} was assumed to be that moment

at which the beam was just on the verge of cracking.

In the beam tests, the observed flexural cracking load was usually higher than the theoretical cracking load, since it was based on a positive visual identification of a crack. Thus, in an attempt to arrive at the theoretical cracking moment, a value of 0.9 times the observed cracking moment was inserted in equation A.8. The force P in equation A.8 was taken as the effective prestressing force. It could be assumed that the increase in the reinforcement strain from the start of the test to cracking compensated for relaxation in the prestressing cables. The values of f_r calculated are shown in Table A.1 and are also plotted in Figure A.3. Values predicted by equation A.9 and A.13 are also presented.

From Table A.1, it can be seen that beams 13 and 2A which had the same concrete strengths and the same amount of reinforcement, had almost the same calculated modulus of rupture. Beams 3A and 3B with concrete strengths of 3500 psi and steel areas of 0.4624 sq. inch, showed calculated f_r values of 638 and 705 psi respectively. However, beam 1B with the same concrete strength as beams 3A and 3B and steel area of 0.2312 sq. inch, had a calculated f_r value of 259 psi.

Thus, although the method of computing f_r is rather approximate, there is an indication that the amount of reinforcement present in the beam may have some effect on the modulus of rupture and in turn on the cracking moment of the beam. In general, the plot of calculated modulus of rupture against concrete strength illustrated in Figure A.3, showed a scatter of points. Equation A.9 seems to yield an average curve, yet there were large variations from this curve. The curve obtained using

TABLE A.1

MODULUS OF RUPTURE

Beam No.	f'_c psi	f_r calculated psi	$9.5\sqrt{f'_c}$ psi	$\frac{3000}{3 + \frac{12,000}{f'_c}}$ psi
4	4800	161	658	545
10	4300	755	625	517
11	4000	296	600	500
12	3600	284	570	474
13	3400	381	554	460
1A	4300	629	624	517
2A	3400	383	554	460
3A	3500	638	562	466
4A	6000	516	735	600
5A	6800	562	782	630
6A	6900	623	790	633
1B	3500	259	562	466
2B	4200	713	615	510
3B	3500	705	562	466
4B	6300	302	753	610
5B	6500	649	765	620
6B	5900	652	730	595

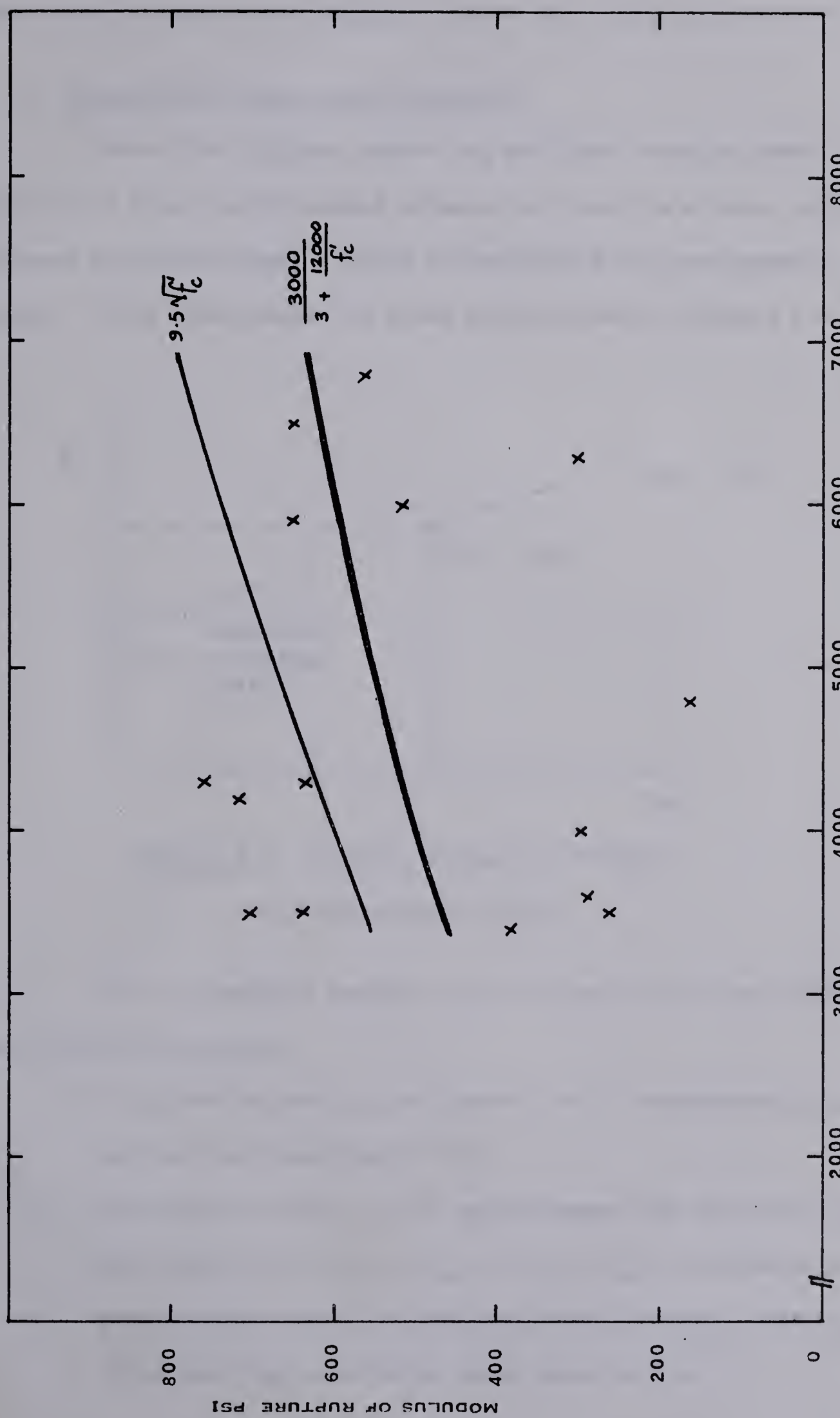

FIGURE A.3 MODULUS OF RUPTURE VS. CONCRETE STRENGTH

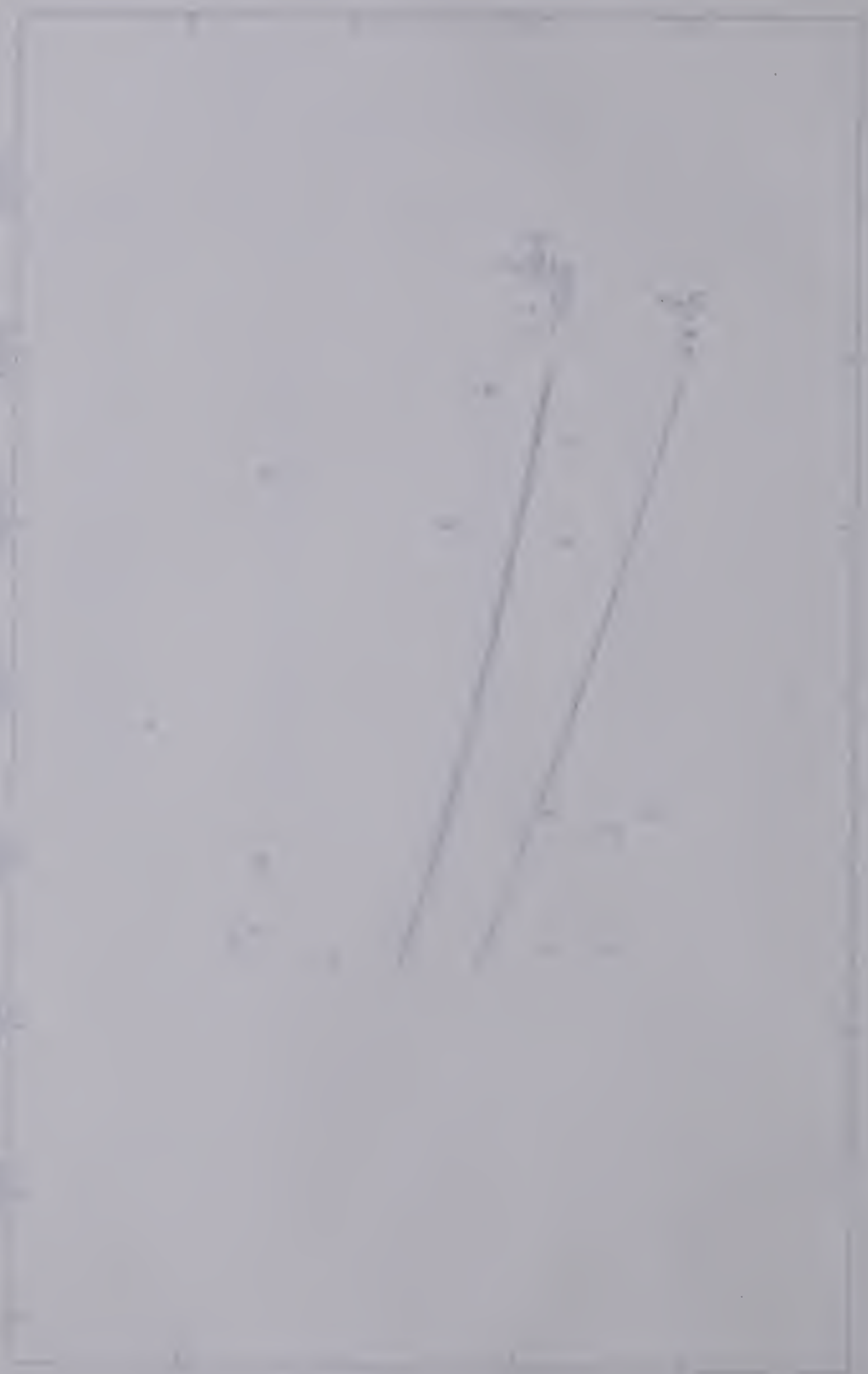

equation A.13 tended to be slightly higher than the average curve.

A.3.4 Intermediate Moments and Curvature

After the ultimate moment and modified cracking moments were obtained, a linear relationship between the concrete strains and the increase in reinforcement strains corresponding to these moments was derived. This relationship is shown qualitatively in Figure A.4.

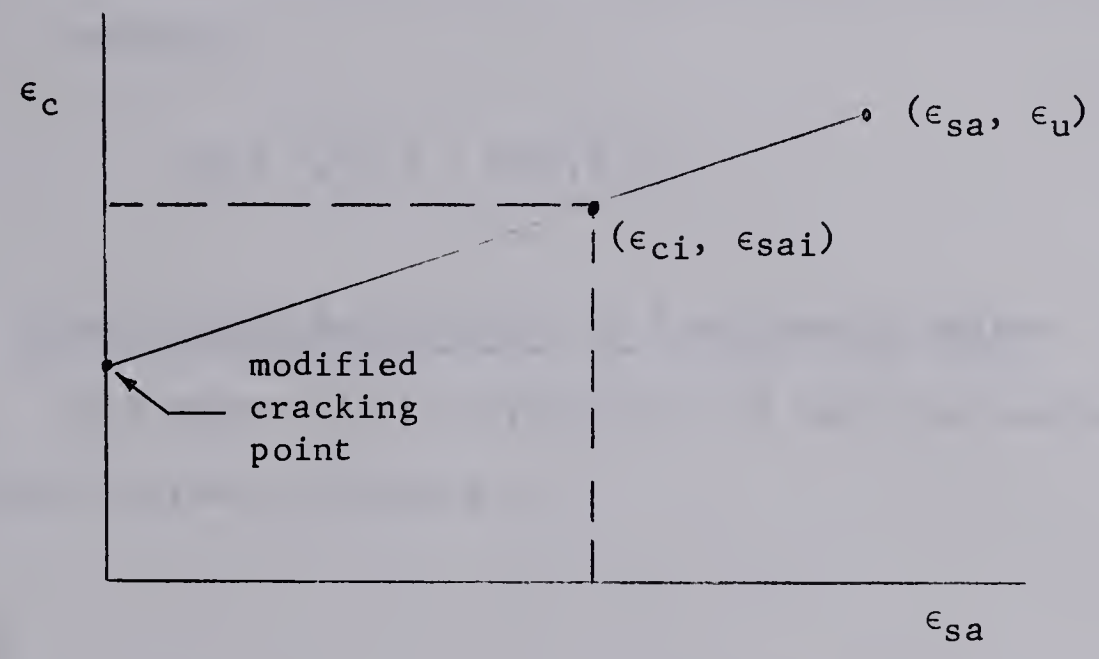

Figure A.4 Concrete Strain vs Increase in Reinforcement Strain

The intermediate moments and curvatures were then computed by the following procedure.

i. A concrete strain ϵ_{ci} was chosen and a corresponding ϵ_{sai} was derived (see Figure A.4).

ii. The tensile stress in the reinforcement was obtained from the total strain, $\epsilon_{si} = \epsilon_{sai} + \epsilon_{se} + \epsilon_{ce}$, and the stress-strain relationship of the prestressing cables. The tensile force was then calculated using equation A.4.

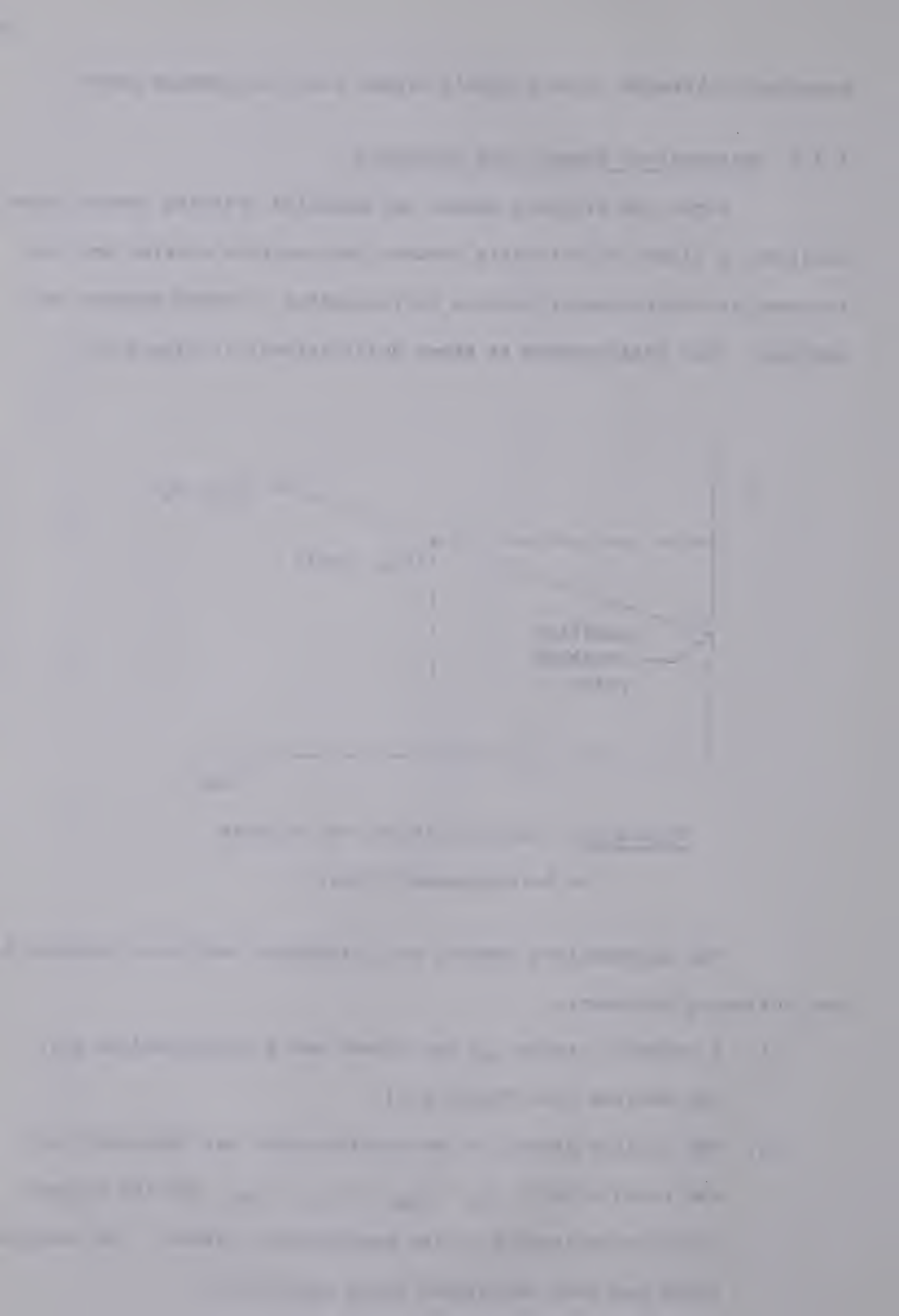

iii. Using the tensile force from step ii, the depth of the compression face was computed from the relationship

$$k_i d = \frac{T}{bC_{fi}} \tag{A.14}$$

where C_{fi} was a known value corresponding to ϵ_{ci} .

iv. With the known value of k_{2i} corresponding to ϵ_{ci} , the moment at an intermediate position was found by using the equation

$$M_i = A_s f_s (1 - k_{2i} k_i)\, d \tag{A.15}$$

A.3.5 Stress-Strain Relationship of Prestressing Cables

The stress-strain relationship of the prestressing cables is shown qualitatively in Figure A.5.

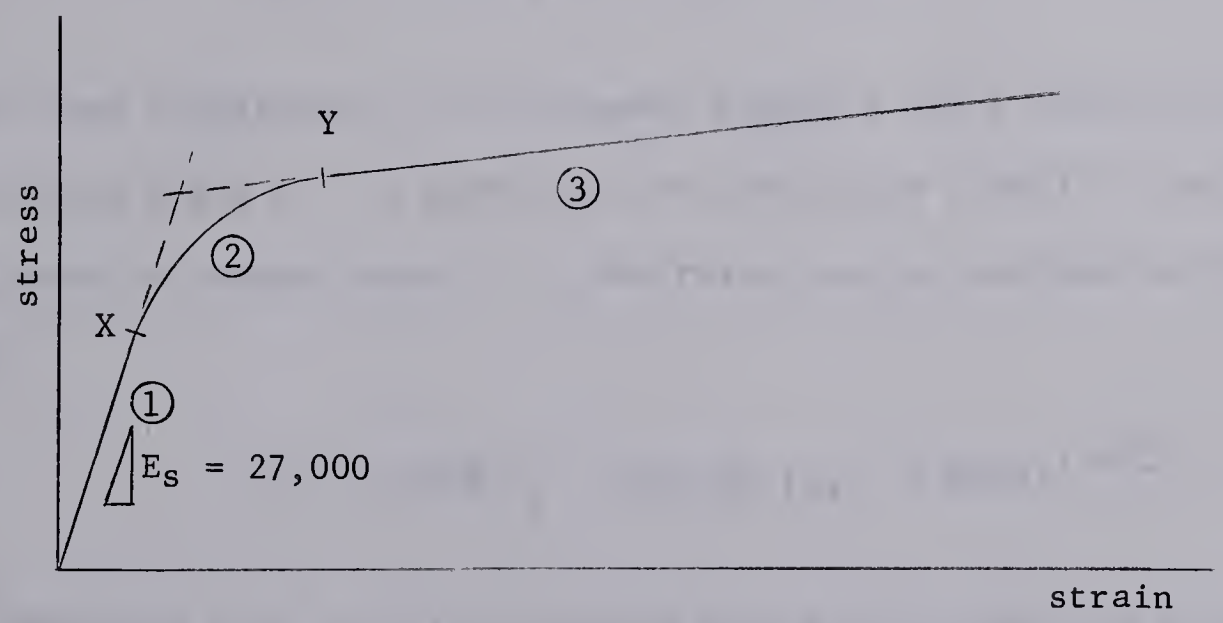

Figure A.5 Stress-Strain Curve for Prestressing Cables

The stress-strain curve consisted of two straight lines joined

by a smooth curve, forming three distinct ranges. In the analysis, three equations for stress in terms of strain were employed. The equation used depended on the range within which the cables were strained.

In the first and third ranges (see Figure A.5) the equations were linear and were given as follows:

in the first range,

$$f_s = 27{,}000\ \epsilon_s \tag{A.16}$$

in the third range,

$$f_s = 254 + 500\ \epsilon_s \tag{A.17}$$

The equation for the second range was obtained by substituting into the equation

$$f_s = 27{,}000\ \epsilon_s - B\ (\epsilon_s - 0.0075)^n \tag{A.18}$$

the known coordinates of the tangent points X and Y and solving for the constants B and n. In equation A.18, the value 0.0075 is the strain ordinate at tangent point X . The relationship obtained for range 2 was ,

$$f_s = 27{,}000\ \epsilon_s - 194{,}100\ (\epsilon_s - 0.0075)^{1.4722} \tag{A.19}$$

In equations A.16 to A.19, stresses were given in ksi and strains in inch per inch. Thus for any value of strain, the corresponding stress value could be readily derived.

Appendix B

FLOW DIAGRAM FOR MAIN PROGRAM

NOTATIONS IN MAIN PROGRAM

Main Do Loops

NO - number of concrete strengths used

N - number of strain values read into program

K - number of beams for each concrete strength

Data Calculated From Stress Blocks

EE(I) - strain values in increments of 0.0002 inch per inch

CF(I) - compressive force factor; this is the area under the stress-strain curve at any strain value divided by the particular strain

FK2(I) - k_2 value corresponding to CF(I)

Beam Data

AS - area of reinforcement in beam

B - width of beam

FH - overall depth of beam

D - effective depth of beam

X - eccentricity of prestressing force

FC - concrete strength obtained from cylinder test

P - effective prestress

ECE - initial concrete prestrain at the level of the reinforcement due to the prestressing force

NOTATIONS IN MAIN PROGRAM (Continued)

Ultimate Condition

MU - ultimate moment M_u

CU - ultimate curvature $\emptyset_u$

FEU - product of compatibility factor and limiting strain ($F\epsilon_u$)

FKU - factor k_u from which the depth of the compression face could be calculated

ESA - increase in reinforcement strain at ultimate condition

ESE - initial prestrain in reinforcement

ESU - total strain in reinforcement at ultimate condition

FS - steel stress

TF - tensile force at ultimate condition

CO - compressive force in concrete at ultimate condition

Cracking Stage

ESCR - total reinforcement strain at cracking

FSCR - reinforcement stress at cracking

TCR - tensile force in reinforcement at cracking

CFCR - compressive force factor at cracking

EECR - compressive concrete strain at cracking

FK2CR - k_2 factor at cracking

MCR - cracking moment

CCR - curvature at cracking

Intermediate Stages

S - slope of ϵ_c vs ϵ_{sa}diagram

ES(I) - increase of reinforcement strain corresponding to concrete strain ϵ_{ci}

NOTATIONS IN MAIN PROGRAM (Continued)

ESN - total reinforcement strain corresponding to ϵ_{ci}

T(I) - tensile force corresponding to ϵ_{ci}

KD(I) - depth to the neutral axis when extreme fibre strain is ϵ_{ci}

M(I) - moment due to tensile force T(I)

C(I) - curvature corresponding to M(I)

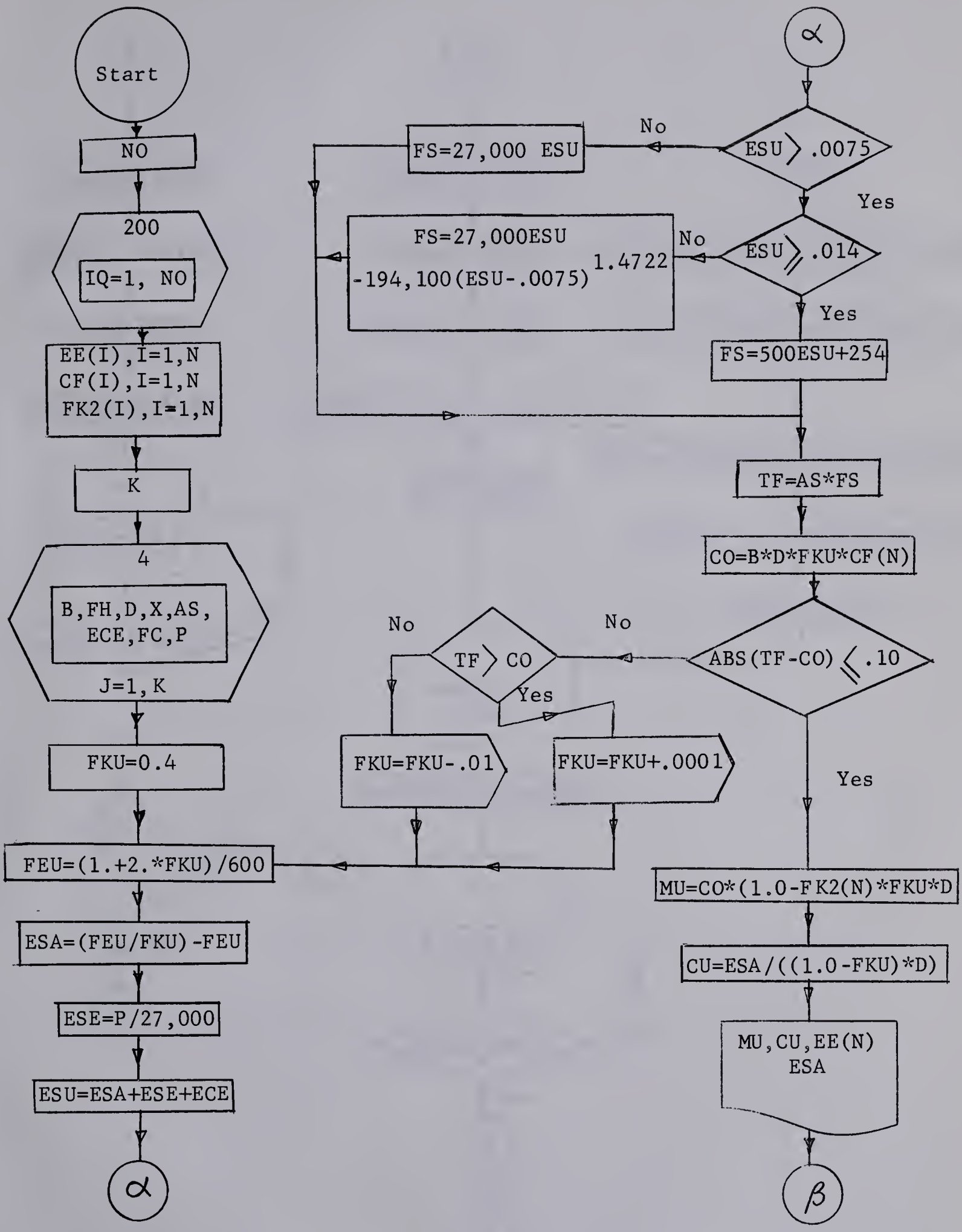
Start
NO
200
IQ=1, NO
EE(I),I=1,N
CF(I),I=1,N
FK2(I),I=1,N
K
4
B,FH,D,X,AS,
ECE,FC,P
J=1,K
FKU=0.4
FEU=(1.+2.*FKU)/600
ESA=(FEU/FKU)-FEU
ESE=P/27,000
ESU=ESA+ESE+ECE
α
FS=27,000 ESU
No
ESU > .0075
Yes
FS=27,000ESU
-194,100(ESU-.0075)^1.4722
No
ESU ≥ .014
Yes
FS=500ESU+254
TF=AS*FS
CO=B*D*FKU*CF(N)
No
TF > CO
Yes
FKU=FKU-.01
FKU=FKU+.0001
No
ABS(TF-CO) ≤ .10
Yes
MU=CO*(1.0-FK2(N)*FKU*D
CU=ESA/((1.0-FKU)*D)
MU,CU,EE(N)
ESA
β

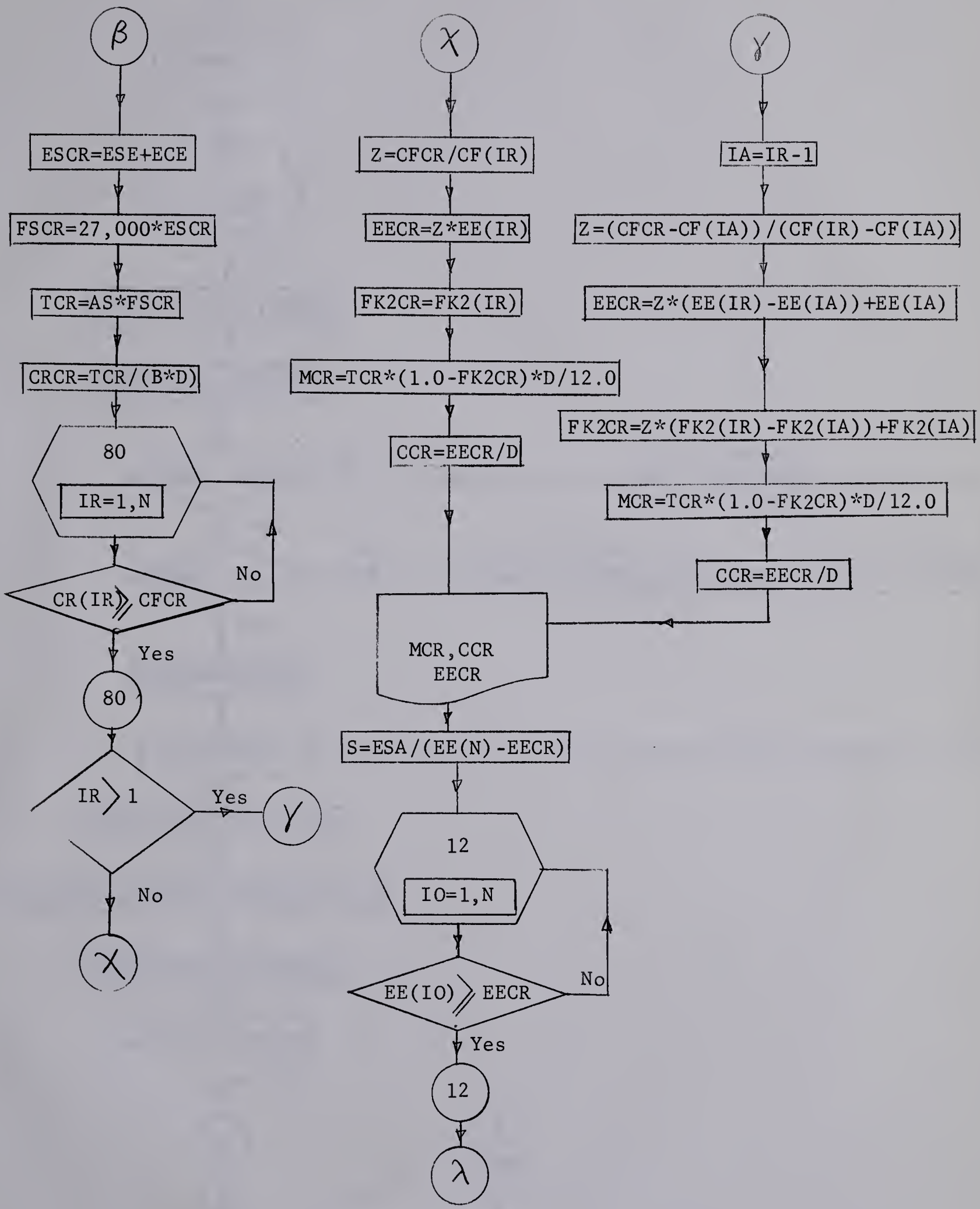
β
ESCR=ESE+ECE
FSCR=27,000*ESCR
TCR=AS*FSCR
CRCR=TCR/(B*D)
80
IR=1,N
CR(IR) ≫ CFCR
No
Yes
80
IR ⟩ 1
Yes
γ
No
χ
χ
Z=CFCR/CF(IR)
EECR=Z*EE(IR)
FK2CR=FK2(IR)
MCR=TCR*(1.0-FK2CR)*D/12.0
CCR=EECR/D
γ
IA=IR-1
Z=(CFCR-CF(IA))/(CF(IR)-CF(IA))
EECR=Z*(EE(IR)-EE(IA))+EE(IA)
FK2CR=Z*(FK2(IR)-FK2(IA))+FK2(IA)
MCR=TCR*(1.0-FK2CR)*D/12.0
CCR=EECR/D
MCR,CCR
EECR
S=ESA/(EE(N)-EECR)
12
IO=1,N
EE(IO) ≫ EECR
No
Yes
12
λ

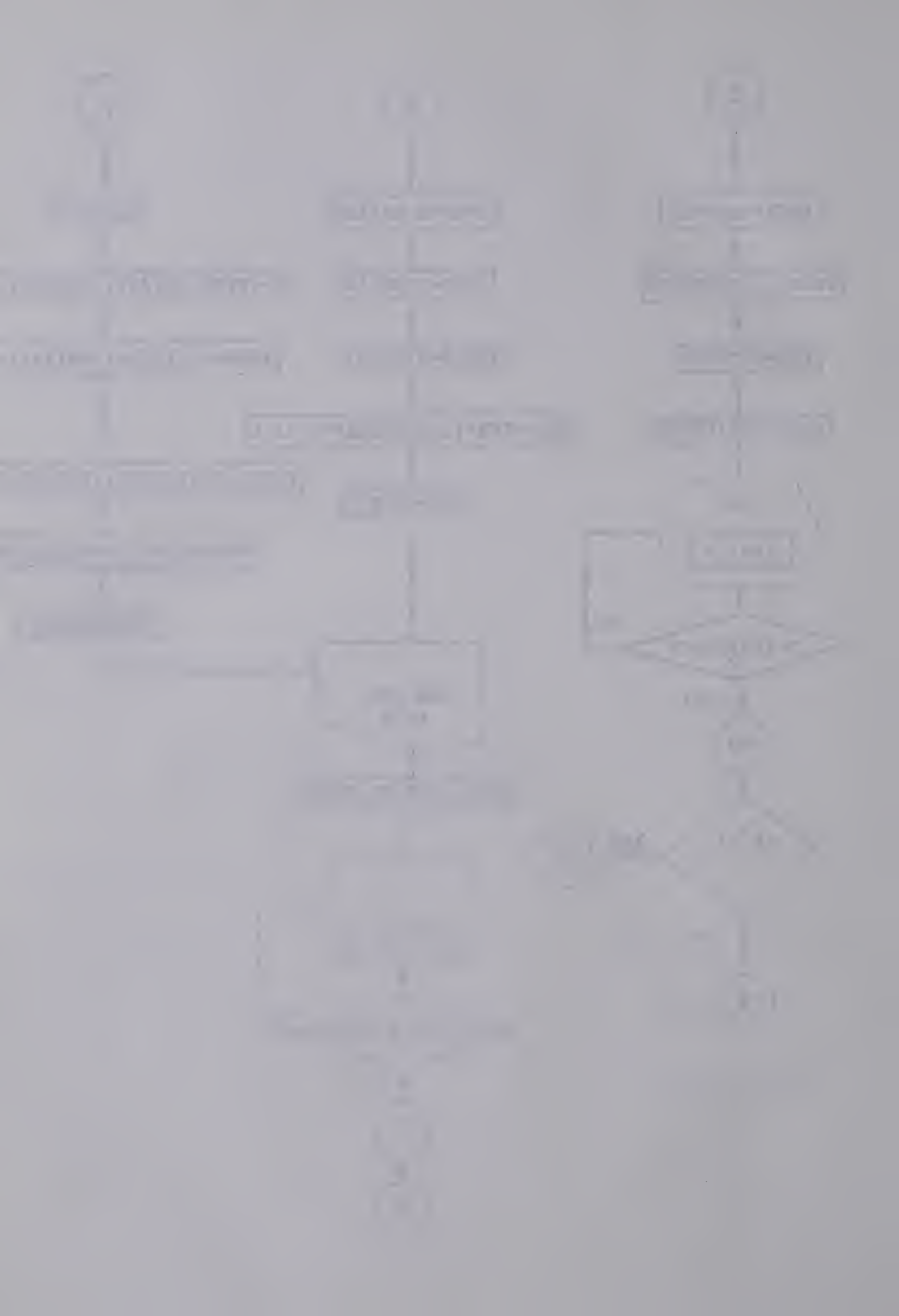

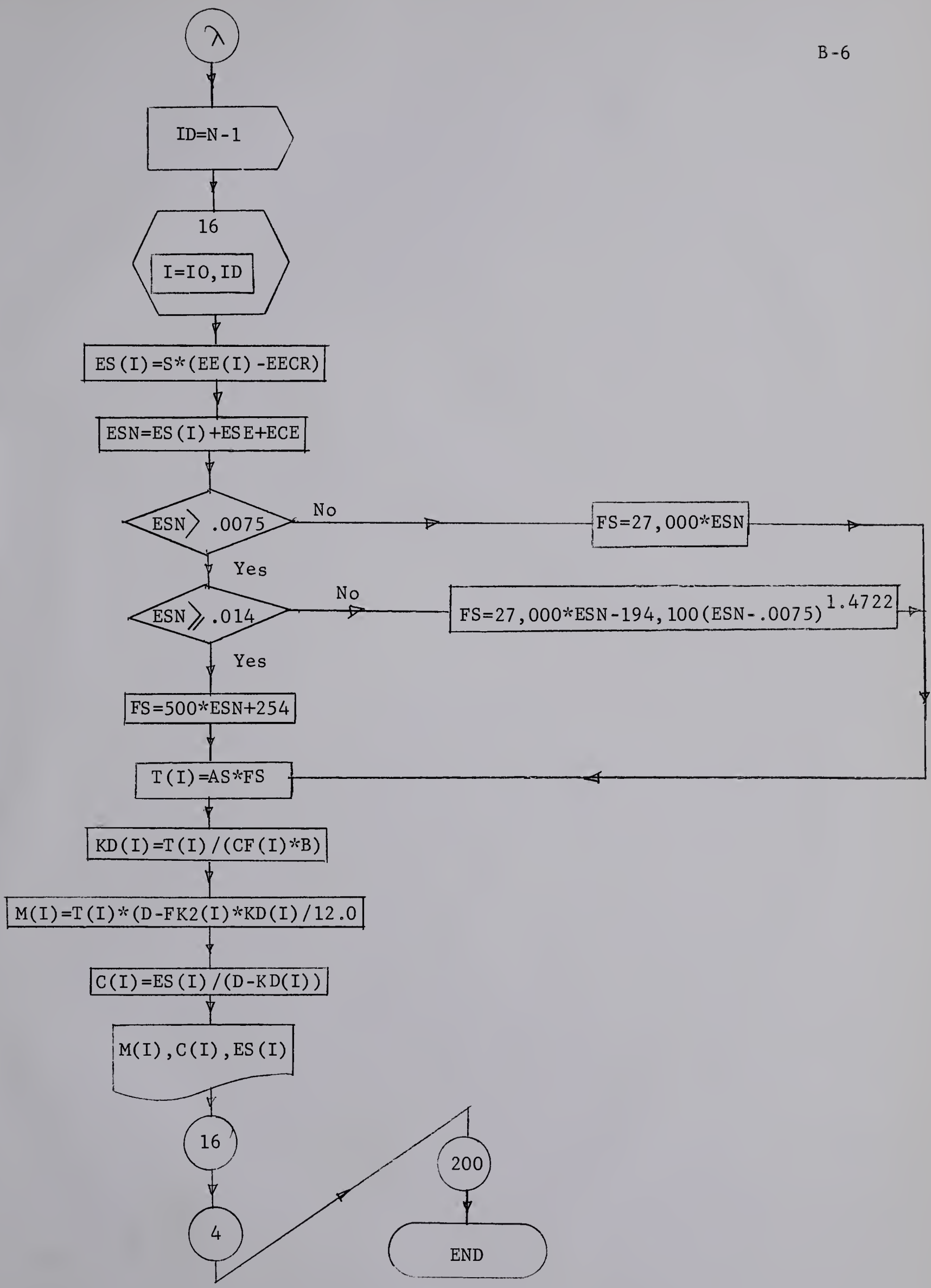
λ
ID=N-1
16
I=IO,ID
ES(I)=S*(EE(I)-EECR)
ESN=ES(I)+ESE+ECE
ESN > .0075
No
FS=27,000*ESN
Yes
ESN >= .014
No
FS=27,000*ESN-194,100(ESN-.0075)^1.4722
Yes
FS=500*ESN+254
T(I)=AS*FS
KD(I)=T(I)/(CF(I)*B)
M(I)=T(I)*(D-FK2(I)*KD(I)/12.0
C(I)=ES(I)/(D-KD(I))
M(I),C(I),ES(I)
16
4
200
END